

LIST OF TABLES

Table 1.1	Known mutational signatures due to DNA damage	8
Table 1.2	Known mutational signatures due to the activity of DNA repair mechanisms	24
Table 2.1	Similarities between simulated mutational signatures	47
Table 3.1	Summary of breast cancer samples and their data sources	72
Table 3.2	Validating consensus mutational signatures found in breast cancer	84
Table 4.1	Validating consensus mutational signatures found in human cancer	97
Table 5.1	Mutational signatures and age of diagnosis	119
Table 6.1	Summary of the deciphered signatures of mutational processes in human cancer	123

LIST OF FIGURES

Figure 1.1	Somatic mutations in cancer versus nucleotide polymorphisms in the germline	5
Figure 1.2	Illustration of mutational processes operative in a cancer	7
Figure 2.1	Simulated examples of mutational signatures defined over different mutational alphabets	46
Figure 2.2	Simulated example of a mutational catalogue of cancer genome	48
Figure 2.3	Simulated example of three mutational signatures active in a single cancer genome	51
Figure 2.4	Simulated example of mutational signatures deciphered from a set of mutational catalogues	54
Figure 2.5	Deciphering mutational signatures from a set of 100 simulated mutational catalogues.	61
Figure 2.6	Design for simulating four mutational signatures with different similarities between them	63
Figure 2.7	Deciphering mutational signatures with different similarities between them	63
Figure 2.8	Deciphering mutational signatures from different sets of cancer genomes	64
Figure 2.9	Dependencies between mutational signatures and mutational catalogues of cancer genomes	64
Figure 2.10	Dependencies between mutational signatures and numbers of somatic mutations	65
Figure 2.11	Deciphering mutational signatures with different contributions in mutational catalogues	66
Figure 2.12	Deciphering errors of exposures and accuracy of mutational signatures	67
Figure 2.13	Evaluating the error rate of identified contributions of mutations signatures	68
Figure 3.1	Mutational signatures extracted from 119 breast cancer genomes	73
Figure 3.2	Breast cancer whole-genome mutational signatures with indels and dinucleotides	75
Figure 3.3	Breast cancer whole-genome mutational signatures with strand-bias	76
Figure 3.4	Signature BC-WG-2 with additional sequence context	77
Figure 3.5	Signature BC-WG-6 with additional sequence context	78
Figure 3.6	Mutational signatures extracted from 884 breast cancer exomes	79
Figure 3.7	Breast cancer exome mutational signatures with indels and dinucleotides	80
Figure 3.8	Breast cancer exome mutational signatures with strand-bias	81
Figure 3.9	Clustering of breast cancer signatures derived from whole-genome and exome data	82
Figure 3.10	Contributions of mutational signatures in a selected set of 25 breast cancer samples	85
Figure 3.11	Summary of the contributions of the mutational signatures in breast cancer	85
Figure 3.12	Samples harbouring <i>BRCA1/2</i> mutations and contributions of mutational signatures	87
Figure 3.13	Estrogen receptor positive/negative samples and contributions of mutational signatures	88
Figure 3.14	Age of diagnosis and mutations due to different mutational signatures	88
Figure 4.1	Samples used for deciphering signatures of mutational processes in human cancer	91
Figure 4.2	Mutational burden in human cancer	92
Figure 4.3	Clustering of mutational signatures	94
Figure 4.4	Types of statuses for validating mutational signatures	95
Figure 4.5	Consensus validated mutational signatures in human cancer	98

Figure 4.6	Consensus mutational signatures that failed validation	99
Figure 4.7	Consensus mutational signatures for which it is not possible to perform validation	99
Figure 4.8	Consensus mutational signatures with strand-bias	101
Figure 4.9	Signatures of mutational processes and the cancer types in which they are found	104
Figure 4.10	Prevalence of validated mutational signatures across all cancer types	105
Figure 4.11	Contributions of mutational signatures in a selected set of cancer types	107
Figure 5.1	Samples harbouring <i>BRCA1/2</i> mutations and contributions of Signature 3	114
Figure 5.2	Associating exposures of mutational signatures to cigarette smoking	116
Figure 5.3	Associating molecular or clinical features with the activity of mutational signatures	118

LIST OF ABBREVIATIONS

8-oxoG	7,8-dihydro-8-oxoguanine
AID	Activation-induced cytosine deaminase
APEX1	Apurinic/aprimidinic endonuclease
API	Application programming interface
APOBEC	Apolipoprotein B mRNA editing enzyme, catalytic polypeptide-like
BAM	Binary sequence alignment and mapping
BER	Base excision repair
BIR	Break-induced replication
BSS	Blind source separation
CGP	Cancer Genome Project
CPD	Cyclobutane pyrimidine dimer
D-loop	Displacement-loop
DA-NER	Domain associated nucleotide excision repair
dbSNP	Single Nucleotide Polymorphism Database
DNA	Deoxyribonucleic acid
dNTP	Deoxynucleoside triphosphate
DSBR	Classical double-strand break repair
FDR	False discovery rate
GG-NER	Global genome-wide nucleotide excision repair
GLM	Generalized linear model
GRCh37	Genome Reference Consortium human genome (build 37)
IARC	International Agency for Research on Cancer
ICA	Independent component analysis
ICGC	International Cancer Genome Consortium
IGHV	Immunoglobulin gene hypermutation
Indel	Small insertion/deletion
LP-BER	Long patch base excision repair
MMEJ	Microhomology mediated end joining
MMR	DNA mismatch repair
NER	Nucleotide excision repair
NHEJ	Non-homologous end joining

NHLBI	National Heart, Lung, and Blood Institute
NMF	Nonnegative matrix factorization
PAH	Polycyclic aromatic hydrocarbons
PCR	Polymerase chain reaction
Pol	Polymerase
POL II	RNA polymerase II
POLE	DNA polymerase epsilon catalytic subunit A
RFC	Replication factor C
RNA	Ribonucleic acid
RNS	Reactive nitrogen species
ROS	Reactive oxygen species
SDSA	Synthesis-dependent strand annealing
SNP	Single nucleotide polymorphism
SP-BER	Short patch base excision repair
SSA	Single-strand annealing
TC-BER	Transcription coupled base excision repair
TC-NER	Transcription coupled nucleotide excision repair
TCGA	The Cancer Genome Atlas
TET	Ten-eleven translocation methylcytosine dioxygenase
TP53	Tumour protein p53
UCSC	University of California, Santa Cruz
UV	Ultraviolet
UV-A	Ultraviolet A
UV-B	Ultraviolet B
UV-C	Ultraviolet B

APPENDIX I: Alphabets of mutational types

This appendix contains information for the alphabets of mutation types used throughout the course of this thesis. These alphabets were termed Ξ_6 , Ξ_{96} , Ξ_{99} , Ξ_{192} , and Ξ_{1536} in chapter 2 and each one will be discussed in more details in the next few sections.

Mutational alphabet Ξ_6

The Ξ_6 alphabet is perhaps the simplest possible alphabet as it considers only the six types of somatic substitutions: **C>A**, **C>G**, **C>T**, **T>A**, **T>C**, **T>G**. All mutations are denoted using the pyrimidine of the Watson-Crick base pair as the reference and, in this appendix, these substitutions are coloured consistently with the way they are plotted in the majority of figures throughout this thesis.

Mutational alphabet Ξ_{96}

The Ξ_{96} alphabet provides greater resolution for examining the six types of single nucleotide variants (*i.e.*, the Ξ_6 alphabet) by including the immediate sequence context of each mutated base. In this alphabet, a mutation type contains a somatic substitution and both the 5' and 3' base next to the somatic mutation. For example, a **C>T** mutation can be characterized as ...**TpCpG**...>...**TpTpG**... (mutated base underlined and presented as the pyrimidine partner of the mutated base pair) generating 96 possible mutation types – (6 types of substitutions) * (4 types of 5' bases) * (4 types of 3' bases). Table listing each of the 96 substitution types, the reference trinucleotide, and the mutated trinucleotide is provided below.

Sub	Ref	Mut	Sub	Ref	Mut
C>A	ApCpA	ApApA	T>A	ApTpA	ApApA
C>A	ApCpC	ApApC	T>A	ApTpC	ApApC
C>A	ApCpG	ApApG	T>A	ApTpG	ApApG
C>A	ApCpT	ApApT	T>A	ApTpT	ApApT
C>A	CpCpA	CpApA	T>A	CpTpA	CpApA
C>A	CpCpC	CpApC	T>A	CpTpC	CpApC
C>A	CpCpG	CpApG	T>A	CpTpG	CpApG
C>A	CpCpT	CpApT	T>A	CpTpT	CpApT
C>A	GpCpA	GpApA	T>A	GpTpA	GpApA
C>A	GpCpC	GpApC	T>A	GpTpC	GpApC
C>A	GpCpG	GpApG	T>A	GpTpG	GpApG
C>A	GpCpT	GpApT	T>A	GpTpT	GpApT

C>A	TpCpA	TpApA	T>A	TpTpA	TpApA
C>A	TpCpC	TpApC	T>A	TpTpC	TpApC
C>A	TpCpG	TpApG	T>A	TpTpG	TpApG
C>A	TpCpT	TpApT	T>A	TpTpT	TpApT
C>G	ApCpA	ApGpA	T>C	ApTpA	ApCpA
C>G	ApCpC	ApGpC	T>C	ApTpC	ApCpC
C>G	ApCpG	ApGpG	T>C	ApTpG	ApCpG
C>G	ApCpT	ApGpT	T>C	ApTpT	ApCpT
C>G	CpCpA	CpGpA	T>C	CpTpA	CpCpA
C>G	CpCpC	CpGpC	T>C	CpTpC	CpCpC
C>G	CpCpG	CpGpG	T>C	CpTpG	CpCpG
C>G	CpCpT	CpGpT	T>C	CpTpT	CpCpT
C>G	GpCpA	GpGpA	T>C	GpTpA	GpCpA
C>G	GpCpC	GpGpC	T>C	GpTpC	GpCpC
C>G	GpCpG	GpGpG	T>C	GpTpG	GpCpG
C>G	GpCpT	GpGpT	T>C	GpTpT	GpCpT
C>G	TpCpA	TpGpA	T>C	TpTpA	TpCpA
C>G	TpCpC	TpGpC	T>C	TpTpC	TpCpC
C>G	TpCpG	TpGpG	T>C	TpTpG	TpCpG
C>G	TpCpT	TpGpT	T>C	TpTpT	TpCpT
C>T	ApCpA	ApTpA	T>G	ApTpA	ApGpA
C>T	ApCpC	ApTpC	T>G	ApTpC	ApGpC
C>T	ApCpG	ApTpG	T>G	ApTpG	ApGpG
C>T	ApCpT	ApTpT	T>G	ApTpT	ApGpT
C>T	CpCpA	CpTpA	T>G	CpTpA	CpGpA
C>T	CpCpC	CpTpC	T>G	CpTpC	CpGpC
C>T	CpCpG	CpTpG	T>G	CpTpG	CpGpG
C>T	CpCpT	CpTpT	T>G	CpTpT	CpGpT
C>T	GpCpA	GpTpA	T>G	GpTpA	GpGpA
C>T	GpCpC	GpTpC	T>G	GpTpC	GpGpC
C>T	GpCpG	GpTpG	T>G	GpTpG	GpGpG
C>T	GpCpT	GpTpT	T>G	GpTpT	GpGpT
C>T	TpCpA	TpTpA	T>G	TpTpA	TpGpA
C>T	TpCpC	TpTpC	T>G	TpTpC	TpGpC
C>T	TpCpG	TpTpG	T>G	TpTpG	TpGpG
C>T	TpCpT	TpTpT	T>G	TpTpT	TpGpT

Mutational alphabet \mathbb{E}_{99}

The \mathbb{E}_{99} alphabet extends \mathbb{E}_{96} by including three additional mutation types, *viz.*, (i) double nucleotide substitutions, (ii) small insertions or deletions at short tandem repeats, and (iii) small insertions or deletions overlapping with microhomologies at breakpoints.

Mutational alphabet Ξ_{192}

The Ξ_{192} alphabet elaborates Ξ_{96} by considering the transcriptional strand on which a substitution resides. In contrast to all other alphabets, Ξ_{192} is defined only in the regions of the genome where transcription occurs, which in these analyses has been limited to the genomic footprints of protein coding genes. For example, the **C>T** mutations at **TpCpA** are split into two categories: the **C>T** mutations at **TpCpA** occurring on the untranscribed strand of a gene and the **C>T** mutations at **TpCpA** occurring on the transcribed strand. Similarly, all 96 mutations types from Ξ_{96} are extended to form the Ξ_{192} alphabet.

Mutational alphabet Ξ_{1536}

The Ξ_{1536} further extends Ξ_{96} by including two bases 5' and 3' to the mutated base resulting in 1,536 possible mutated pentanucleotides - (6 types of substitutions) * (16 types of the two immediate 5' bases) * (16 types of the two immediate 3' bases). For example, using the Ξ_{1536} alphabet, one of the 256 subclasses of a **C>T** mutation is ...**ApTpCpGpC**... > ...**ApTpTpGpC**... For brevity, the complete list of mutation types included in Ξ_{1536} is not provided here.

APPENDIX II: List of analysed samples

This appendix contains a summary list of all samples analysed throughout the course of this thesis. Summarized information is provided for all 7,042 separated by sequencing types (exome sequencing versus whole-genome sequencing), cancer types, and respective data sources. It should be noted that the pilocytic astrocytomas dataset contains a small number of other paediatric low-grade gliomas and paediatric low-grade glioneuronal tumours. Information for each individual sample including its mutational catalogues and somatic mutations (both before and after filtering) could be found at <ftp://ftp.sanger.ac.uk/pub/cancer/AlexandrovEtAl>.

Exome sample types and data sources	Total
ALL	140
doi:10.1038/nature10725	15
doi:10.1038/ng.2508	29
doi:10.1038/ng.2532	42
New unpublished samples	54
AML	147
TCGA data portal	147
Bladder	136
TCGA data portal	136
Breast	844
doi:10.1038/nature10933	63
doi:10.1038/nature11017	9
New unpublished samples	5
TCGA data portal	767
Cervix	38
TCGA data portal	38
CLL	103
doi:10.1038/ng.1032	80
ICGC data portal	23
Colorectum	559
doi:10.1038/nature11282	70
TCGA data portal	489
Oesophageal	146
doi:10.1038/ng.2591	146
Glioblastoma	98
ICGC data portal	50
TCGA data portal	48
Glioma Low Grade	217
TCGA data portal	217

Whole-genome sample types and data sources	Total
ALL	1
New unpublished samples	1
AML	7
doi:10.1038/nature10738	7
Breast	119
doi:10.1016/j.cell.2012.04.024	21
New unpublished samples	98
CLL	28
doi:10.1038/nature10113	4
New unpublished samples	24
Liver	88
ICGC data portal	66
New unpublished samples	22
Lung Adenocarcinoma	24
doi:10.1016/j.cell.2012.08.029	24
Lymphoma B-cell	24
doi:10.1038/ng.2468	1
New unpublished samples	23
Medulloblastoma	100
New unpublished samples	100
Pancreas	15
New unpublished samples	15
Pilocytic Astrocytoma	101
doi:10.1038/ng.2611	38
New unpublished samples	63
Grand Total	507

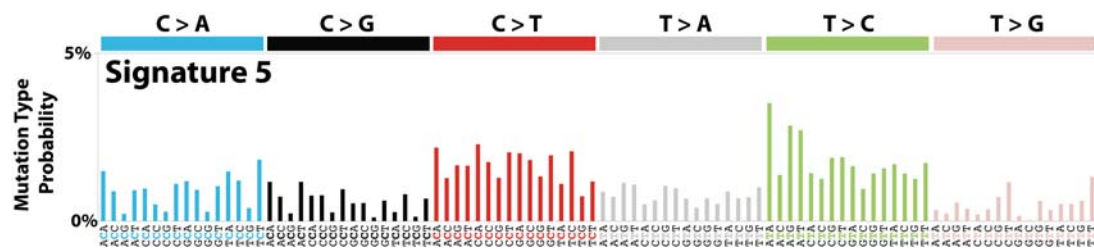
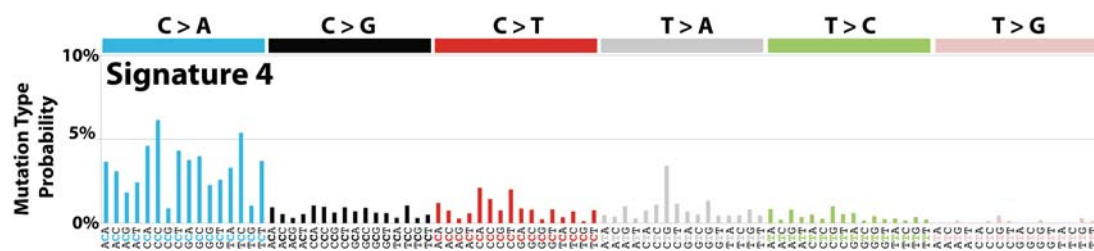
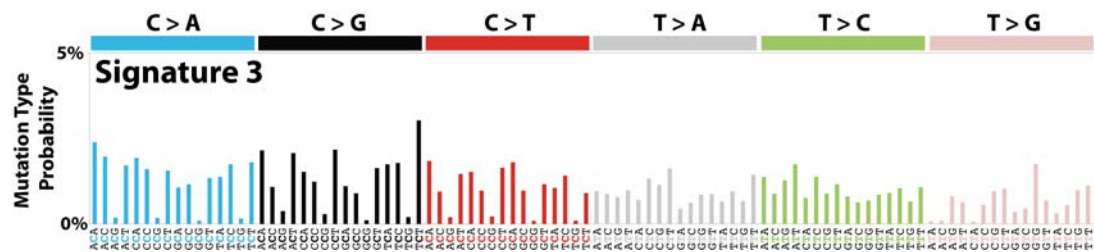
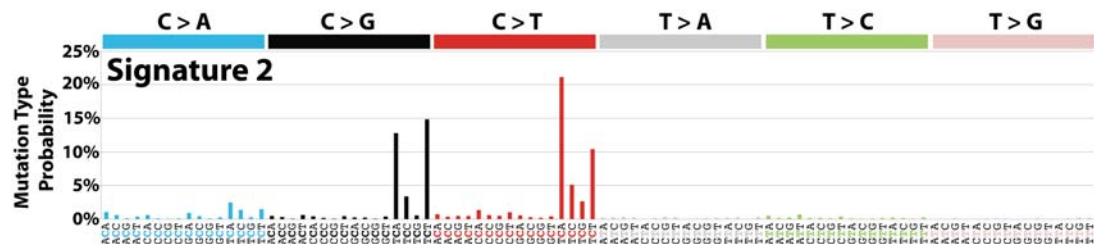
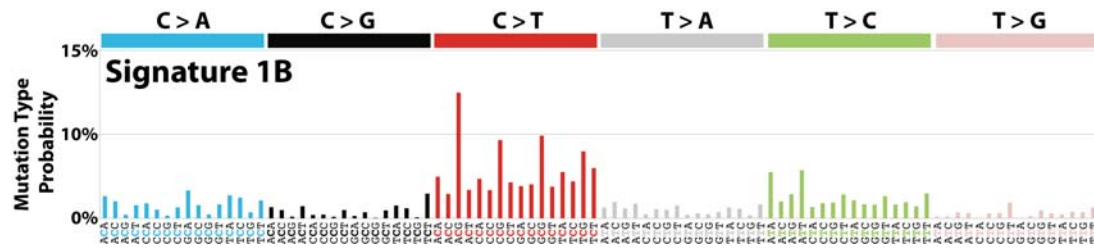
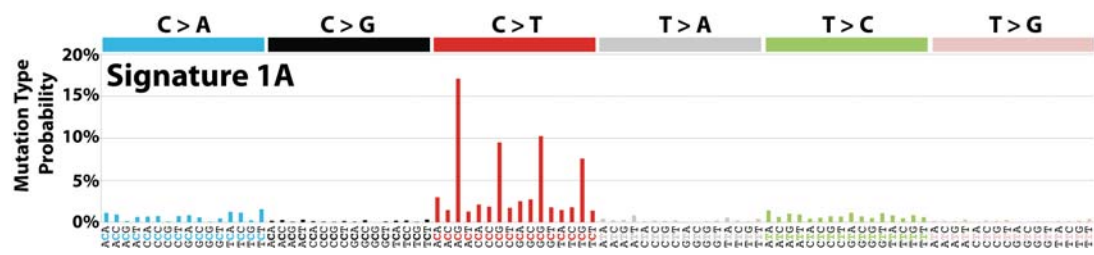
Head and Neck	380
doi:10.1126/science.1206923	12
doi:10.1126/science.1208130	68
TCGA data portal	300
Kidney Chromophobe	65
TCGA data portal	65
Kidney Clear Cell	325
doi:10.1038/ng.1014	10
doi:10.1038/ng.2323	7
TCGA data portal	308
Kidney Papillary	100
TCGA data portal	100
Lung Adenocarcinoma	636
doi:10.1016/j.cell.2012.08.029	150
doi:10.1038/nature07423	30
doi:10.1101/gr.145144.112	75
TCGA data portal	381
Lung Small Cell	70
doi:10.1038/ng.2396	29
doi:10.1038/ng.2405	40
ICGC data portal	1
Lung Squamous	176
TCGA data portal	176
Lymphoma B-cell	24
doi:10.1038/nature10351	16
doi:10.1038/ng.2468	8
Melanoma	396
doi:10.1016/j.cell.2012.06.024	92
doi:10.1038/nature11071	28
doi:10.1038/ng.1041	8
ICGC data portal	1
New unpublished samples	17
TCGA data portal	250
Myeloma	69
New unpublished samples	69
Neuroblastoma	210
doi:10.1038/ng.2493	13
doi:10.1038/ng.2529	197
Ovary	471
doi:10.1126/science.1196333	8
TCGA data portal	463
Pancreas	98
doi:10.1073/pnas.1118046108	22
doi:10.1126/science.120060	10
ICGC data portal	37

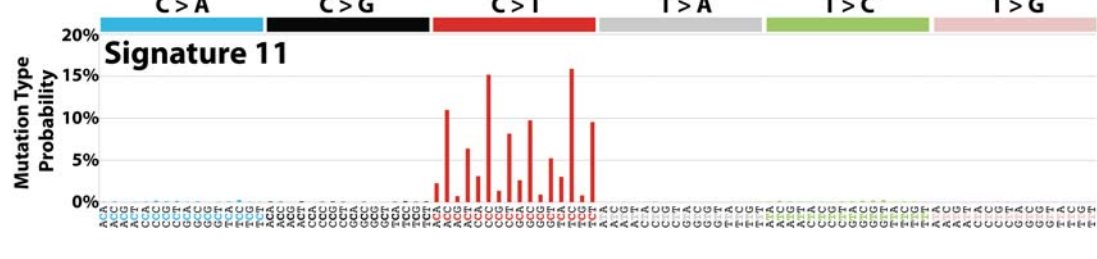
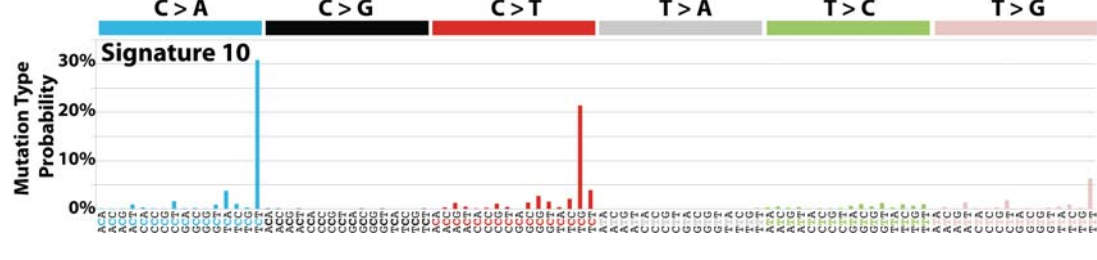
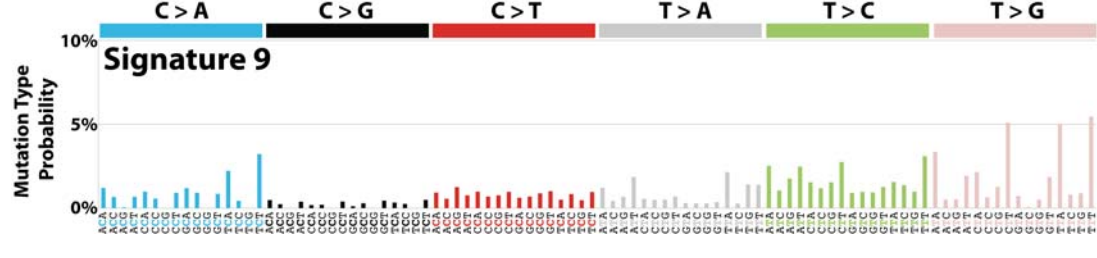
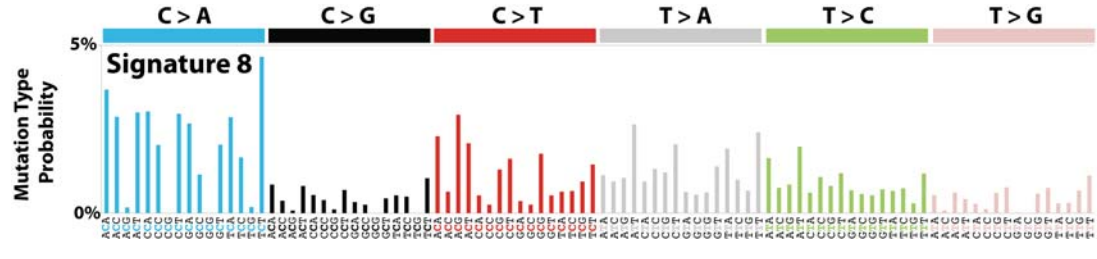
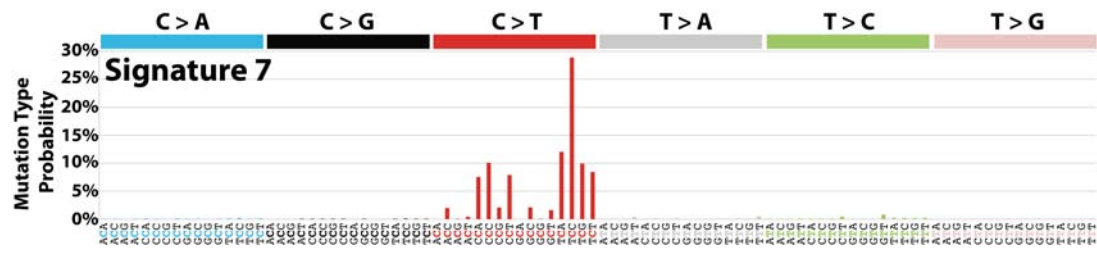
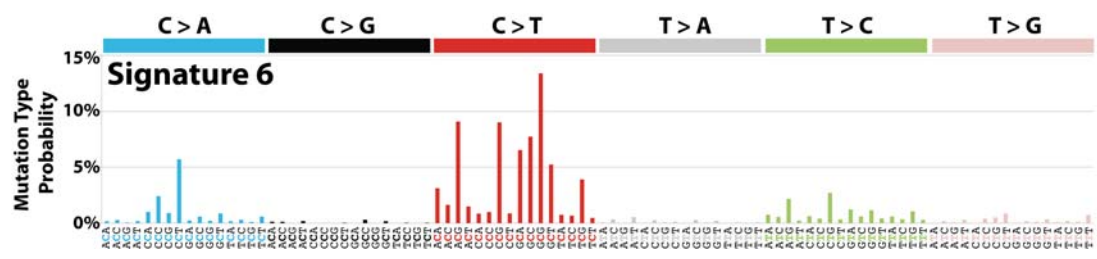
TCGA data portal	29
Prostate	330
doi:10.1038/nature09744	7
doi:10.1038/nature11125	61
doi:10.1038/ng.2279	112
TCGA data portal	150
Stomach	212
doi:10.1038/ng.2246	14
doi:10.1038/ng.982	22
ICGC data portal	10
TCGA data portal	166
Thyroid	304
TCGA data portal	304
Uterus	241
TCGA data portal	241
Grand Total	6,535

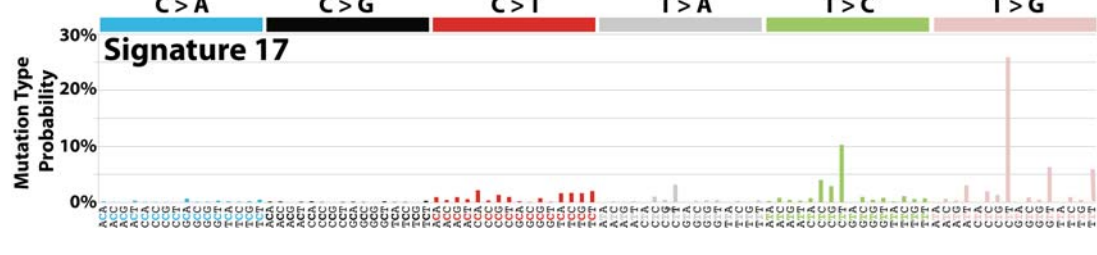
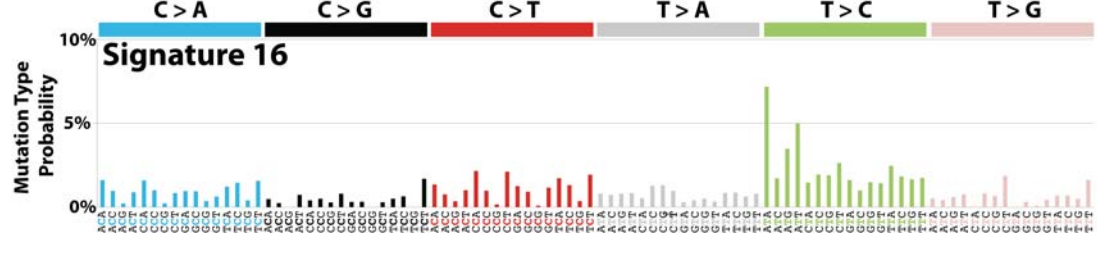
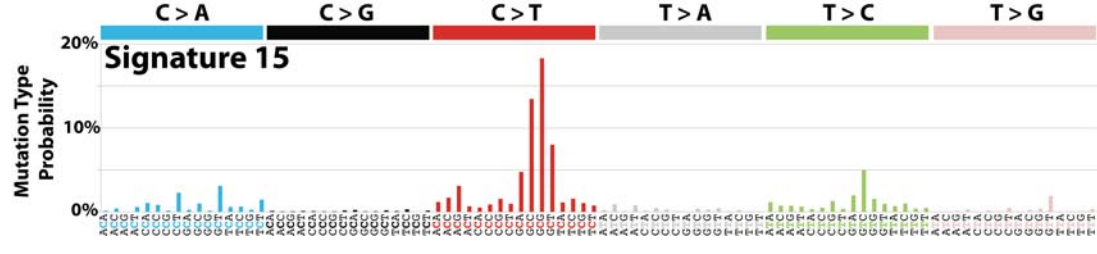
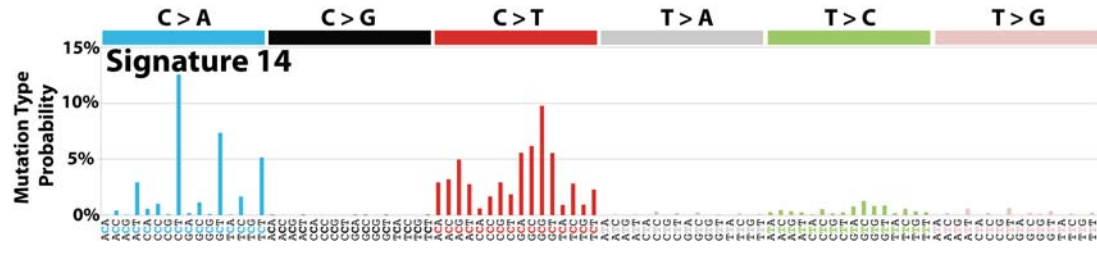
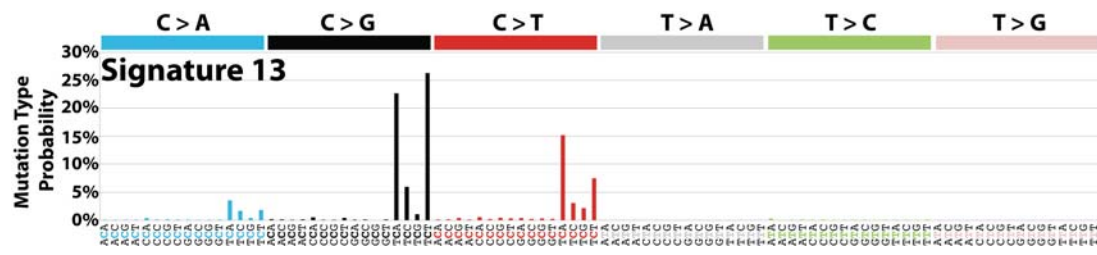
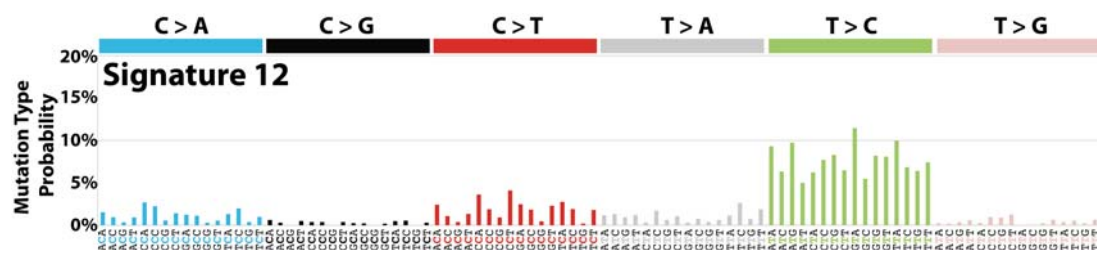
APPENDIX III: Mutational signatures in human cancer

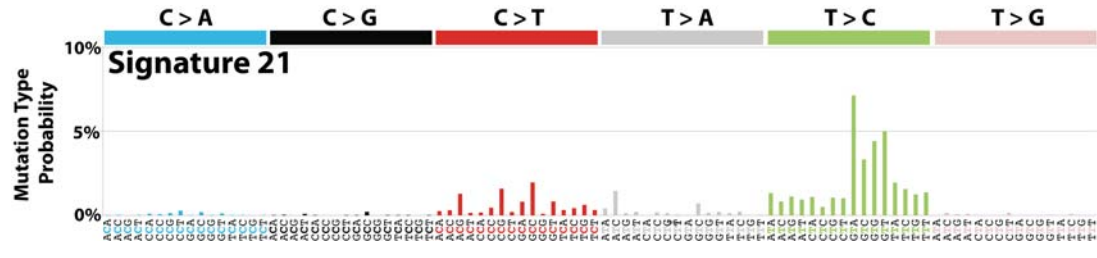
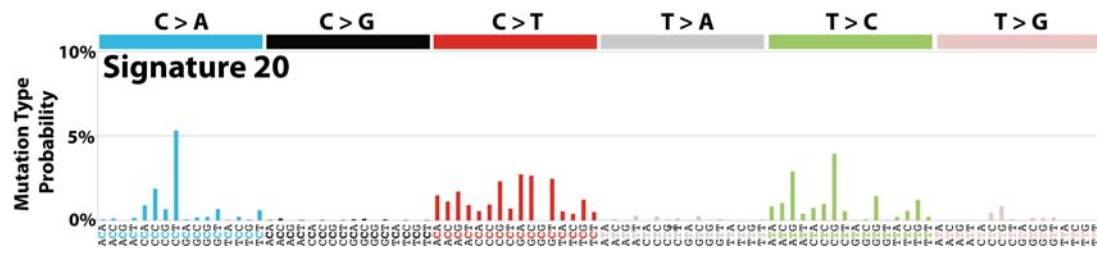
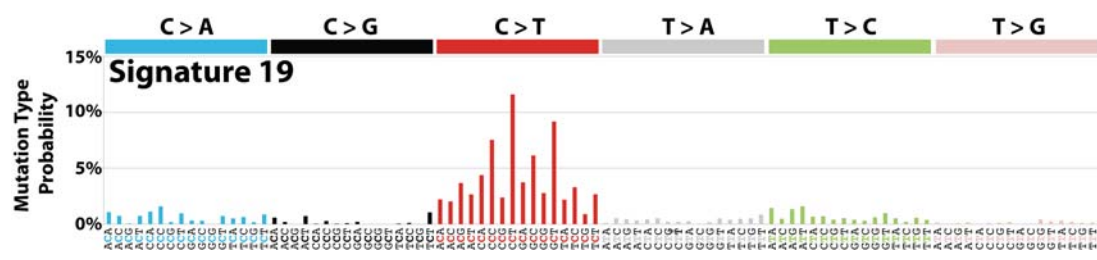
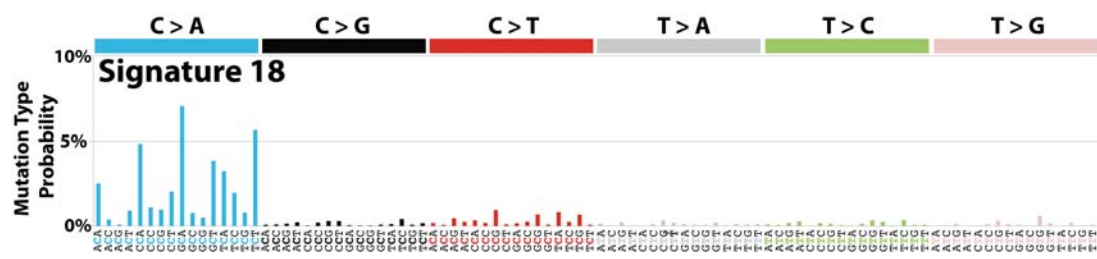
This appendix contains high-resolution figures for the twenty-seven consensus mutational signatures that were deciphered by applying the developed computational approach across the spectrum of human cancer (chapter 4). Each mutational signature is shown using the same plot. Signatures are displayed based on the trinucleotide frequency of the human genome. The probability bars for each of the six types of substitutions as well as the mutated bases are displayed in different colours. The mutation types are displayed on the horizontal axes, while vertical axes depict the percentages of mutations attributed to specific mutation types. The plots are ordered by signature validation types: validated mutational signatures (Signatures 1A, 1B, 2 through 21), mutational signatures that failed validation (Signatures R1, R2, and R3), and mutational signatures for which it was not possible to perform validation (Signatures U1 and U2).

Validated mutational signatures



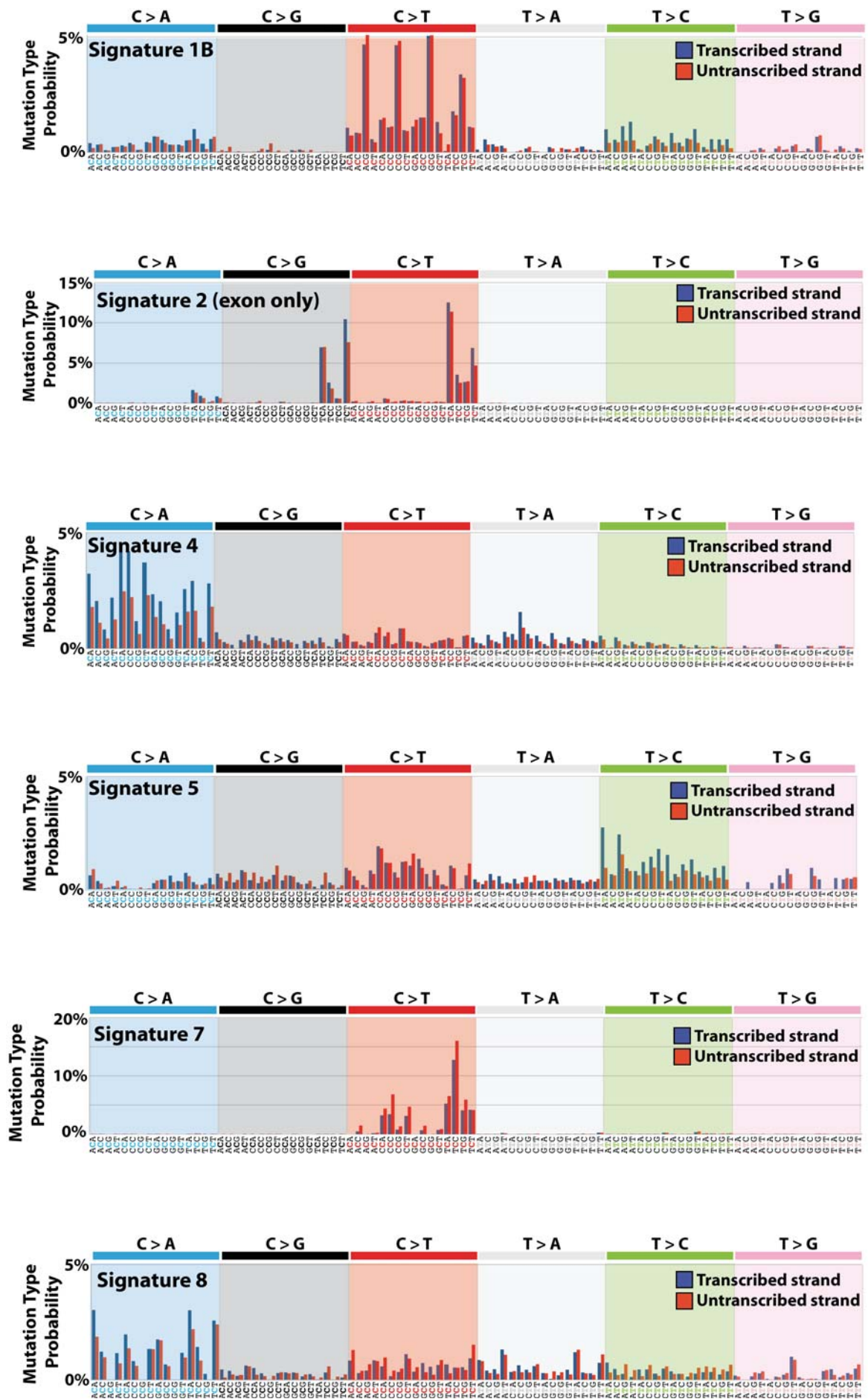






APPENDIX IV: Mutational signatures with transcriptional strand-bias

This appendix contains high-resolution figures for the nine consensus mutational signatures that exhibit transcriptional strand-bias. Each mutational signature is shown using the same figure format based on a 192 substitution classification incorporating the substitution type, the sequence context immediately 5' and 3' to the mutated base and whether the mutated base (in pyrimidine context) is on the transcribed or untranscribed strand. The panels for each of the six types of substitutions as well as the mutated bases are displayed in different colours. Mutations on the transcribed pyrimidine strand are displayed in blue while mutations on the untranscribed strand are displayed in red.

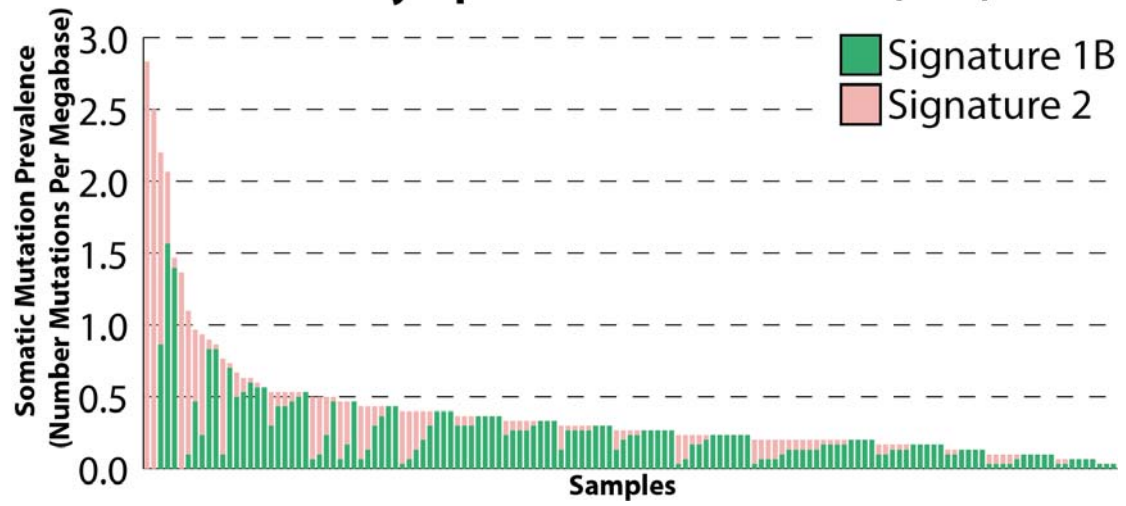


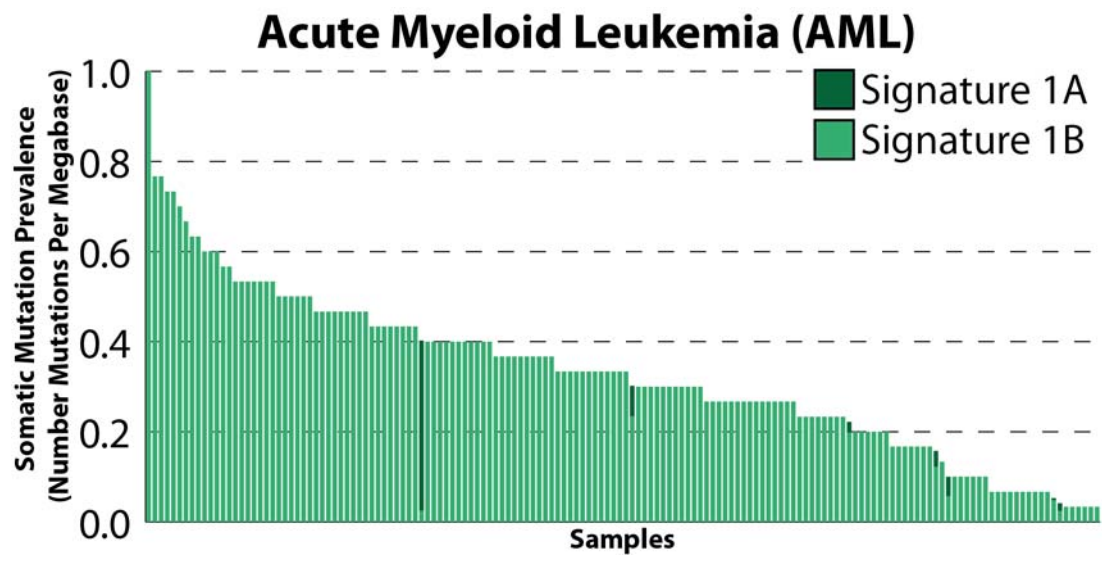
APPENDIX V: Contributions of mutational signatures in individual samples

This appendix contains a high-resolution figure for each of the 30 examined cancer types (chapter 4). Each figure depicts all of the samples in a single cancer type and shows the contributions of the consensus mutational signatures (found in that cancer type) for each sample. All figures use the same format: samples are displayed on the horizontal axis, sorted in descending order based on the numbers of somatic mutations per megabase found in each sample, and the somatic mutation prevalence is displayed on the vertical axis. Mutational signatures are displayed in distinct colours, consistent in all figures. For clarity, several panels are provided (and clearly labelled) when the number of samples is too high or the somatic prevalence differs significantly between samples. Figures are displayed on individual pages, labelled to clearly show the names of the cancer types, and they are ordered alphabetically based on the names of these cancer types. In general, all samples are displayed in each cancer type and the two exceptions are denoted with an asterisk in the appropriate figures and listed below:

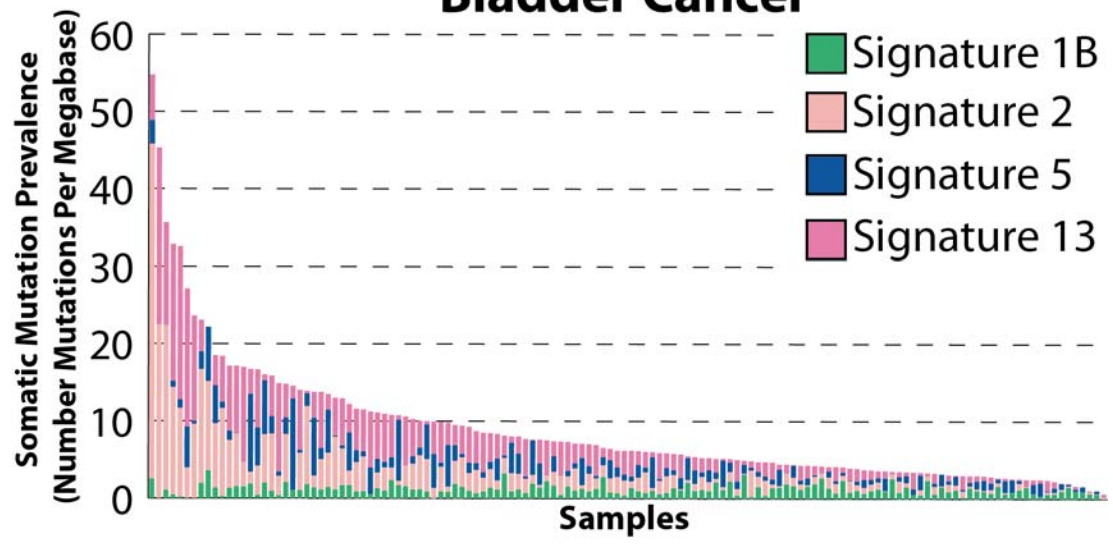
- For clarity, in glioma low grade, one hypermutator sample purely of Signature 14 (254 mutations per MB) is not displayed.
- In lung squamous, one hypermutator sample purely of Signature 7 (72 mutations per MB) is not displayed. Signature 7 is associated with exposure to ultraviolet light, an unlikely carcinogen for lung cancer. As such, this TCGA sample is most likely either a melanoma metastasis or a misannotated sample. Thus, the association between Signature 7 and lung squamous has not been discussed in chapter 4 and this association has not been displayed in Figure 4.9.

Acute Lymphoblastic Leukemia (ALL)

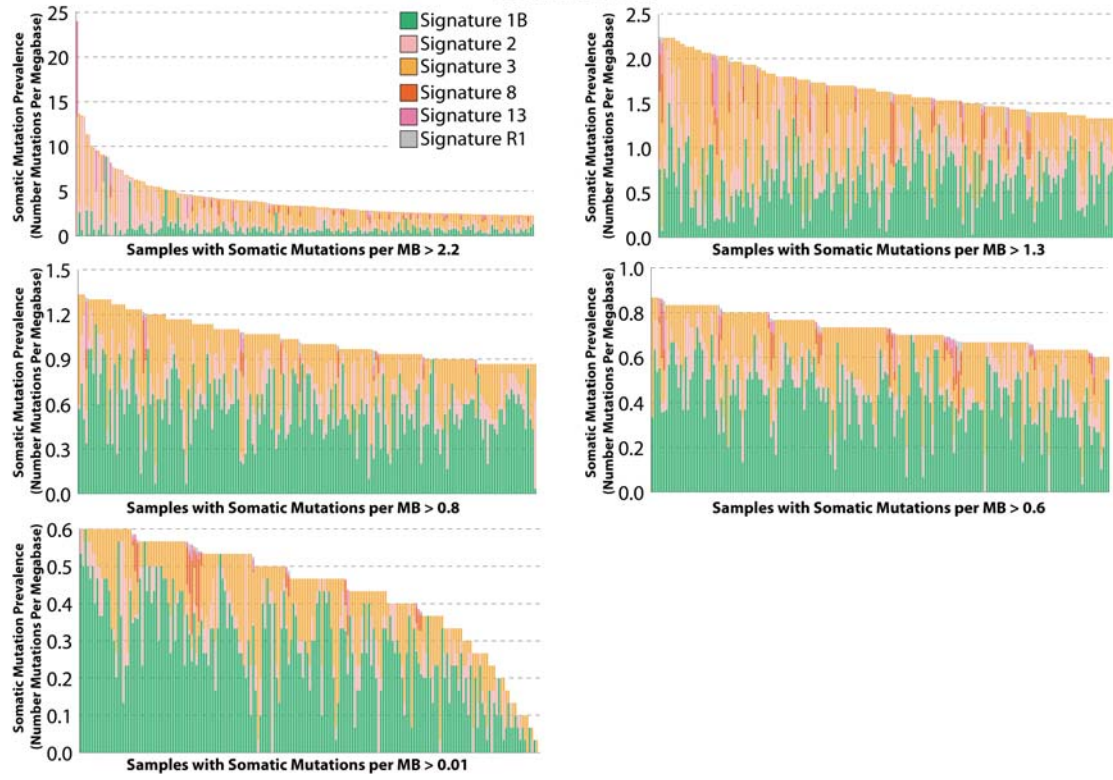




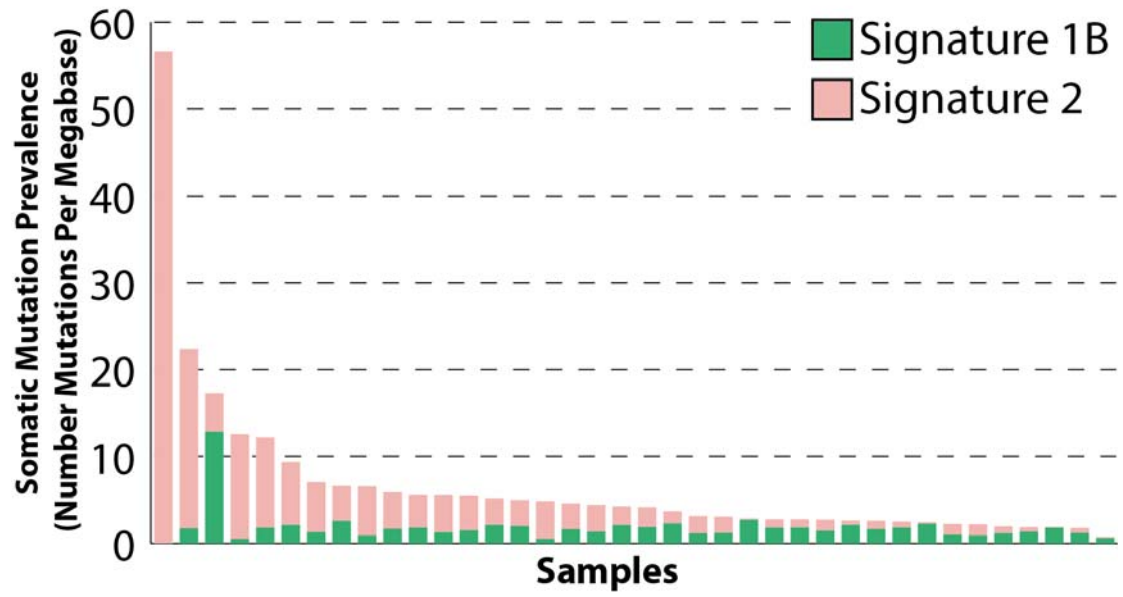
Bladder Cancer



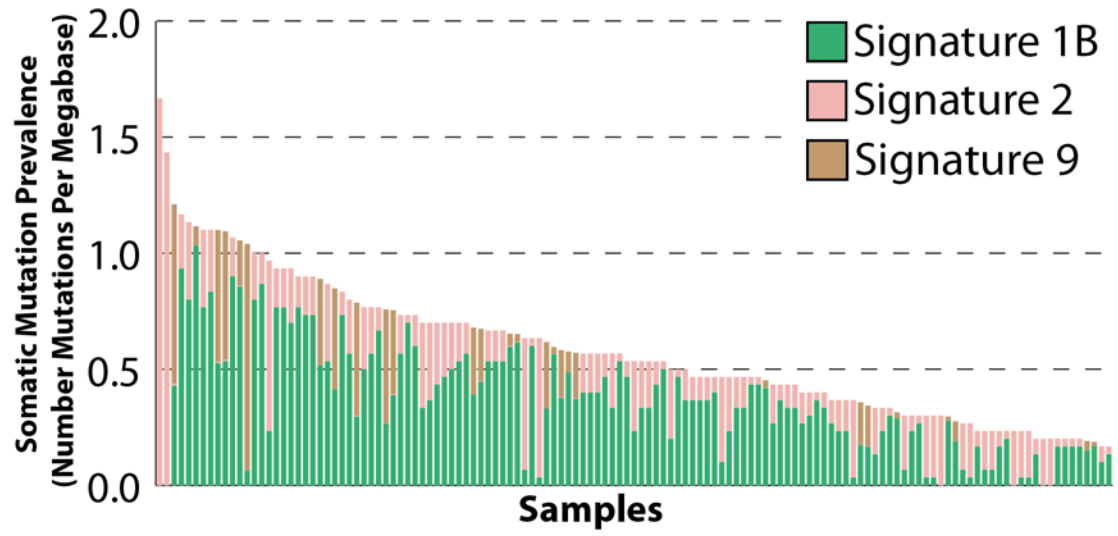
Breast Cancer



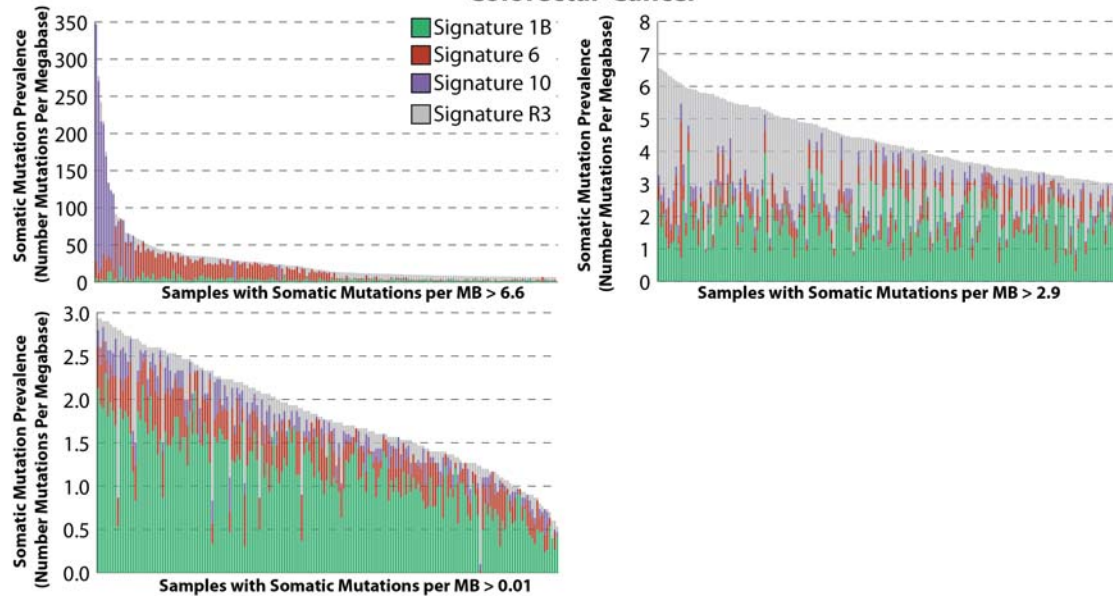
Cervical Cancer



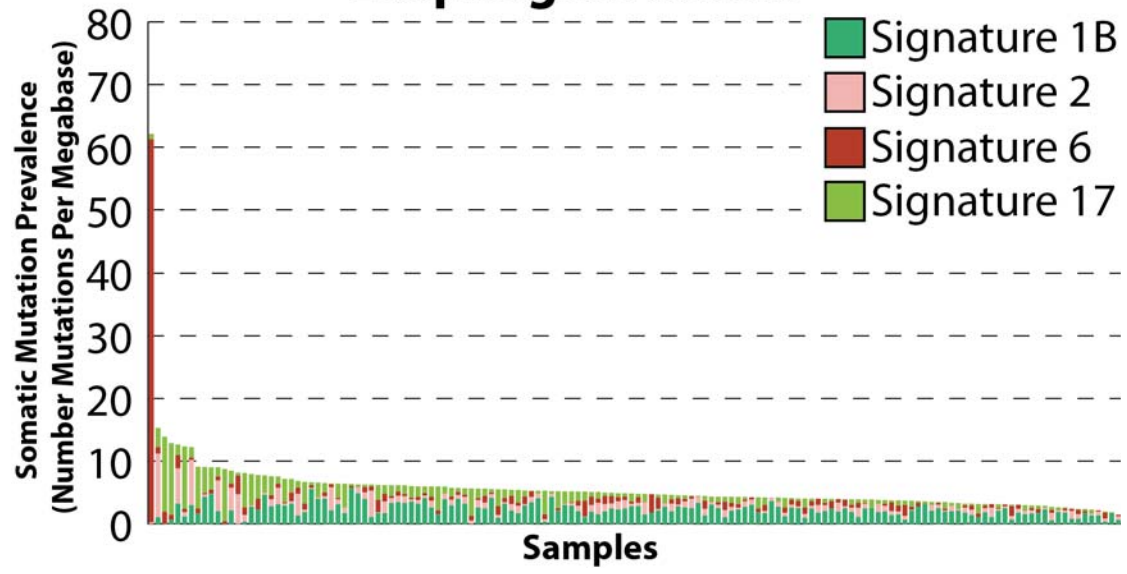
B-cell Chronic Lymphocytic Leukemia (CLL)



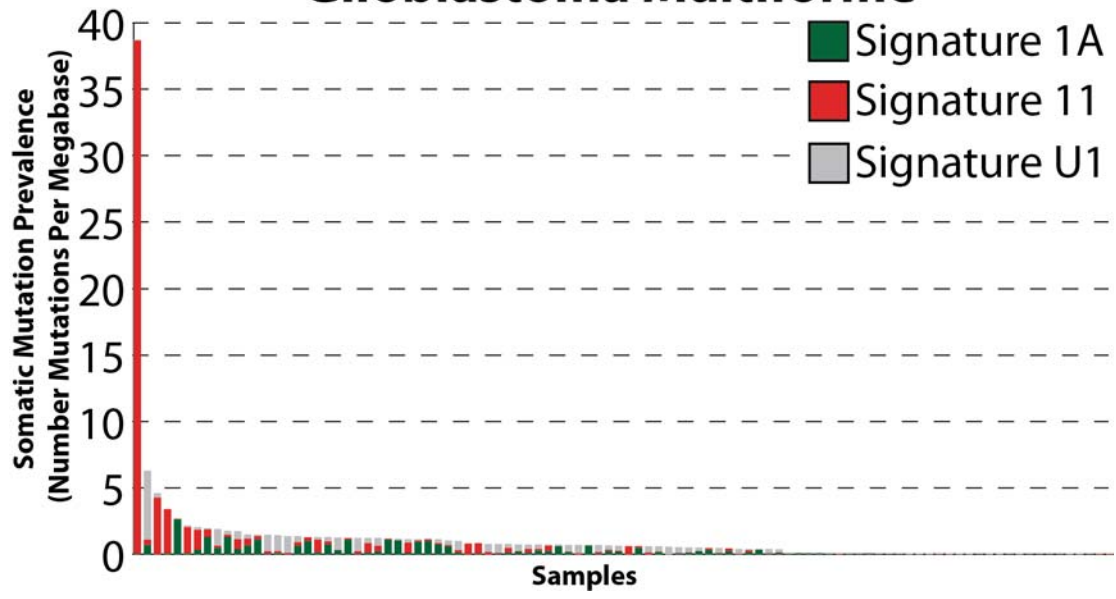
Colorectal Cancer



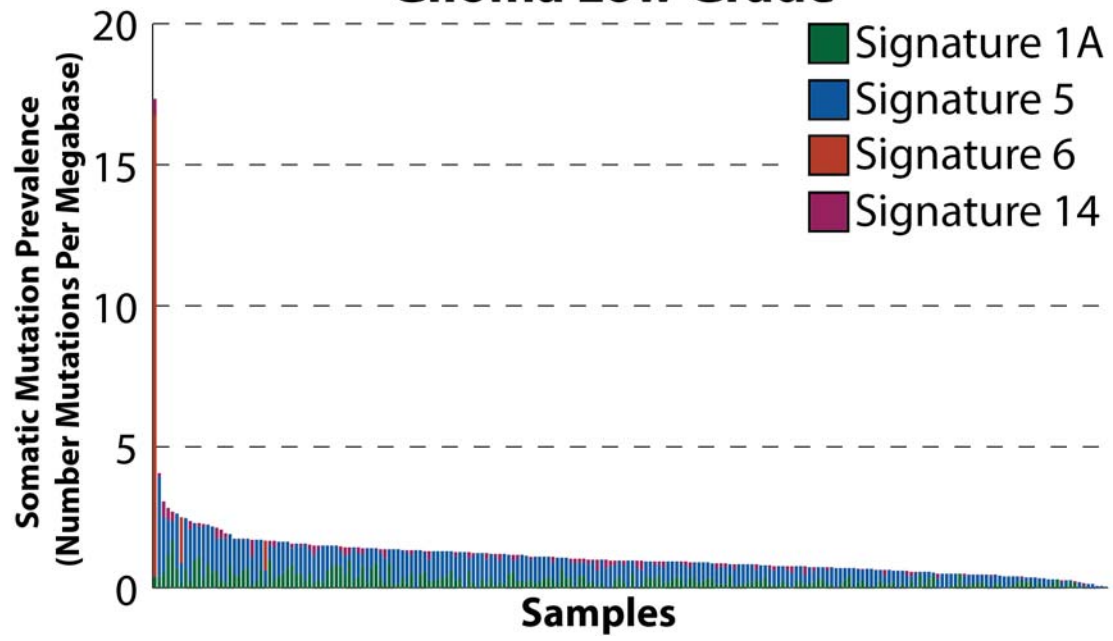
Esophageal cancer

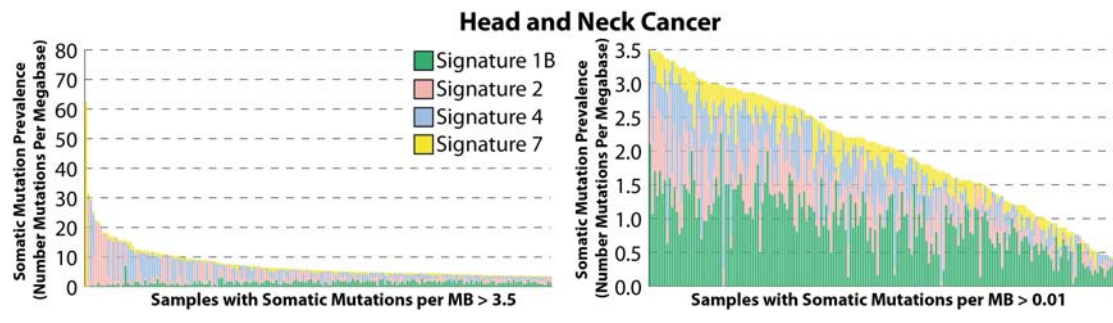


Glioblastoma Multiforme

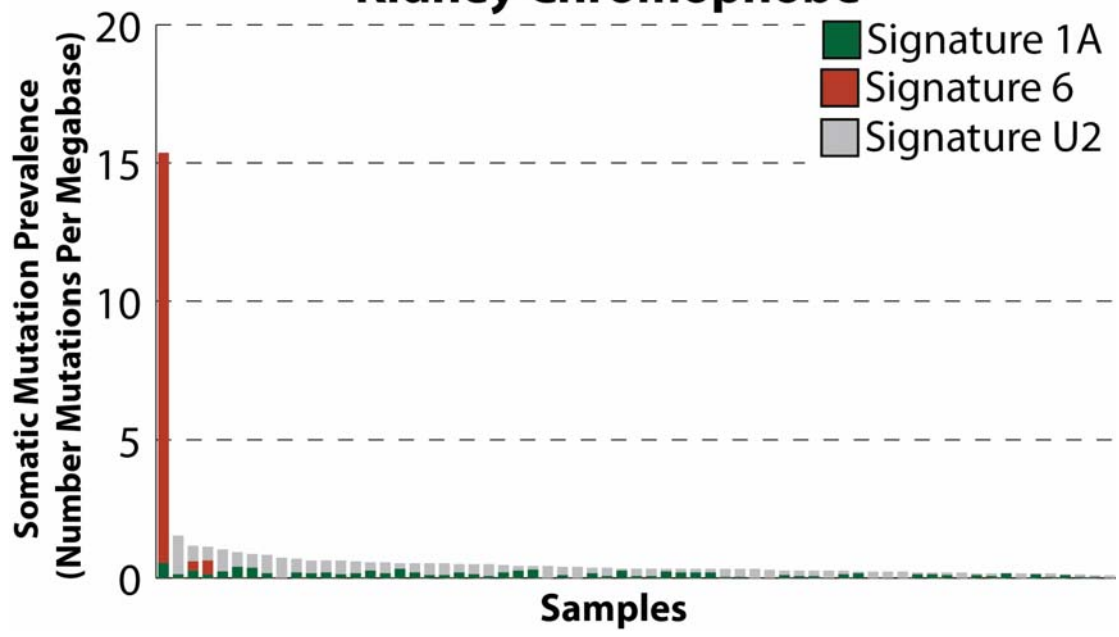


Glioma Low Grade*

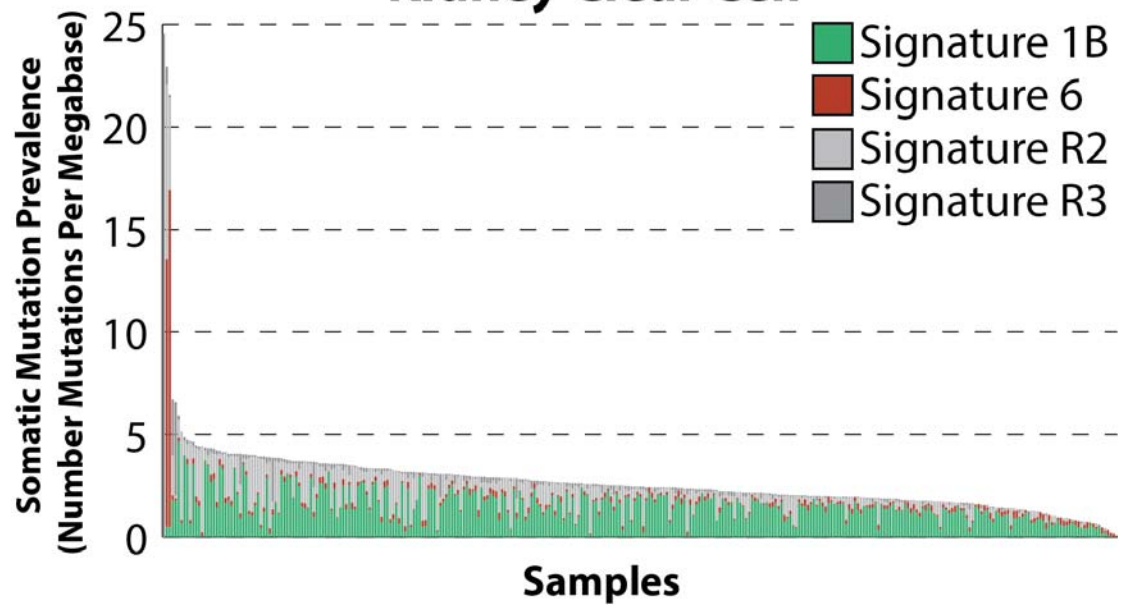




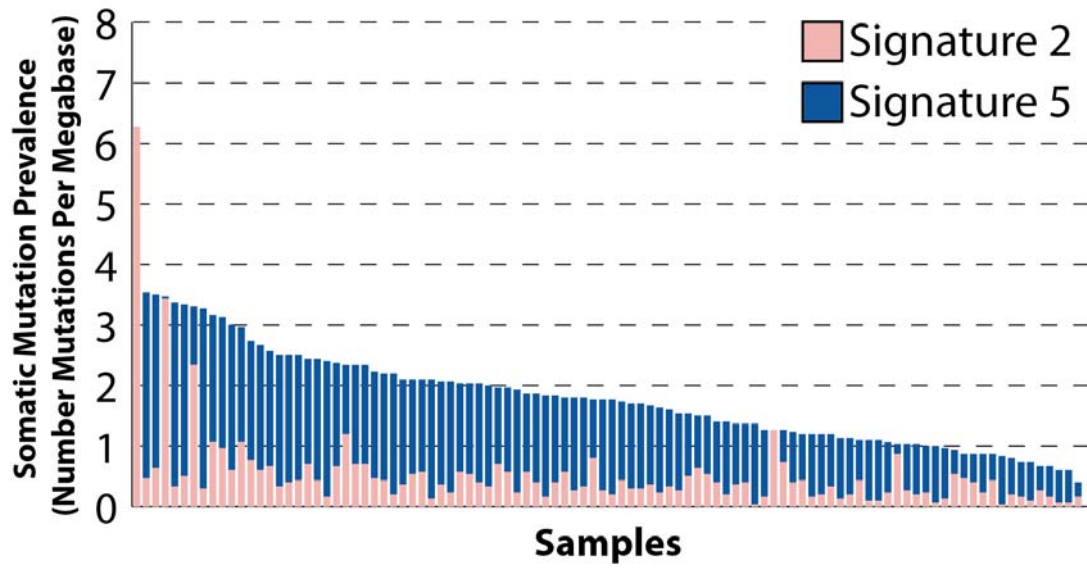
Kidney Chromophobe

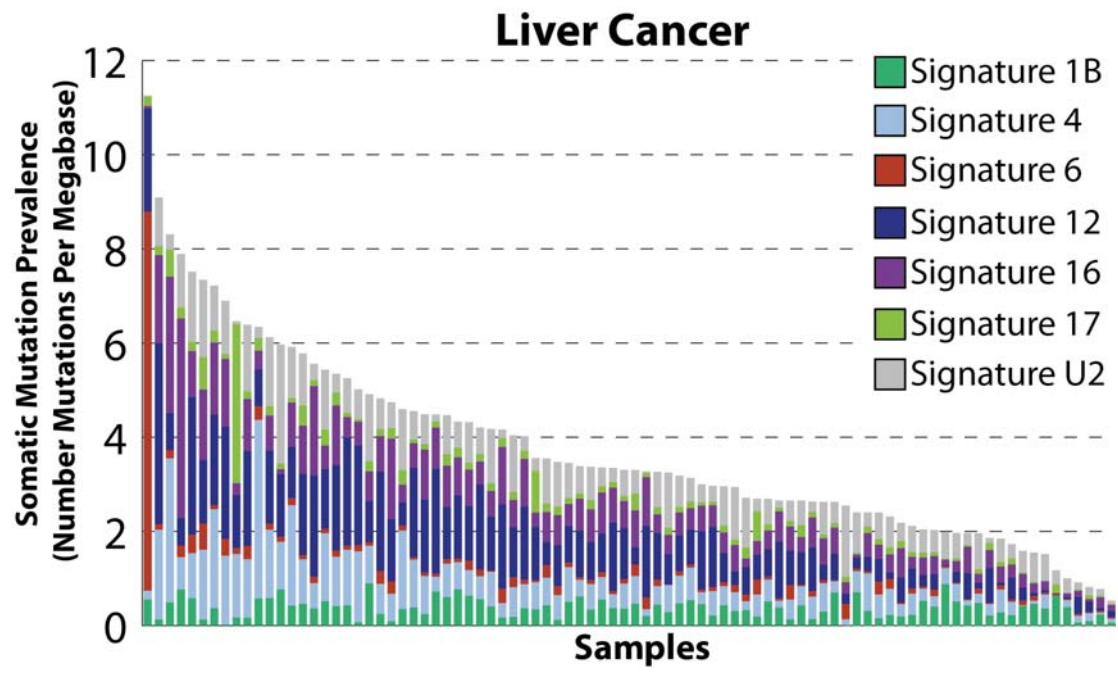


Kidney Clear Cell

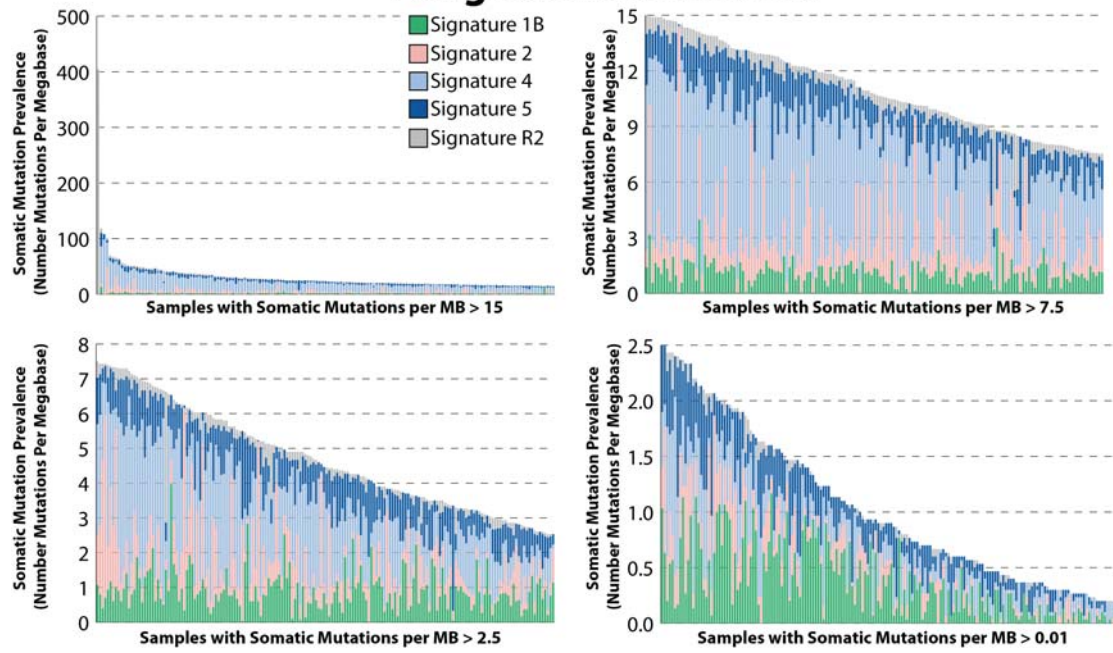


Kidney Papillary

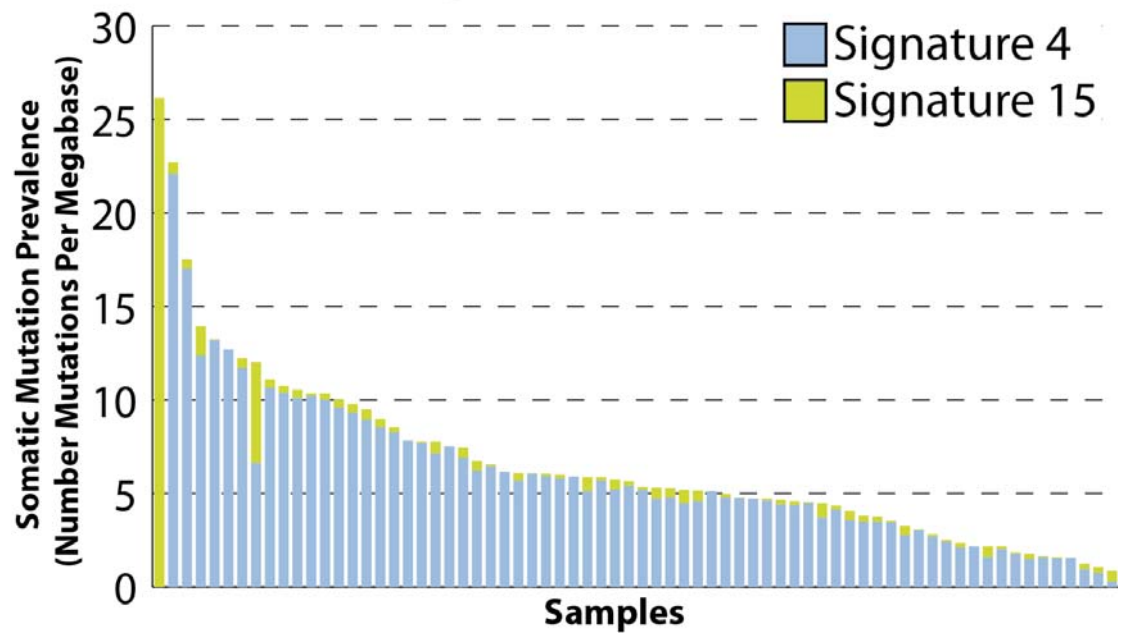




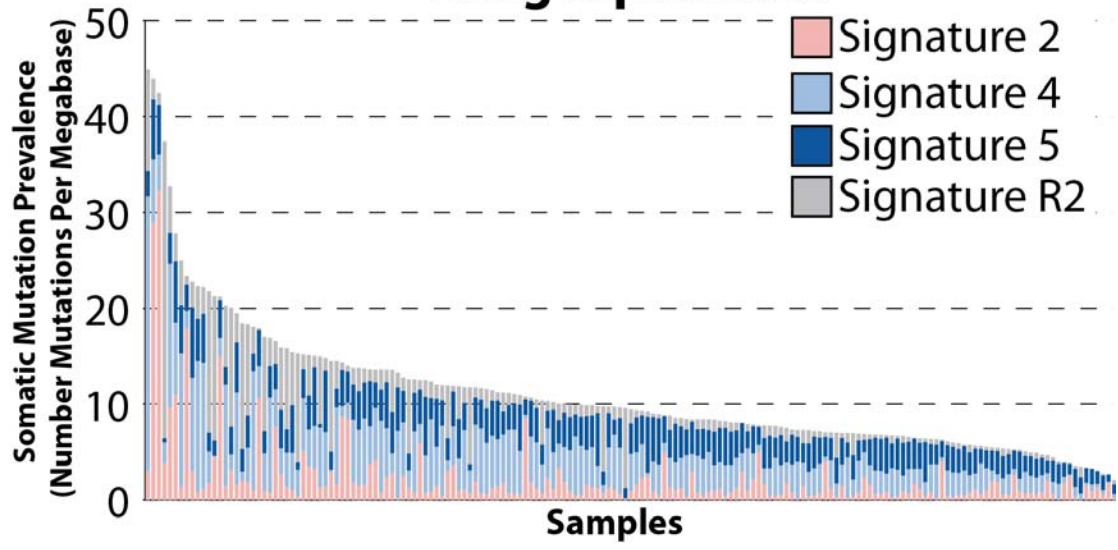
Lung Adenocarcinoma



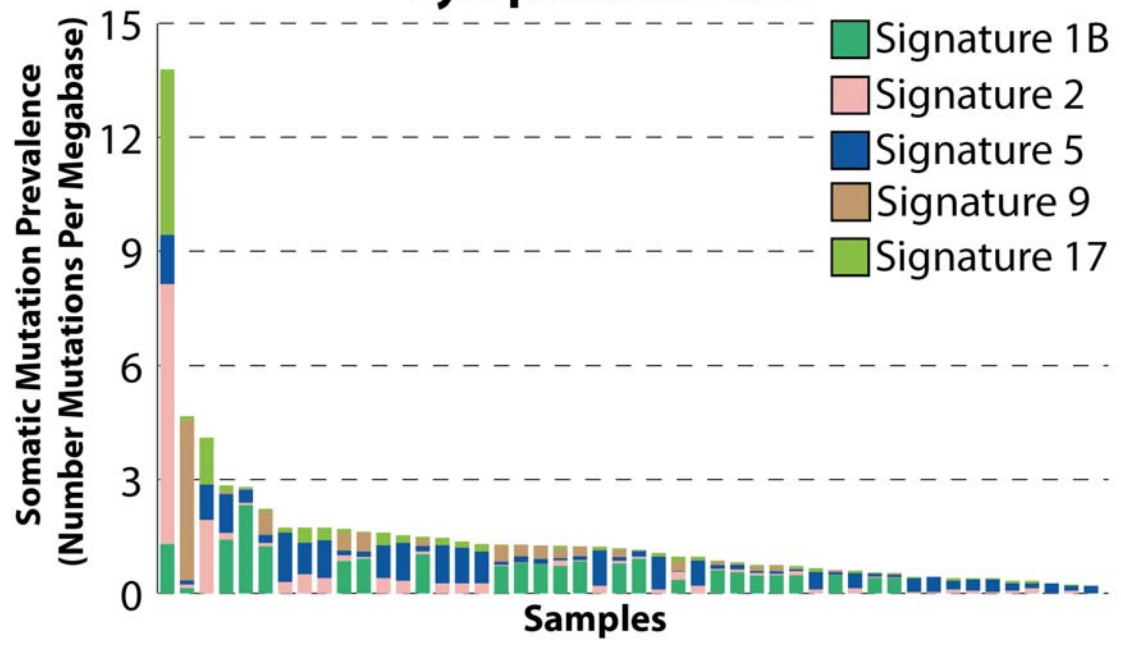
Lung Cancer Small Cell



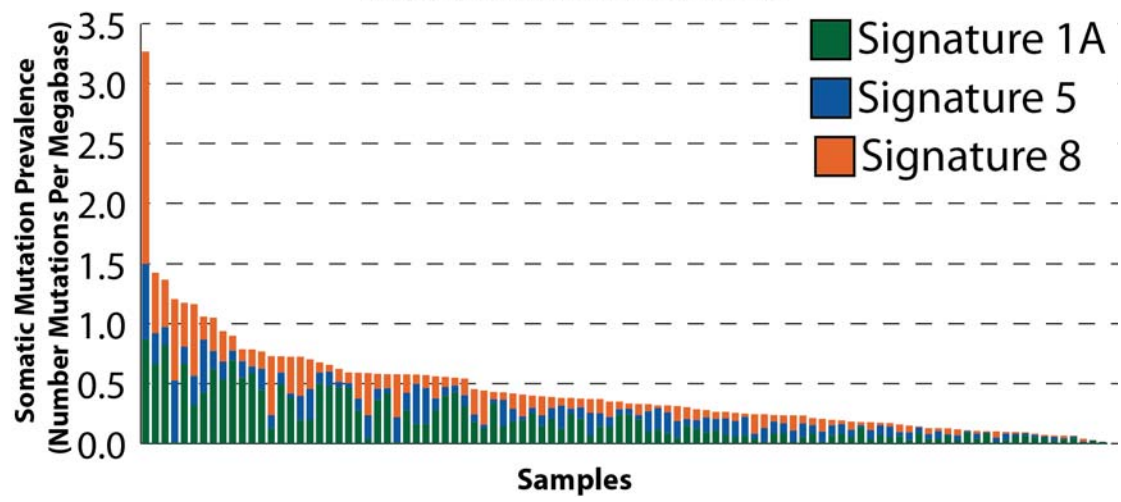
Lung Squamous*

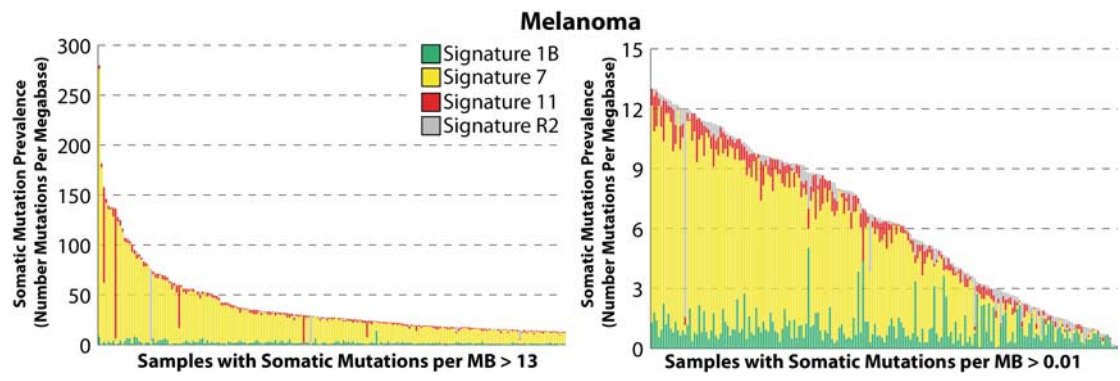


Lymphoma B-cell

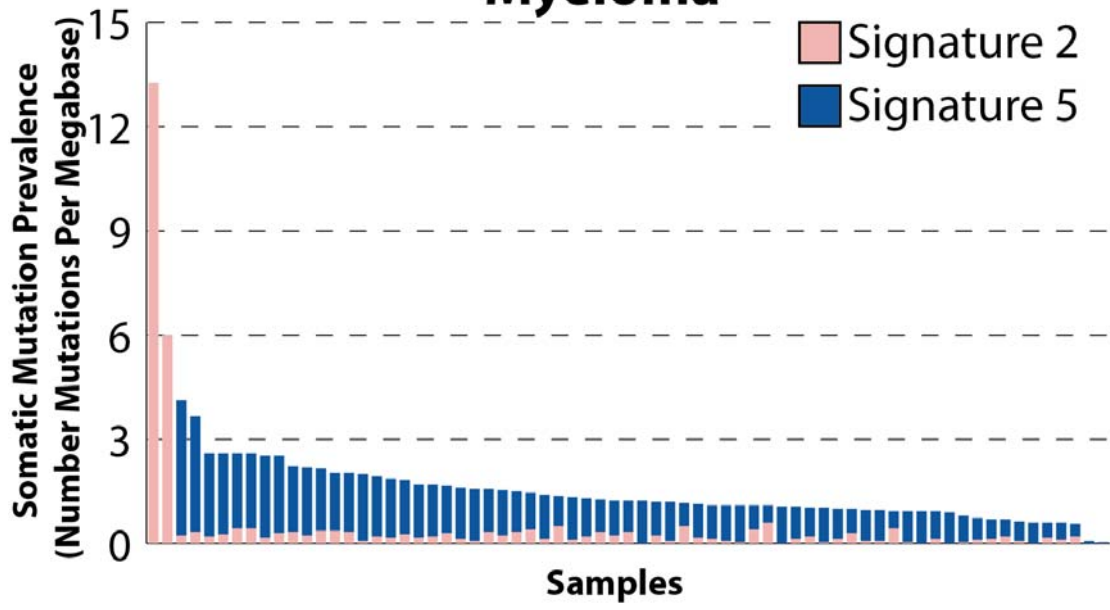


Medulloblastoma

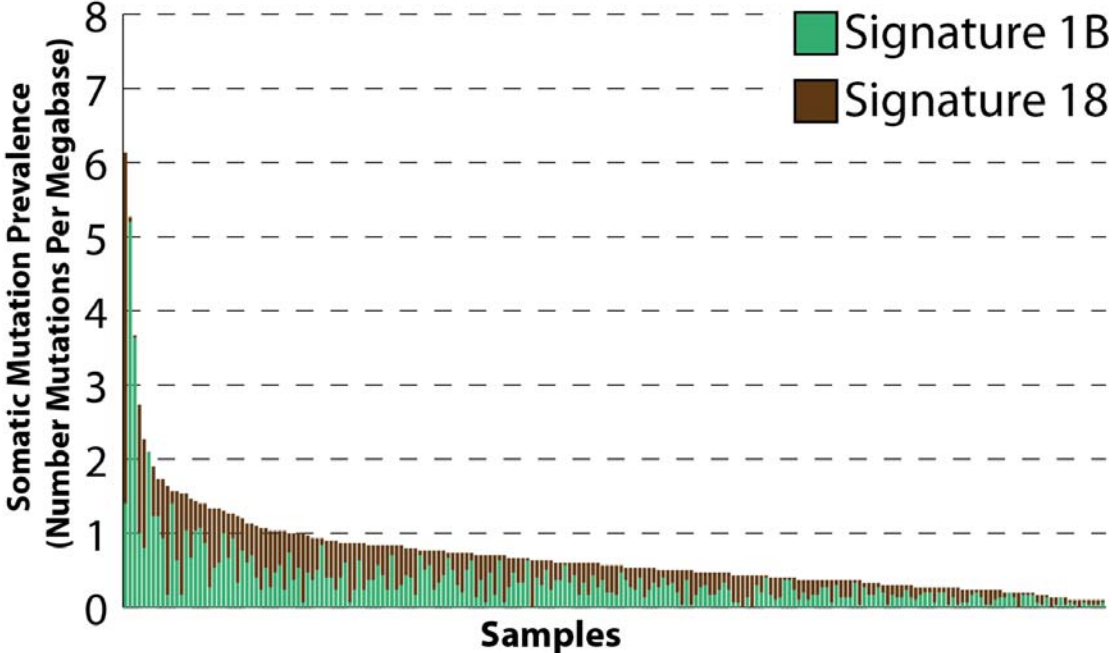




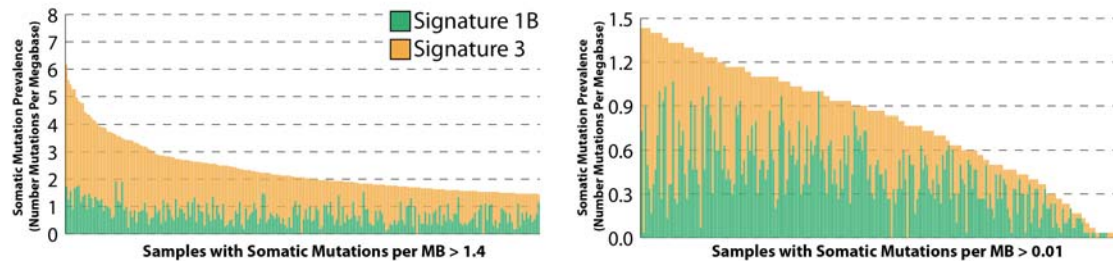
Myeloma



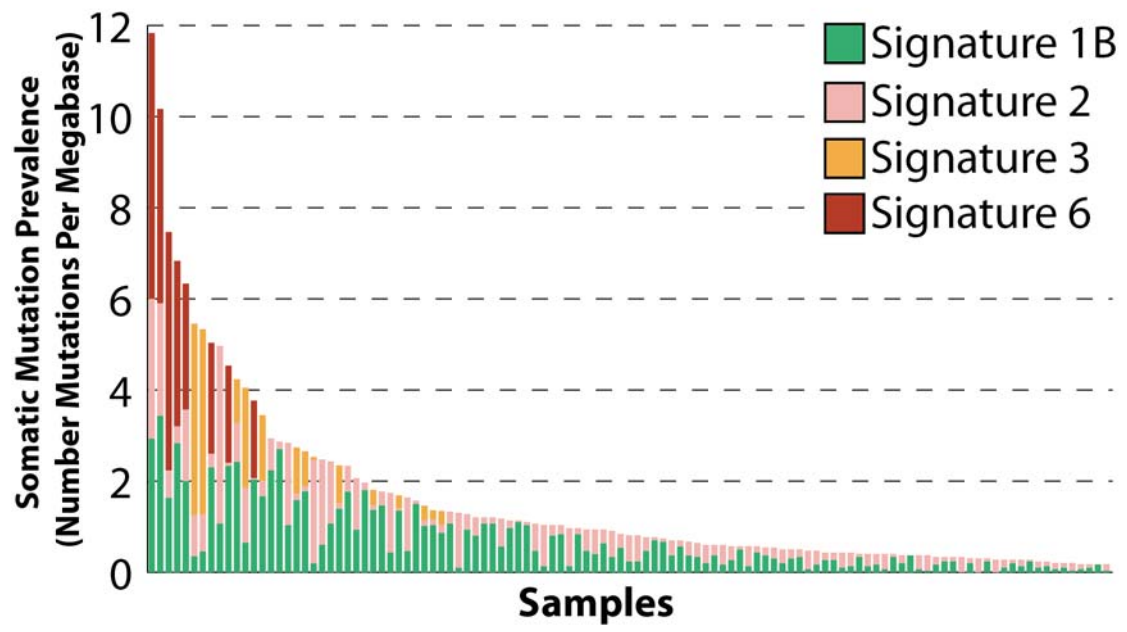
Neuroblastoma



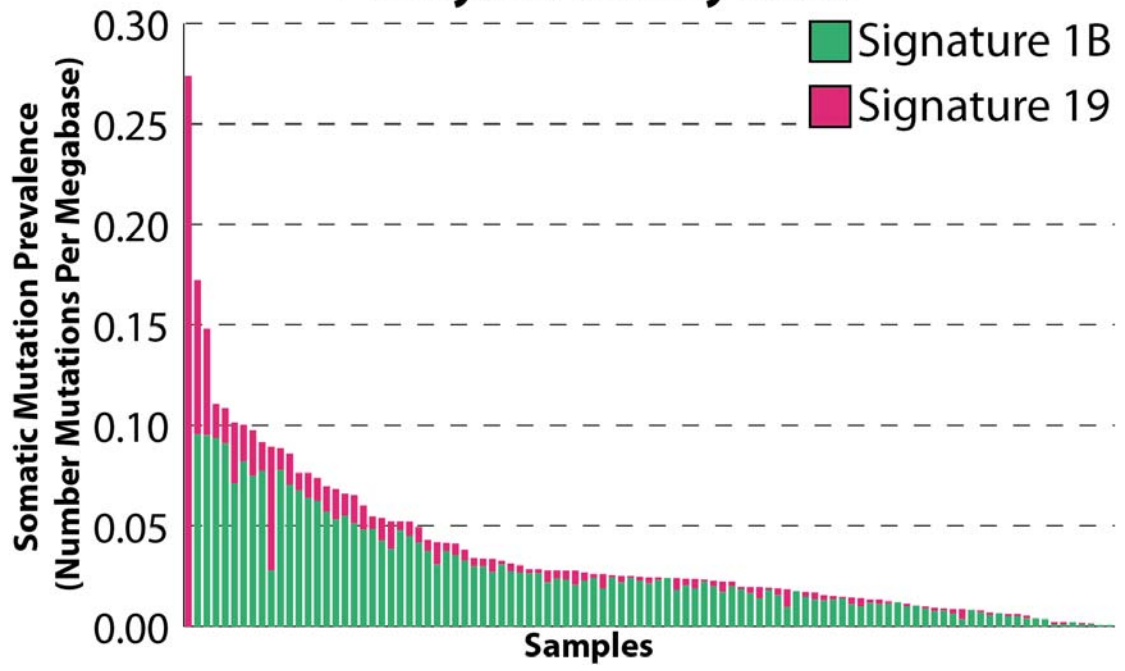
Ovarian Cancer



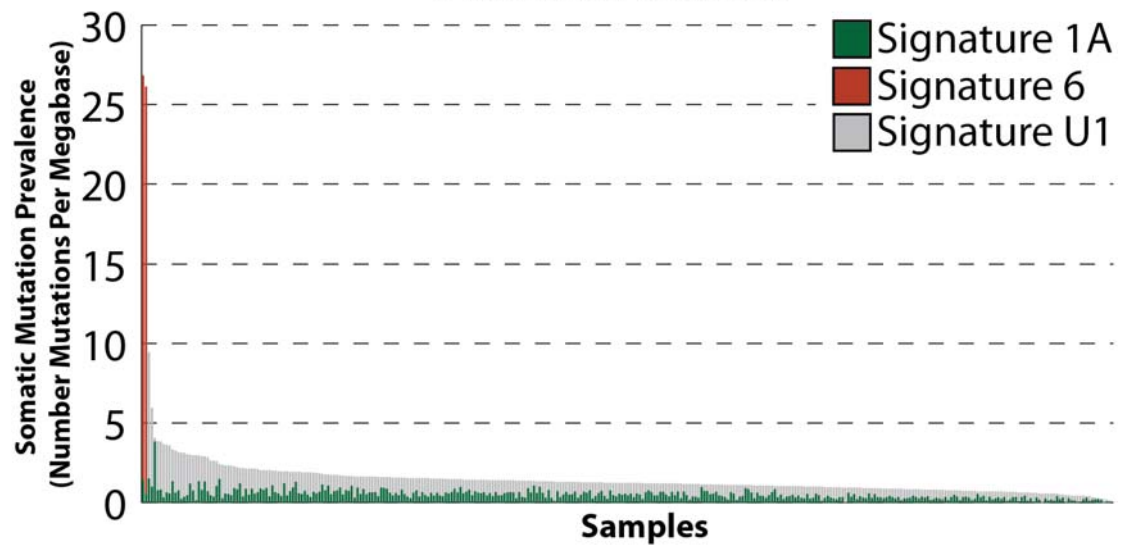
Pancreatic Cancer



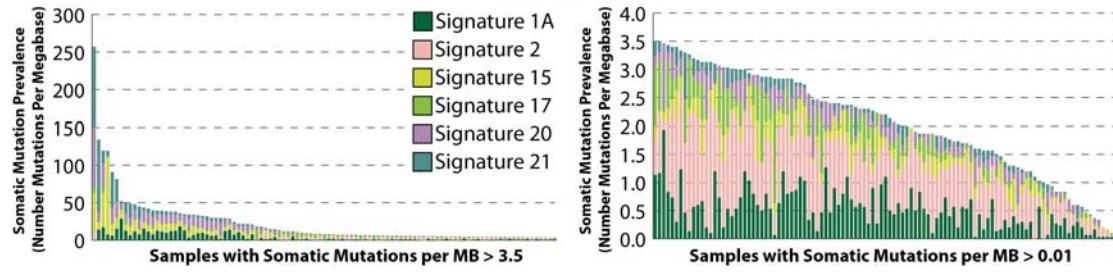
Pilocytic Astrocytoma



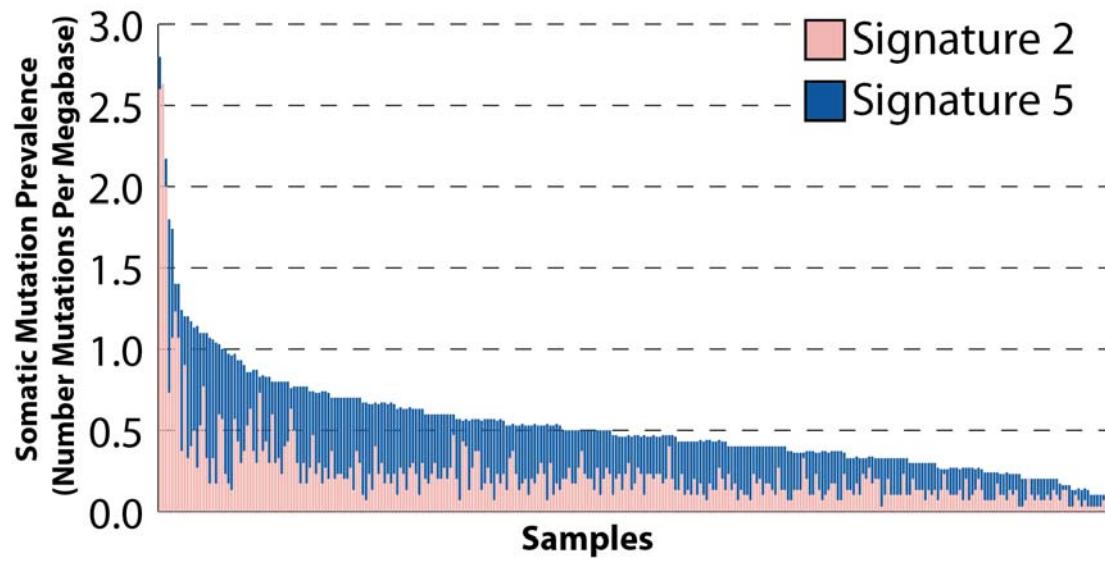
Prostate Cancer



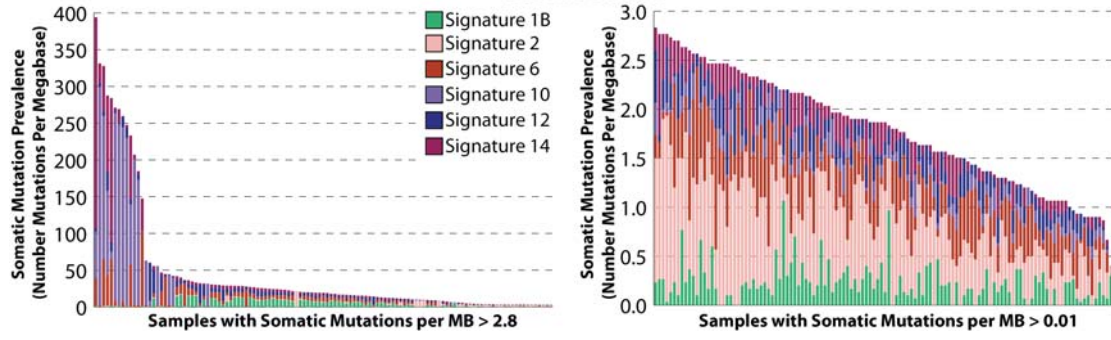
Stomach Cancer



Thyroid Cancer

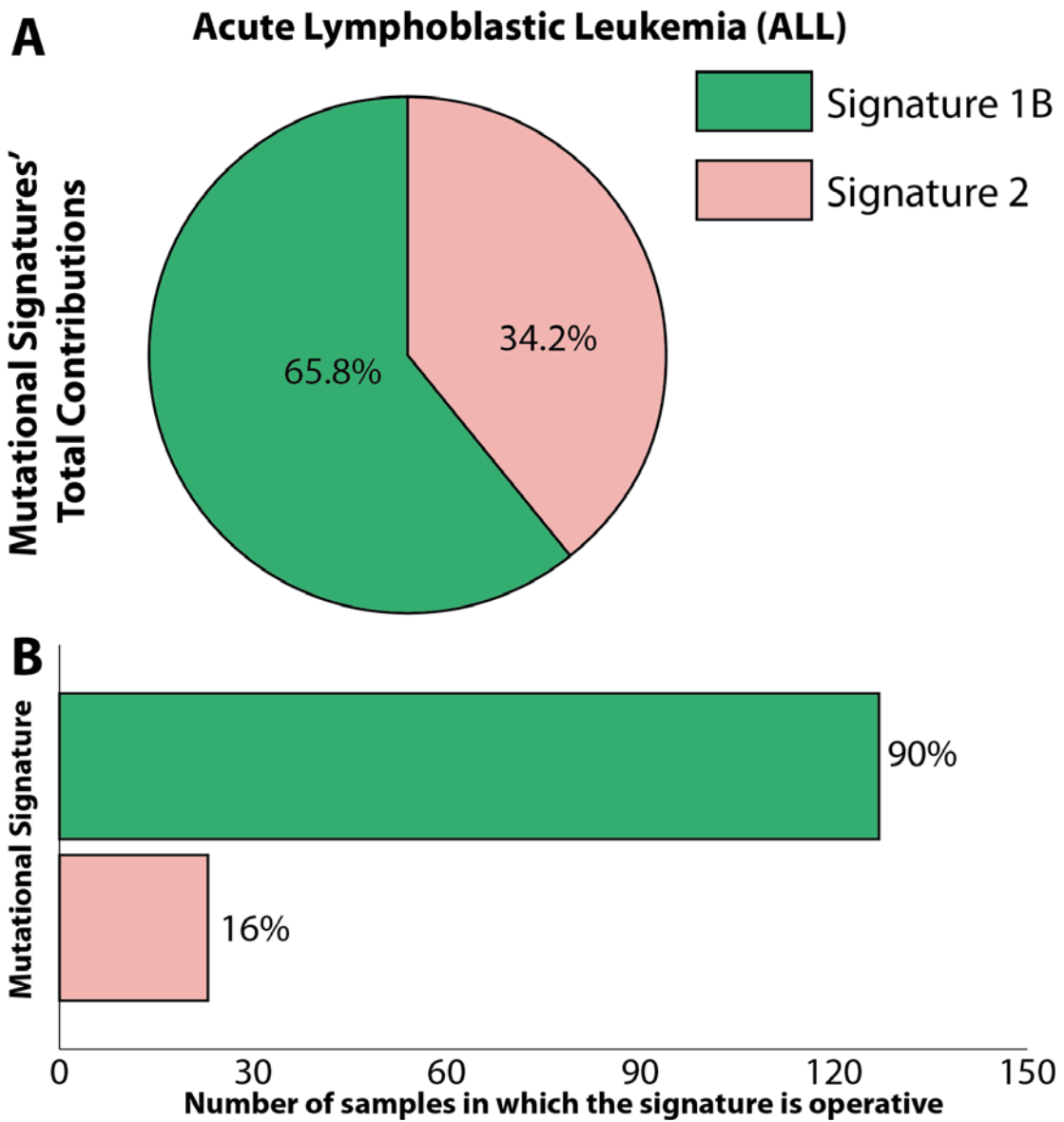


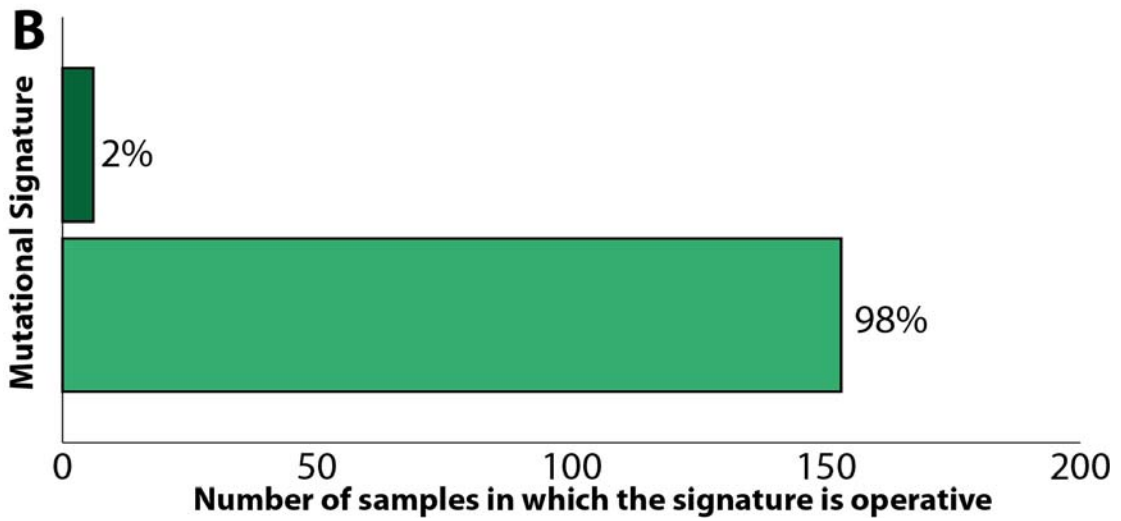
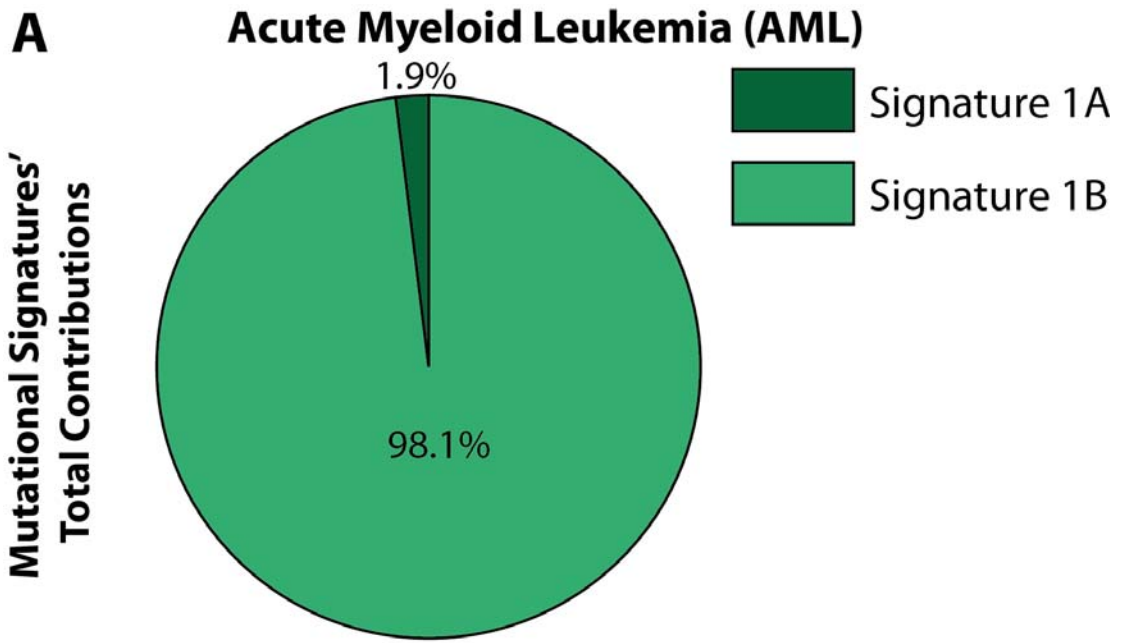
Uterine Cancer

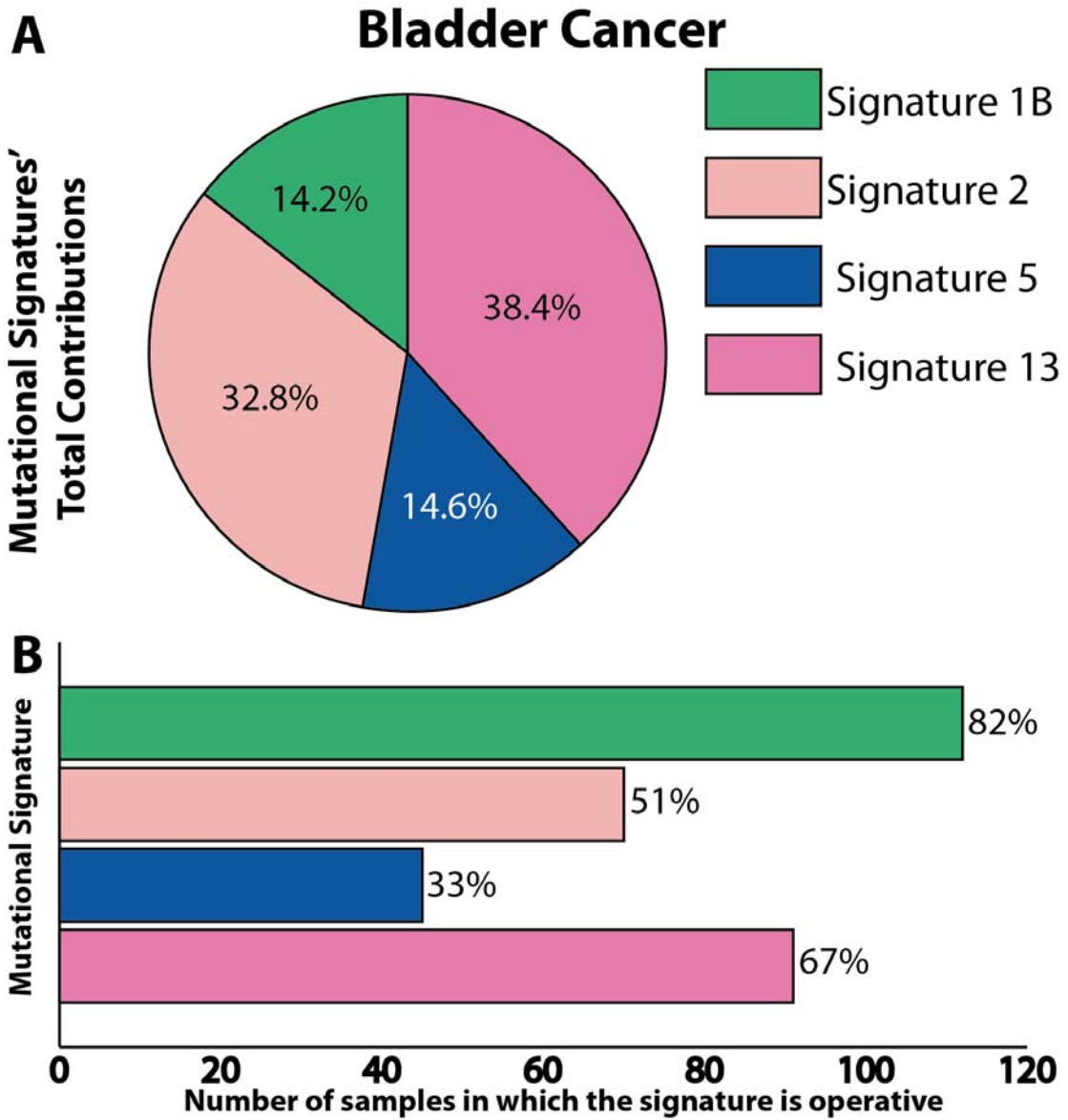


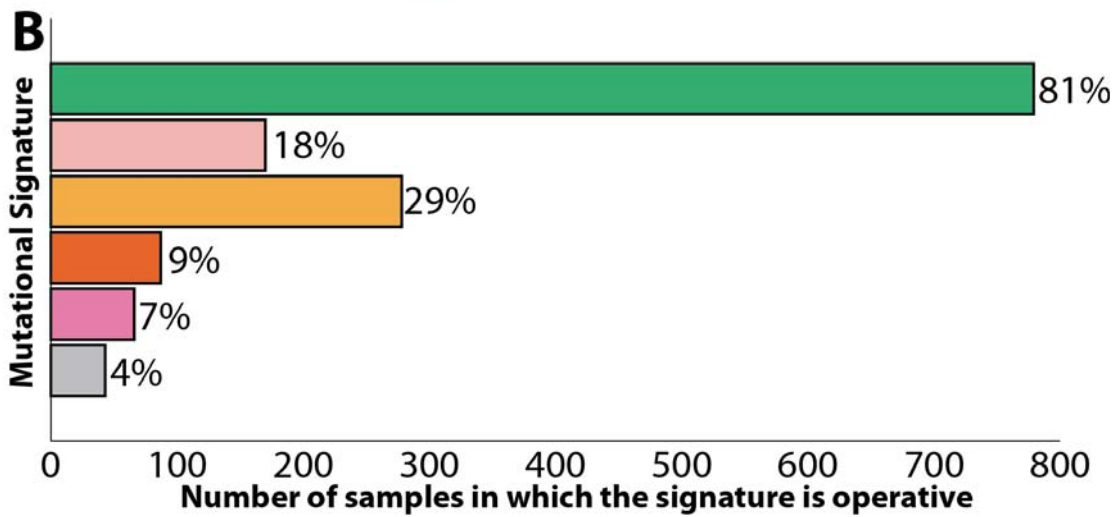
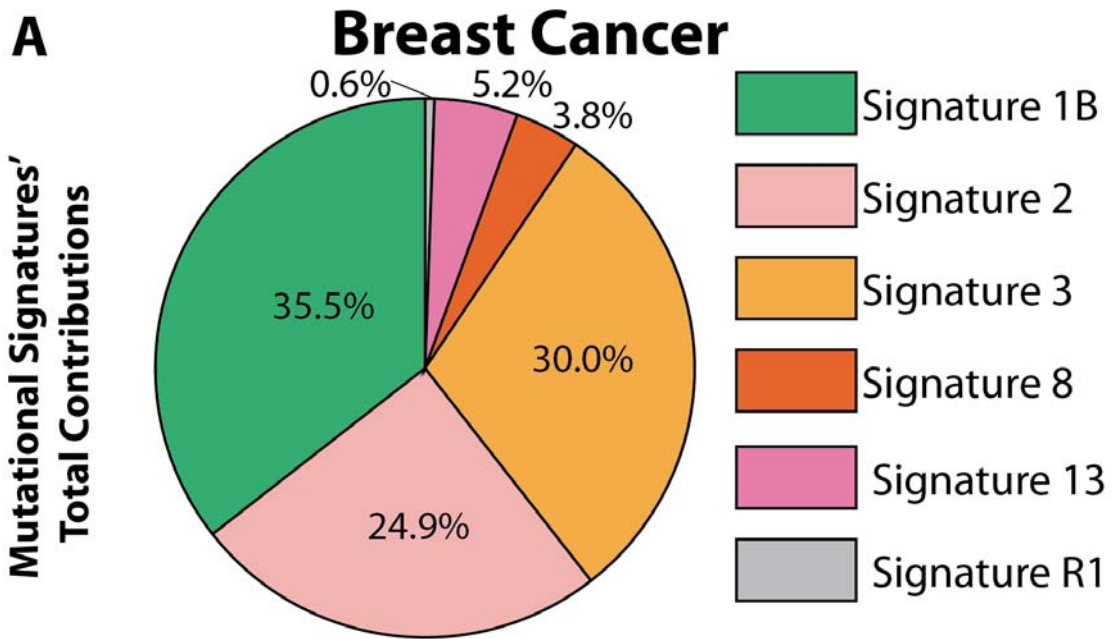
APPENDIX VI: Summary of signatures' contributions in cancer types

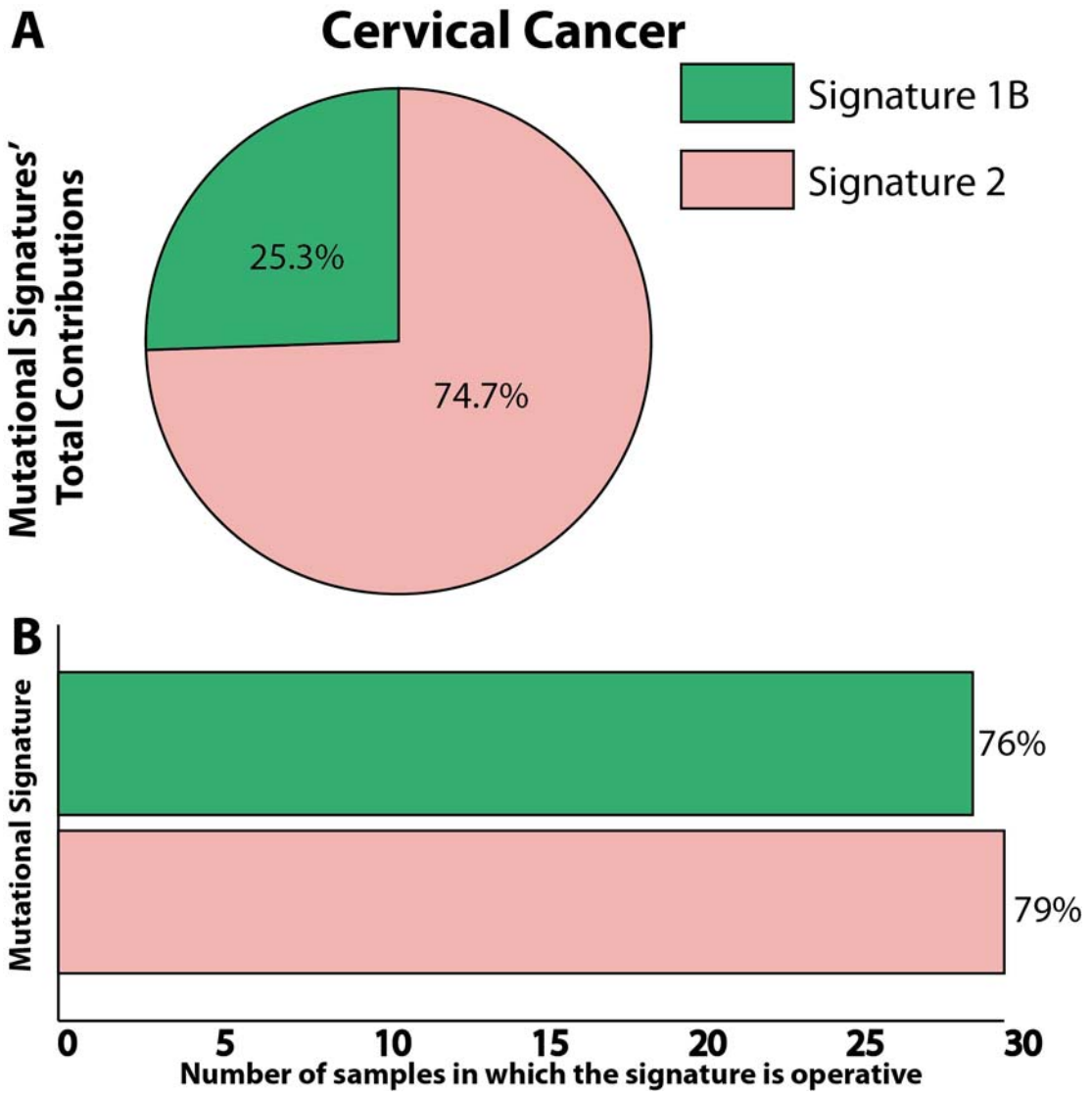
This appendix contains a high-resolution figure for each of the 30 examined cancer types (chapter 4). Each figure depicts a single cancer type and provides a summary of the contributions of the mutational signatures found in this cancer type. All figures have two panels: panel **A** depicting the percentage of total mutations contributed by each of the operative mutational signatures in that cancer type and panel **B** depicting the percentage and number of samples in which each mutational signature contributes significant number of somatic mutations. For most signatures, significant number of mutations in a sample is defined as more than 100 substitutions or more than 25% of all mutations in that sample. Mutational signatures are displayed in distinct colours, consistent in both panels of each figure as well as in all figures in Appendices V and VI. Figures are displayed on individual pages, labelled to clearly show the names of the cancer types, and they are ordered alphabetically based on the names of these cancer types. In general, all samples are included in the summary of each cancer type. The only exception (denoted with an asterisk in the appropriate figure) is one lung squamous hypermutator sample purely of Signature 7 (72 mutations per MB). Signature 7 is associated with exposure to ultraviolet light, an unlikely carcinogen for lung cancer. As such, this TCGA sample is most likely either a melanoma metastasis or a misannotated sample. Thus, the association between Signature 7 and lung squamous has not been discussed in chapter 4 and this association has not been displayed in Figure 4.9.

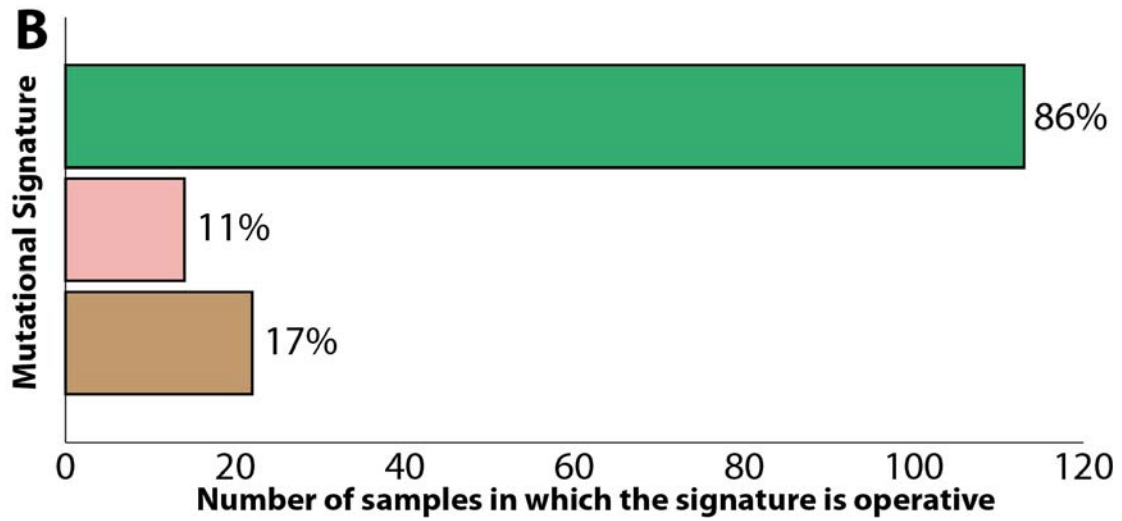
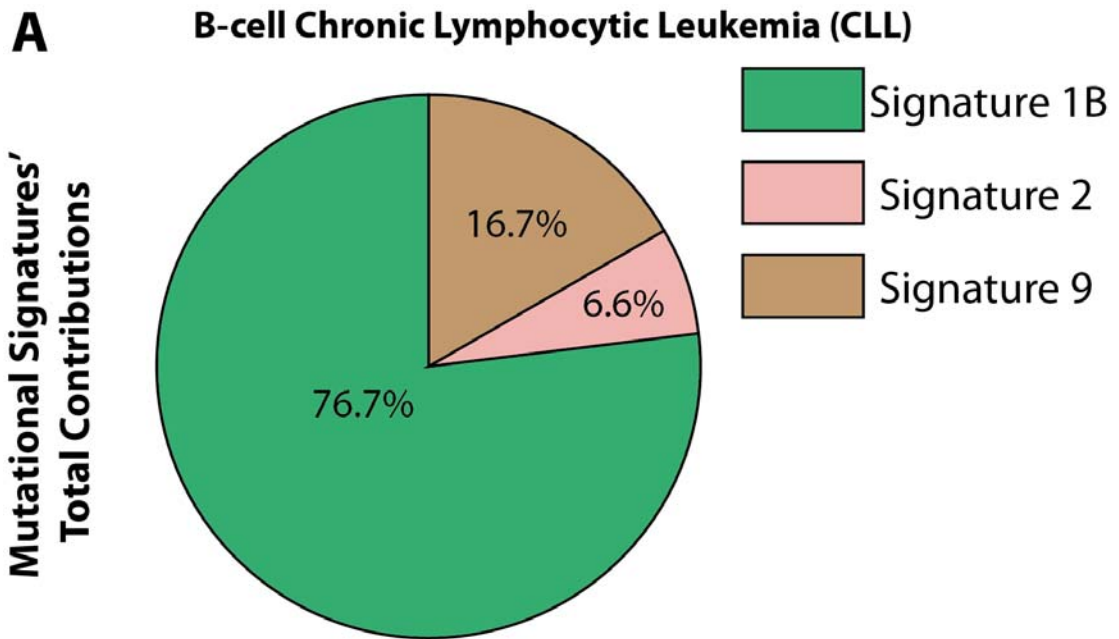


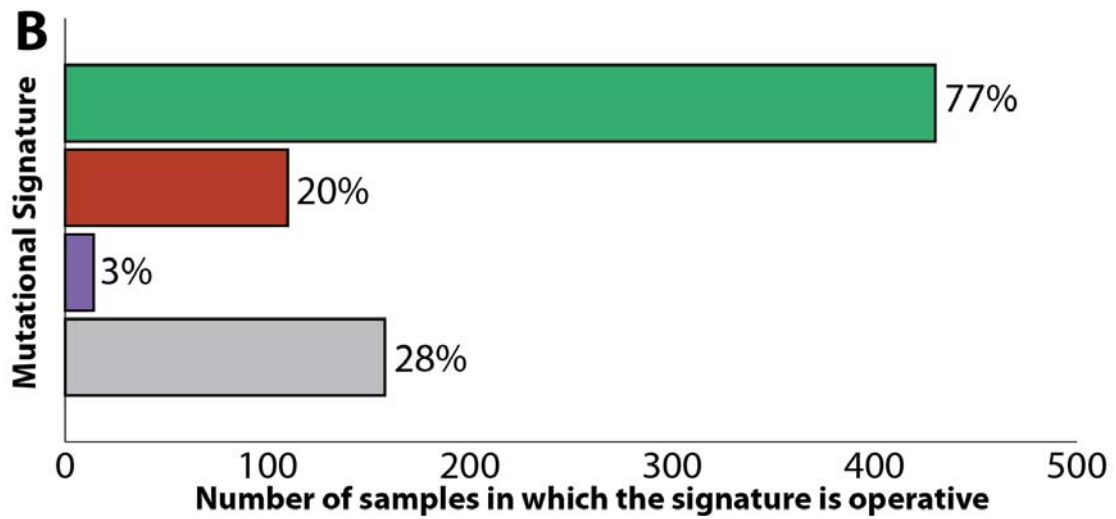
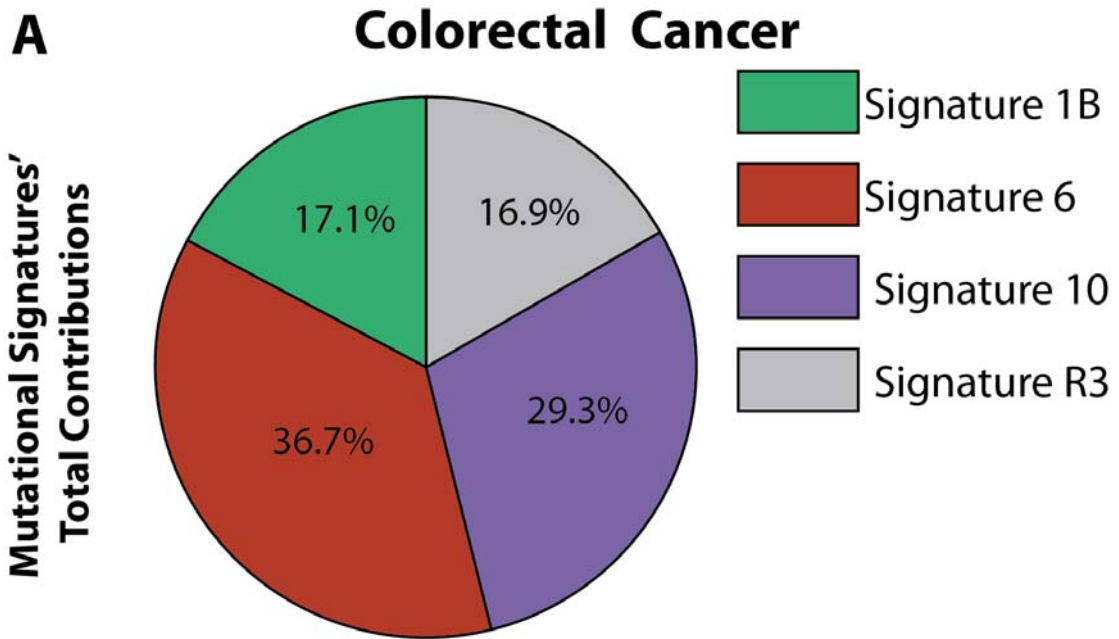


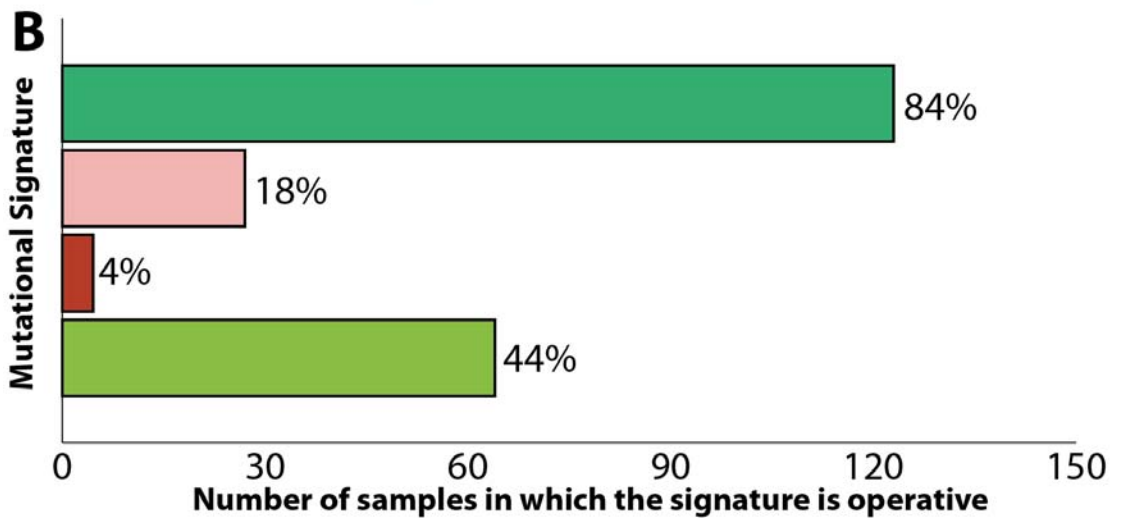
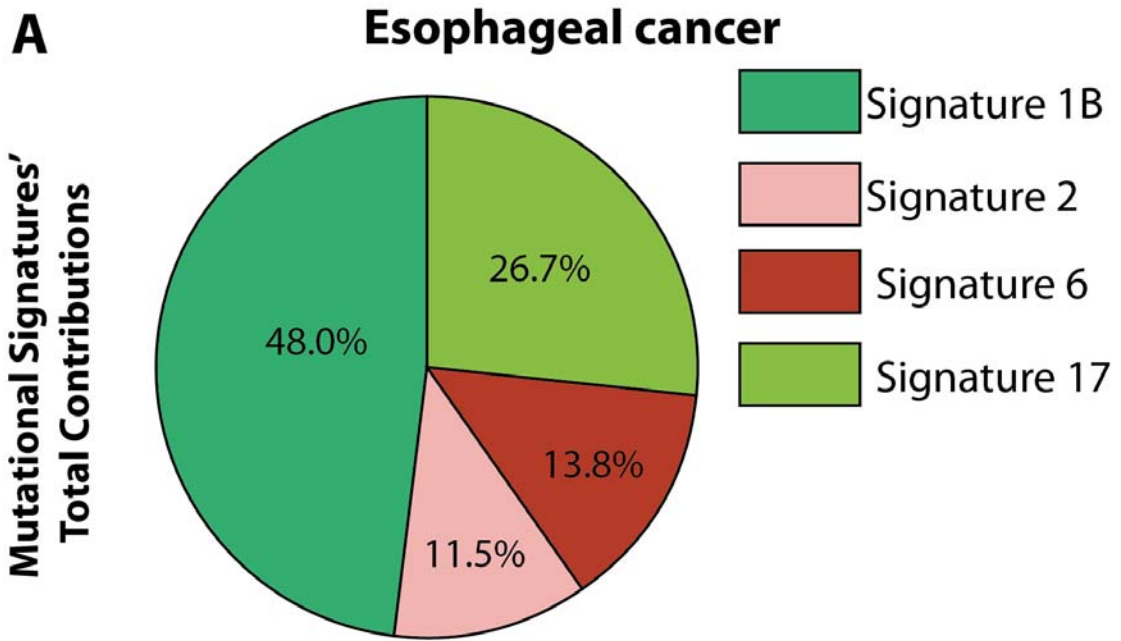


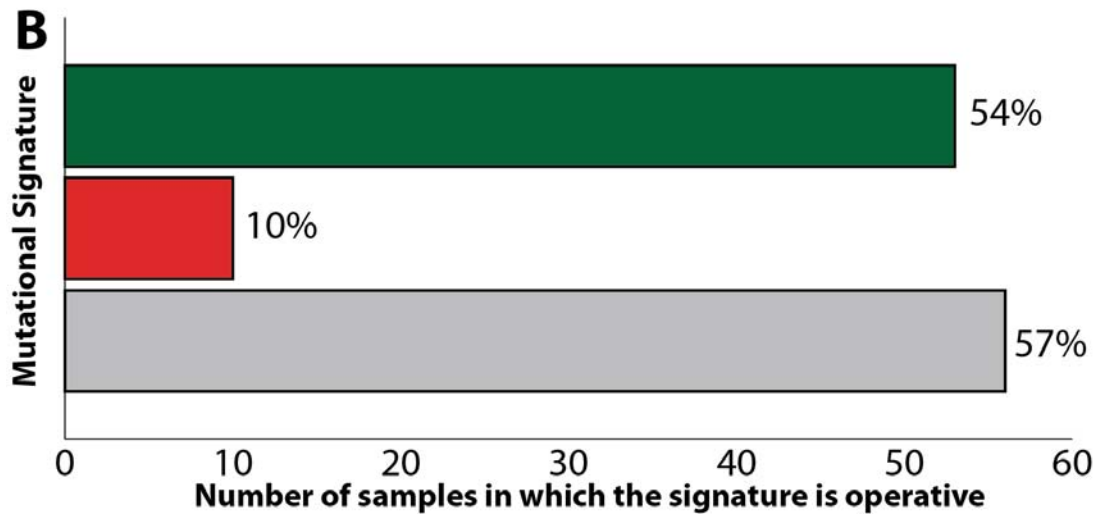
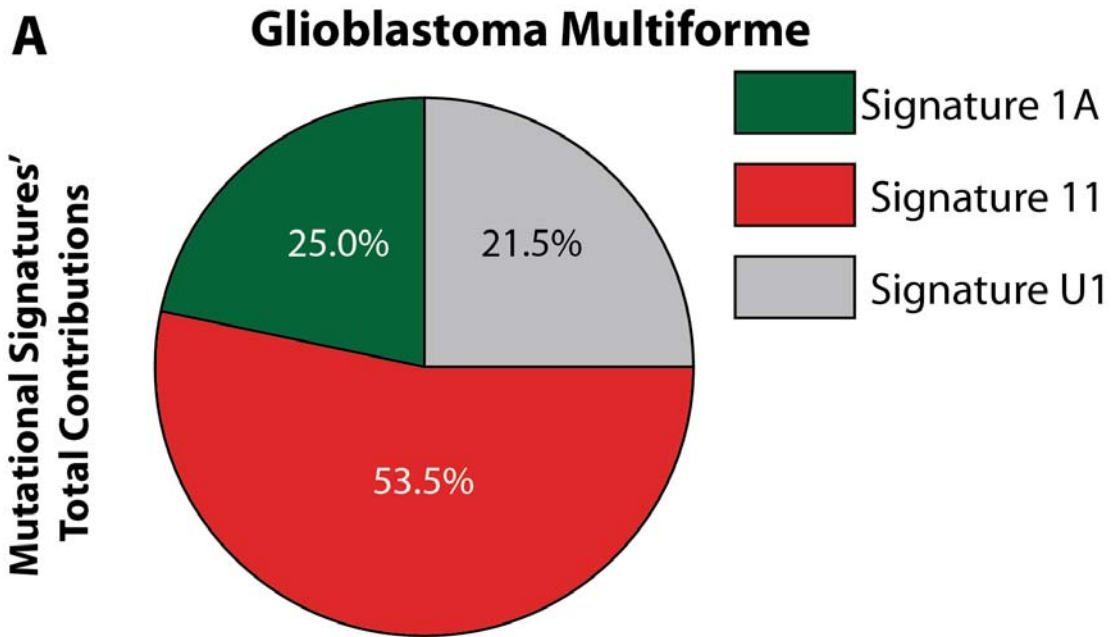


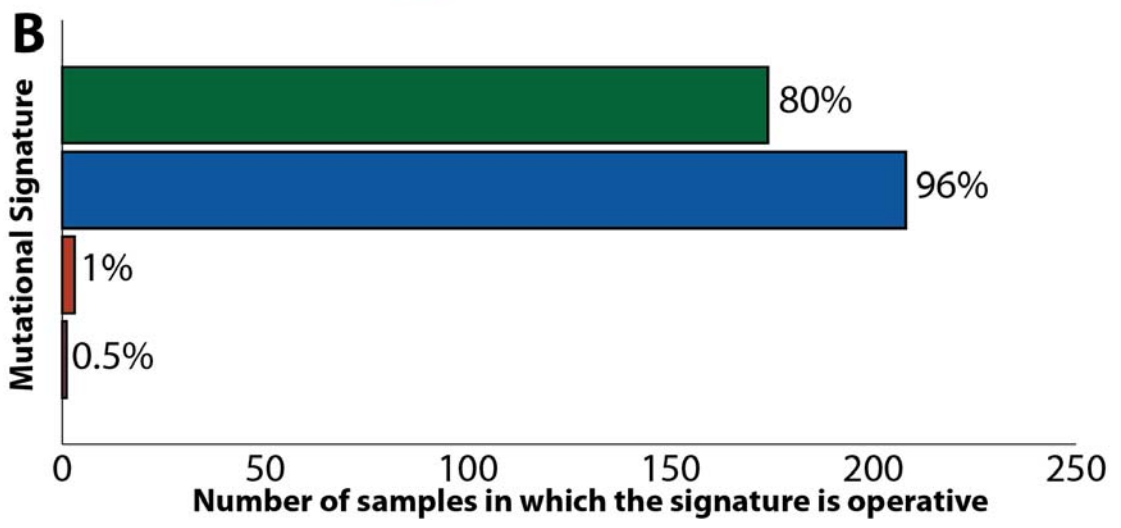
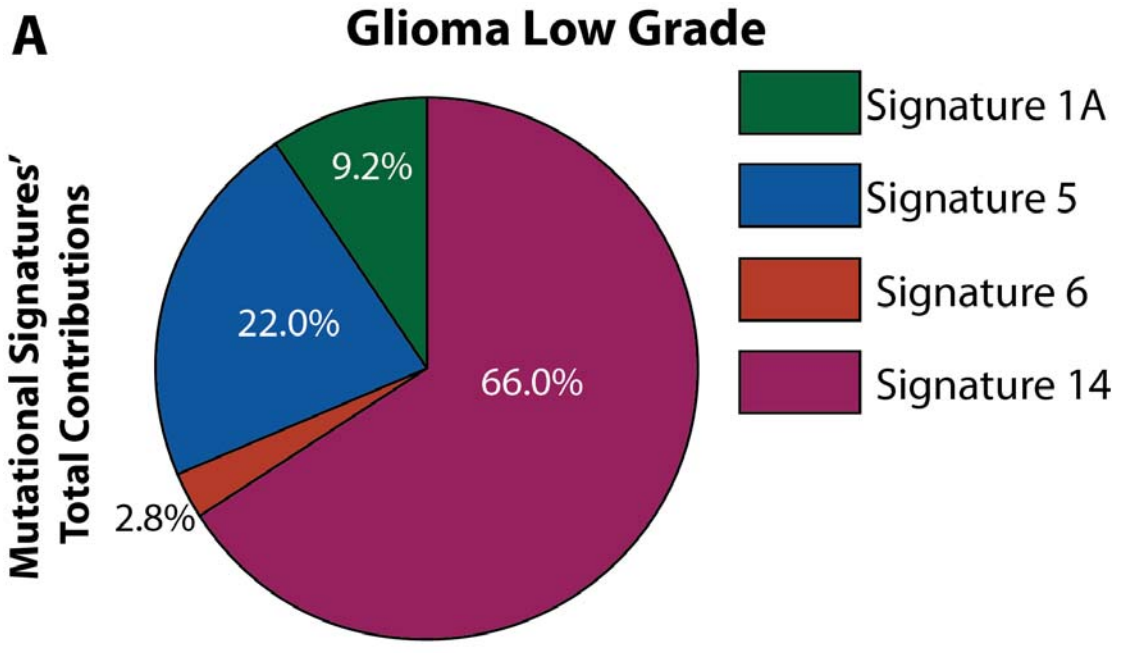


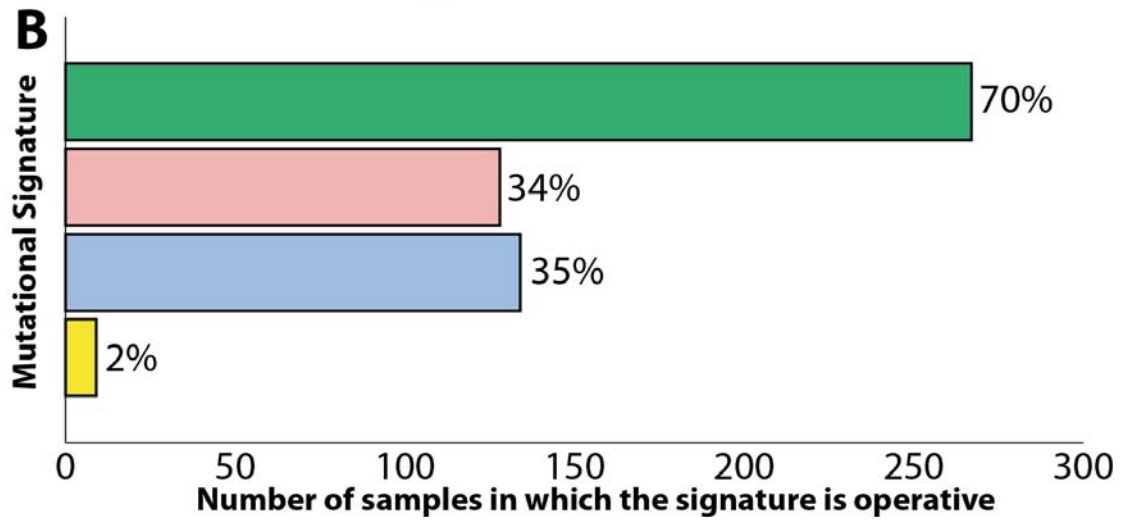
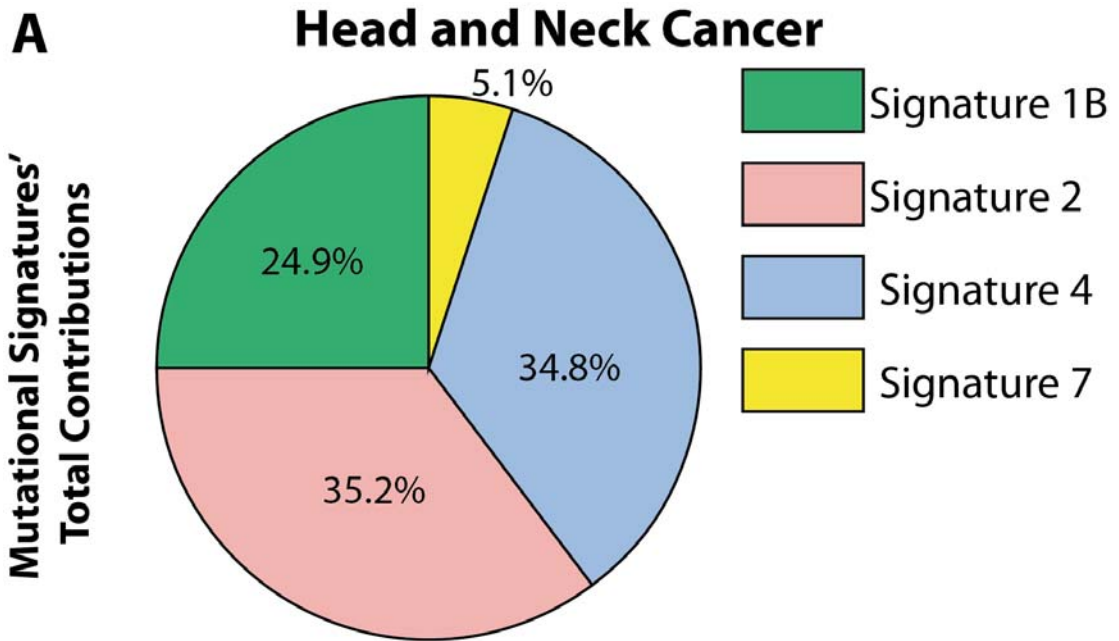


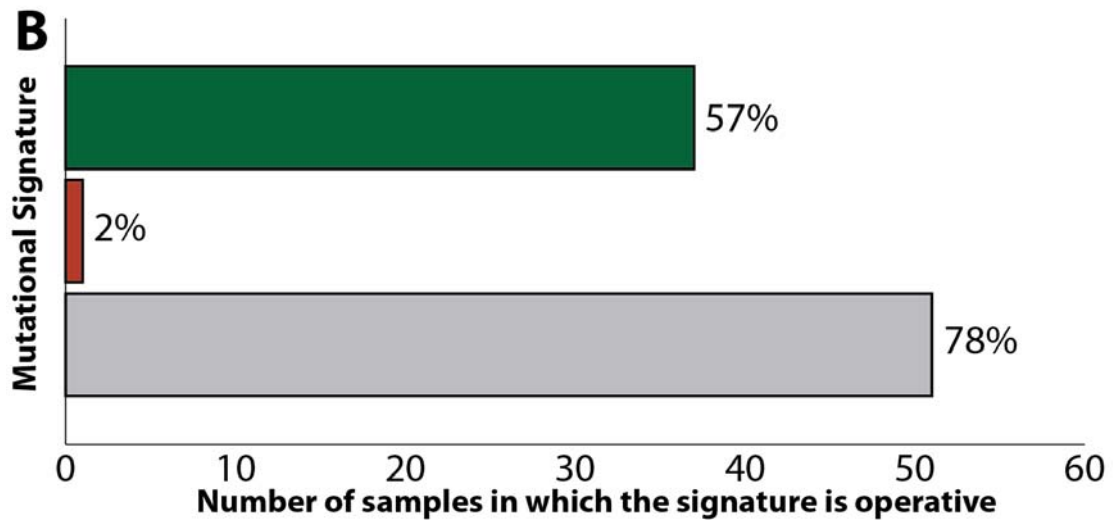
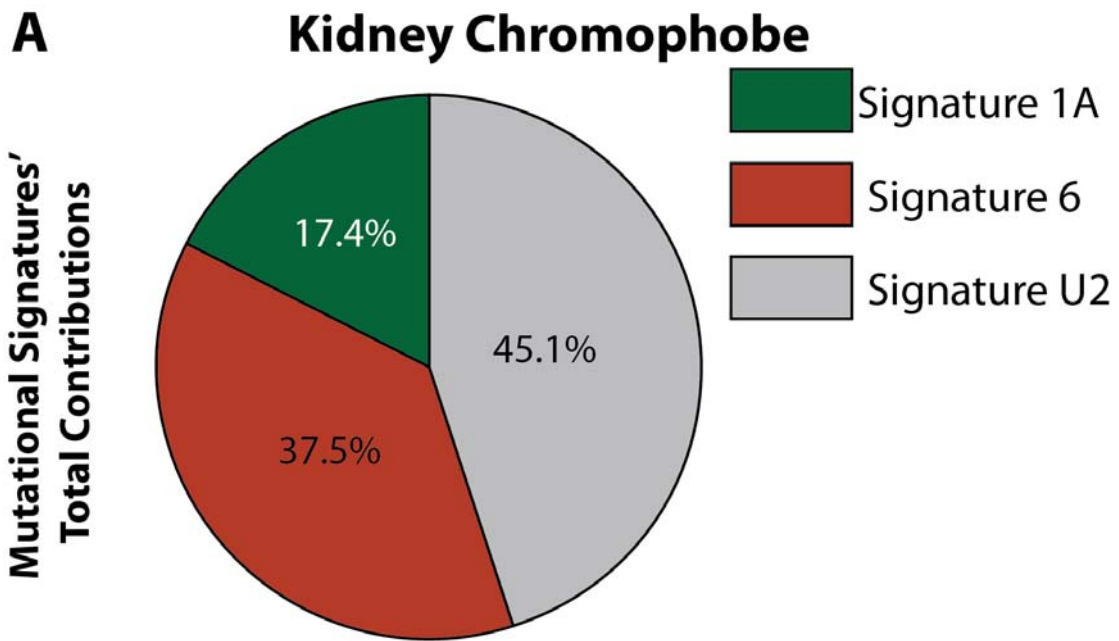


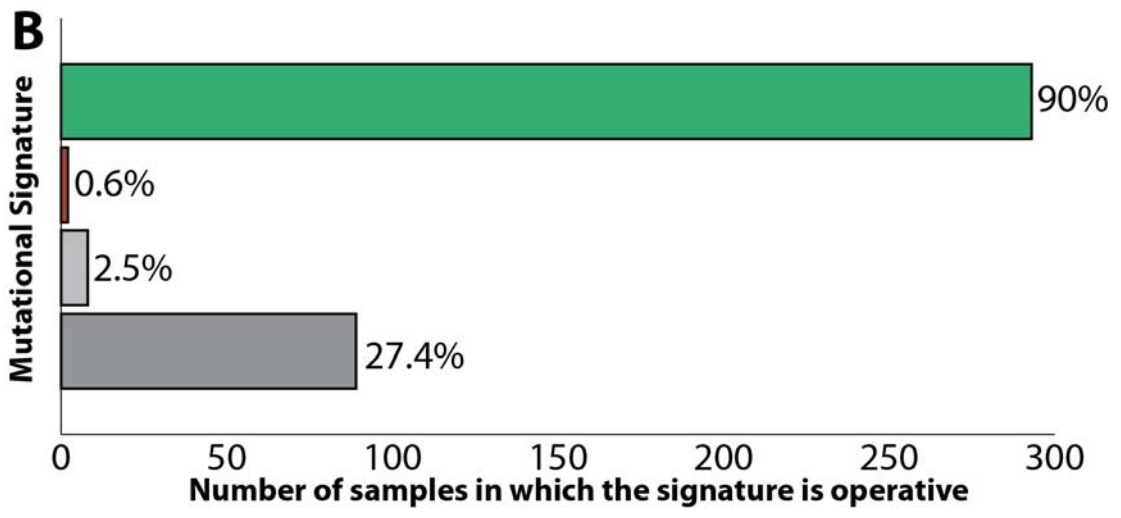
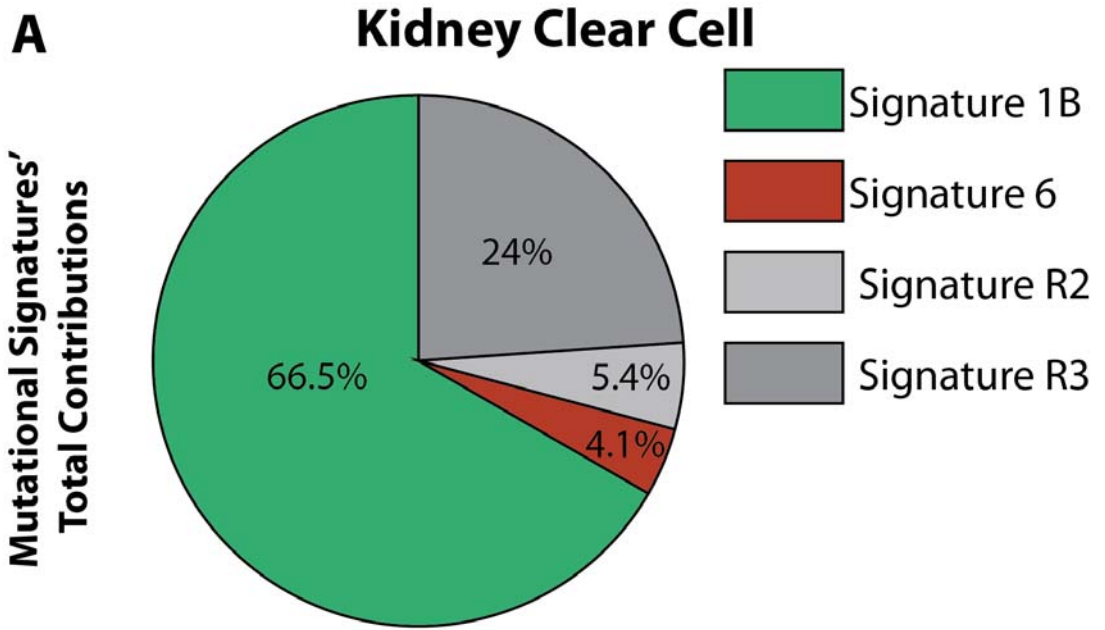


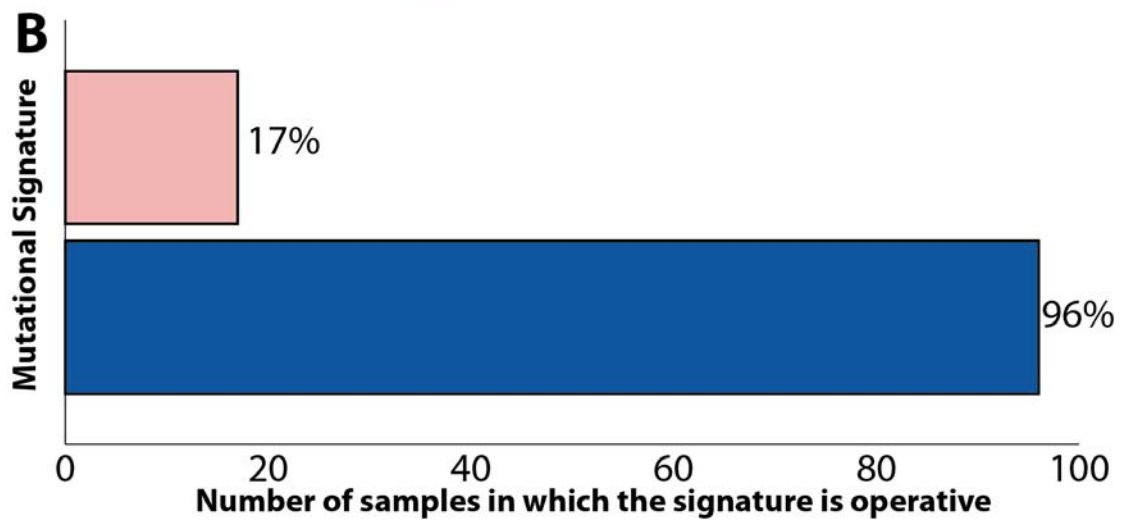
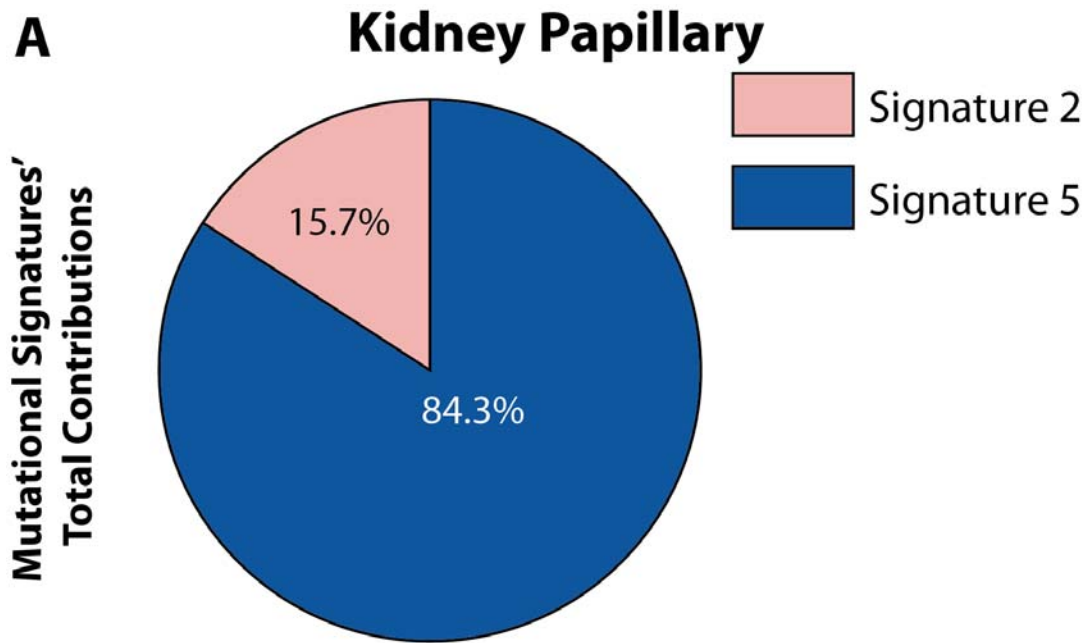


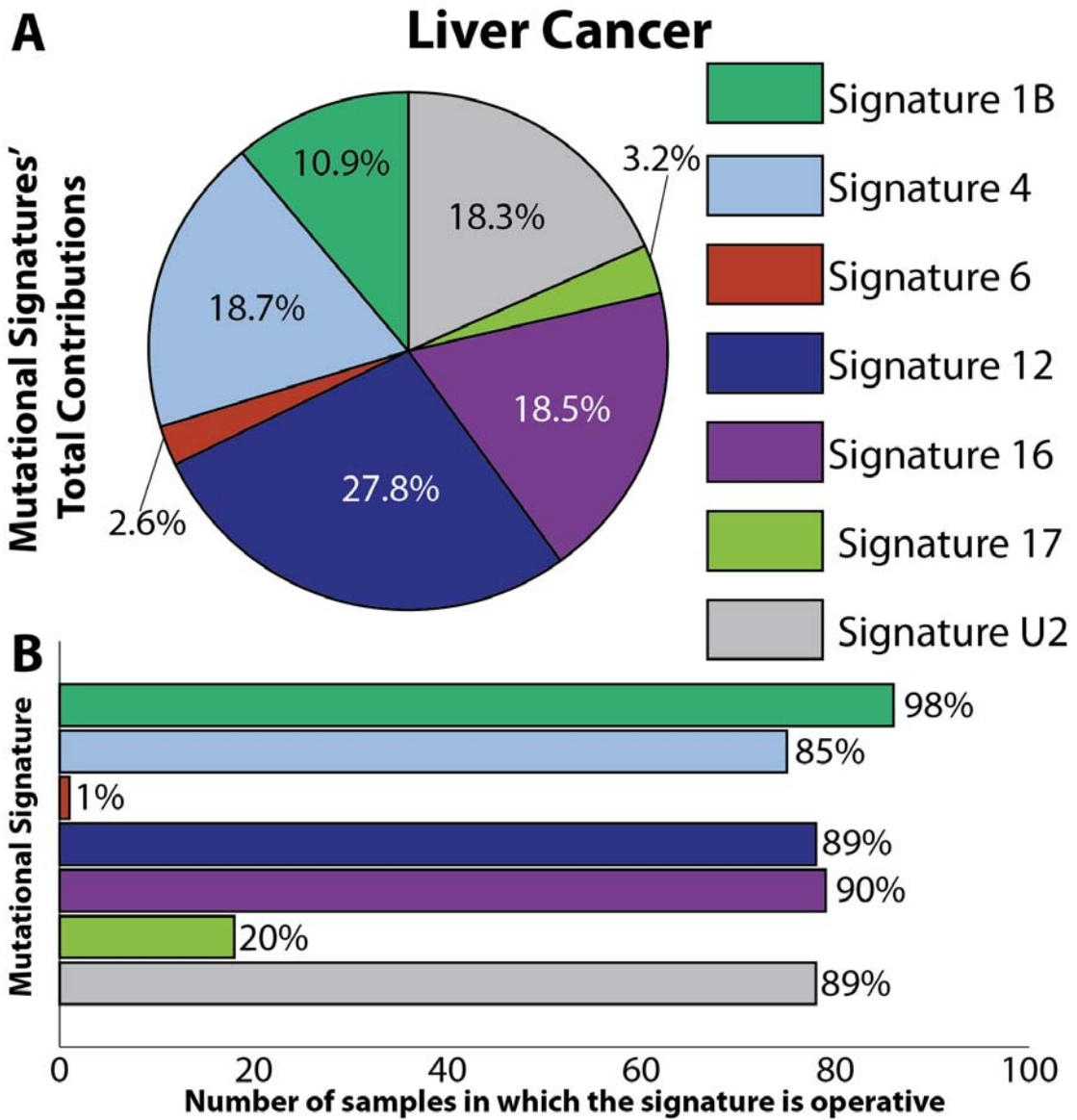


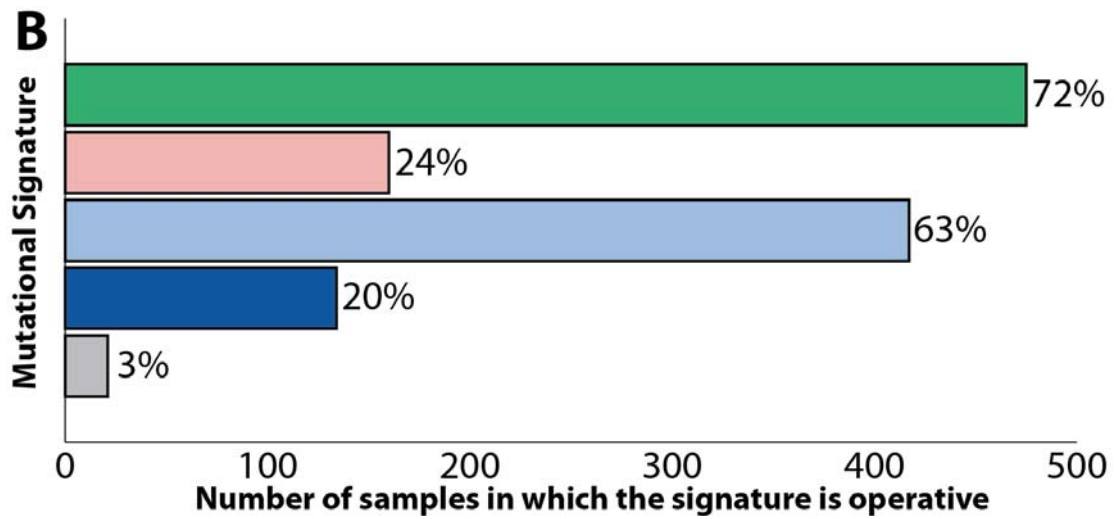
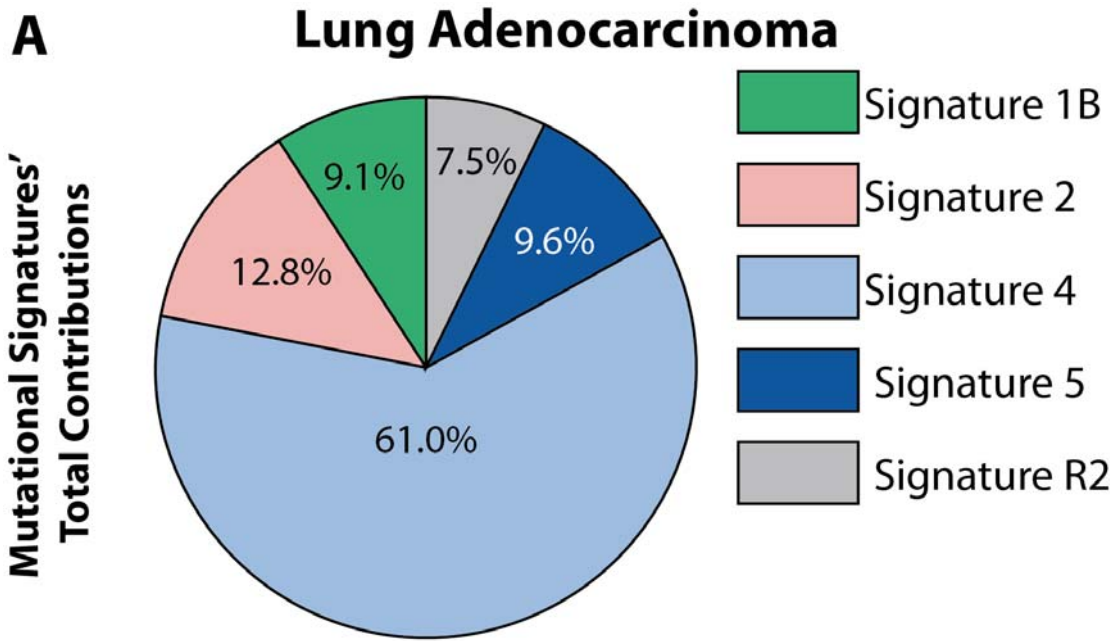


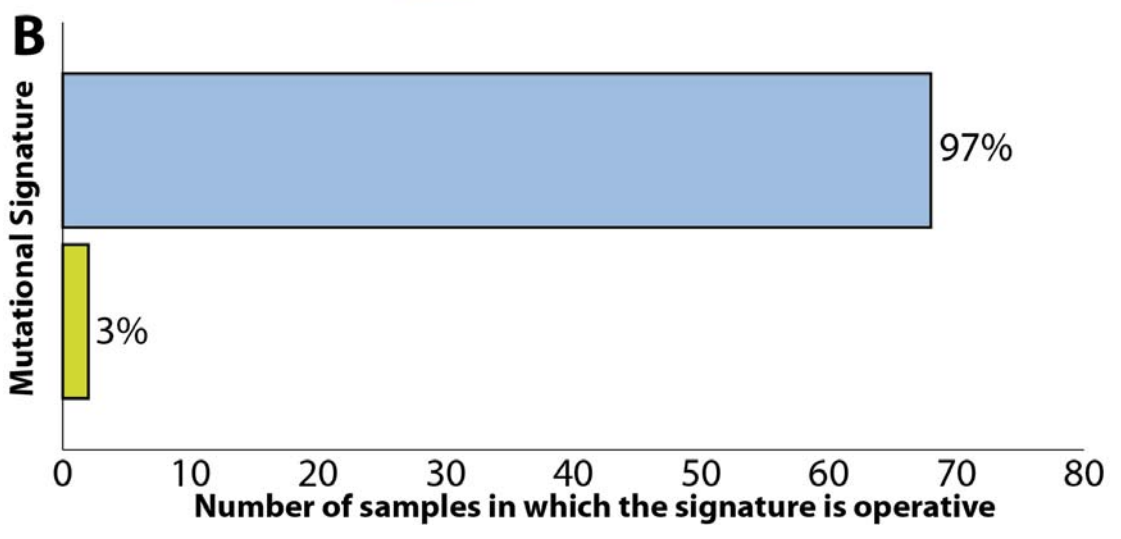
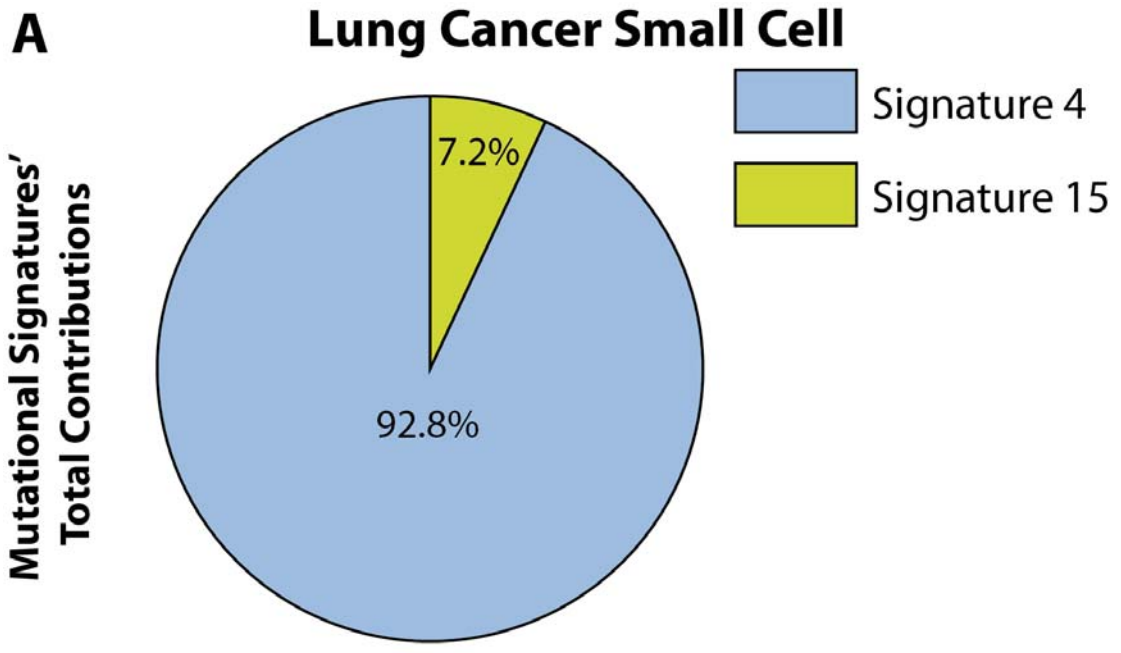


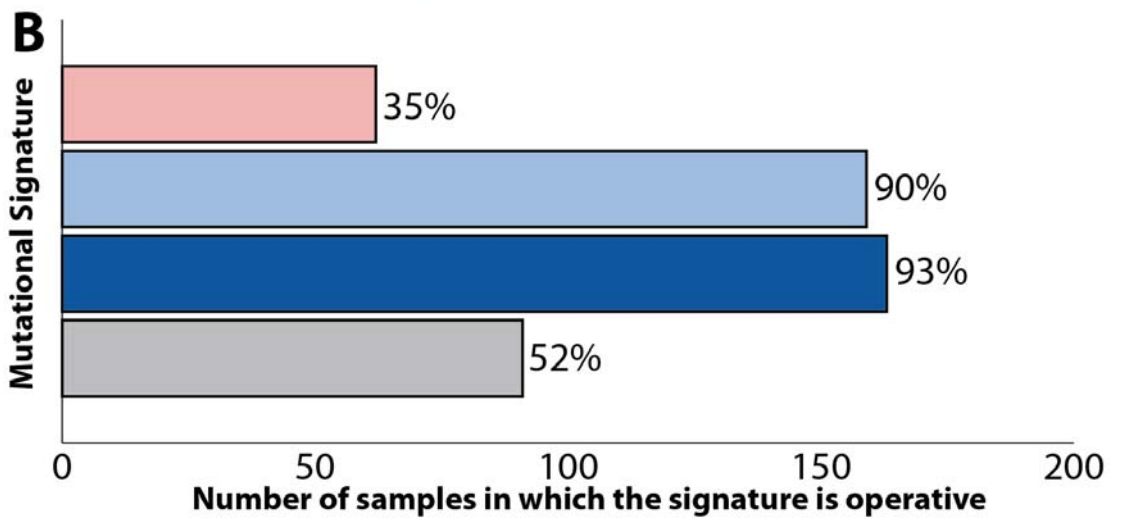
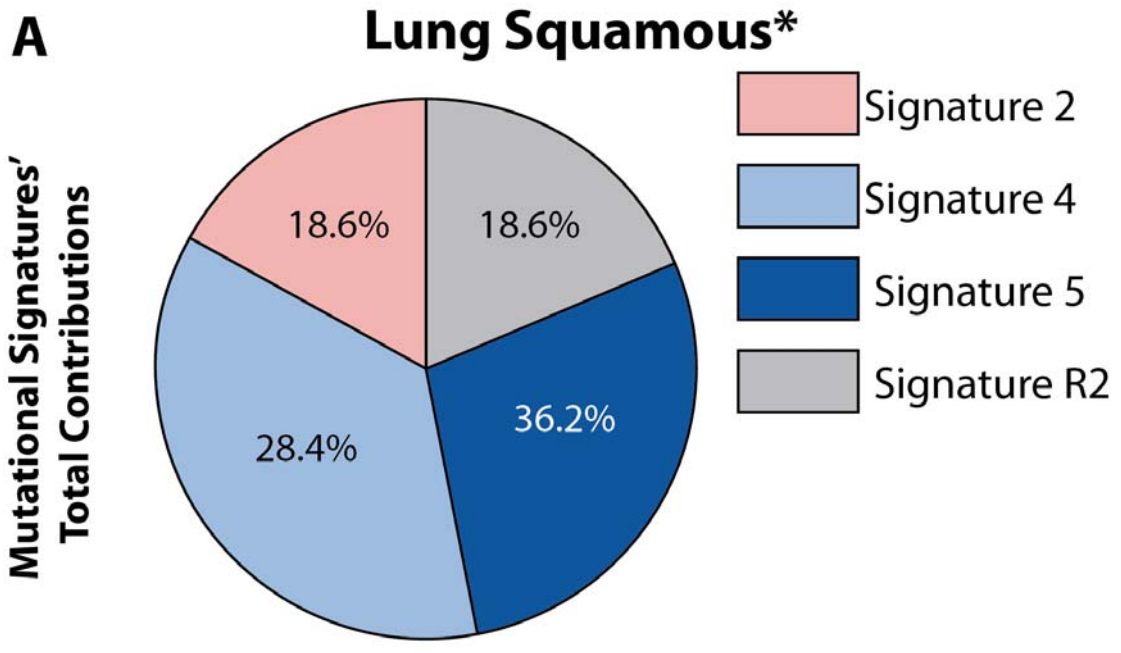


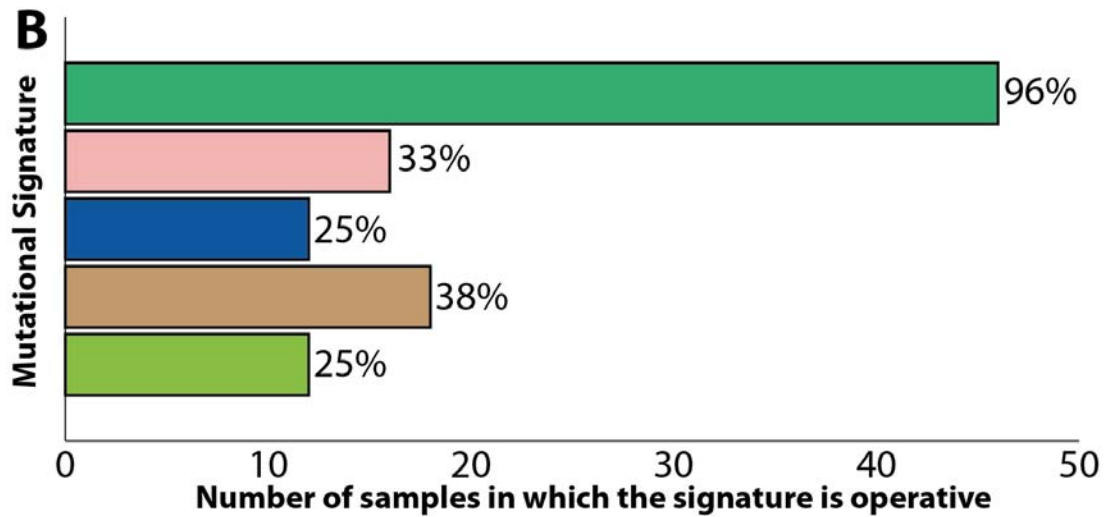
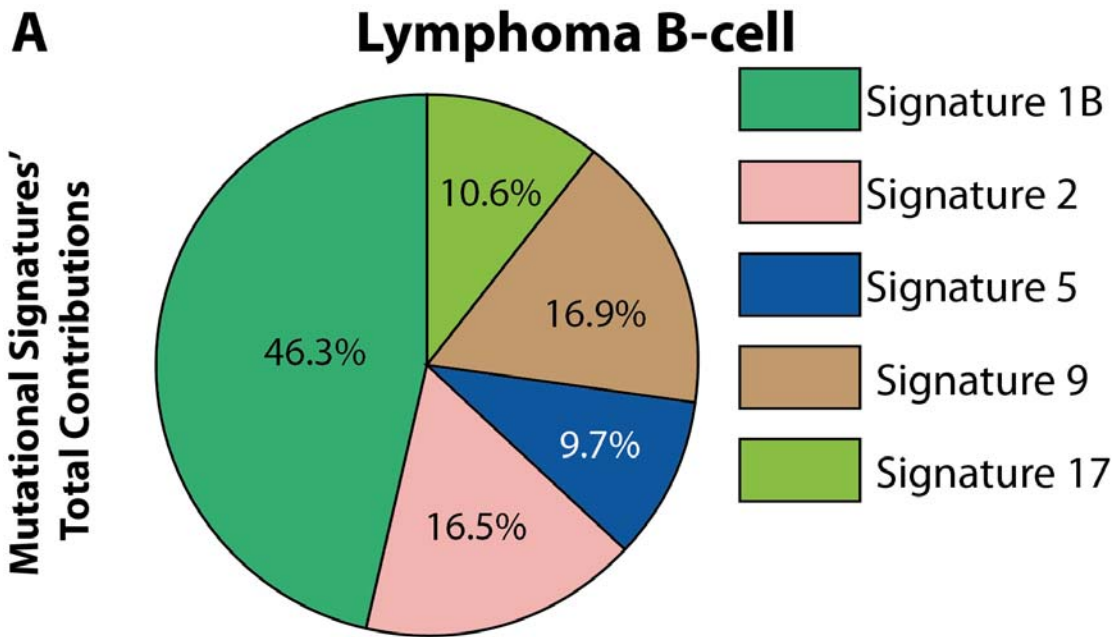


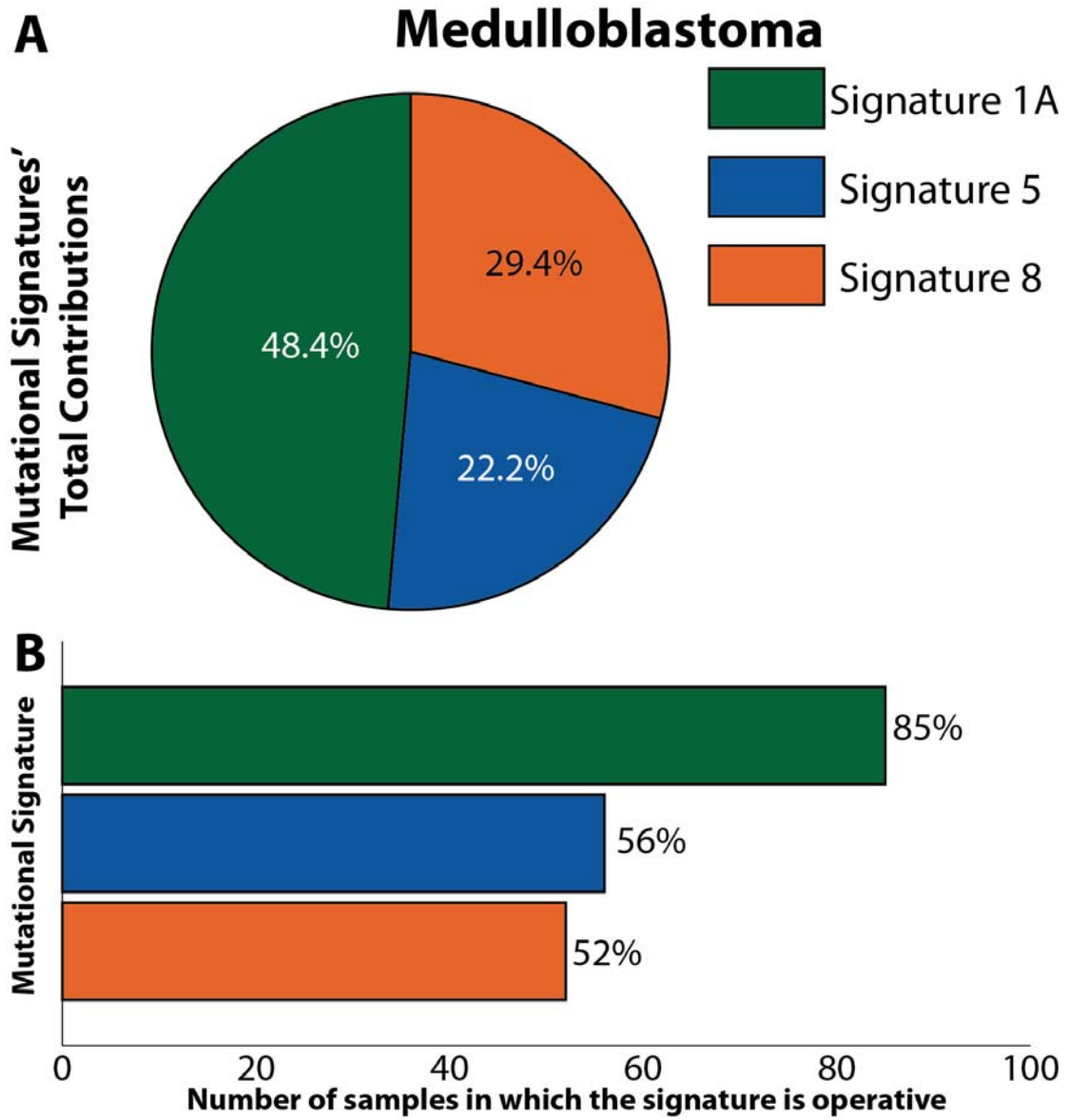


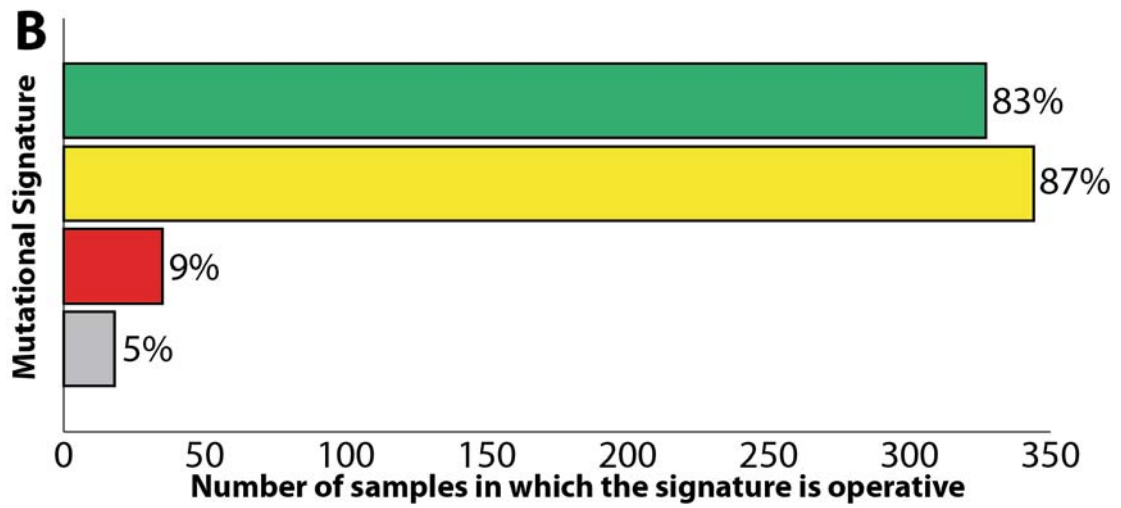
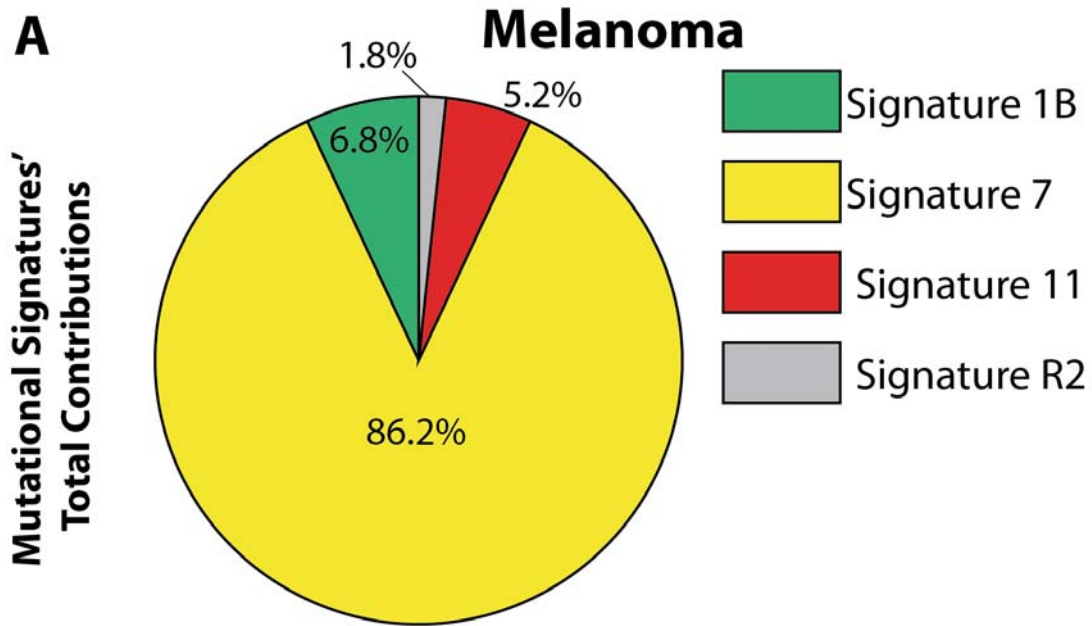


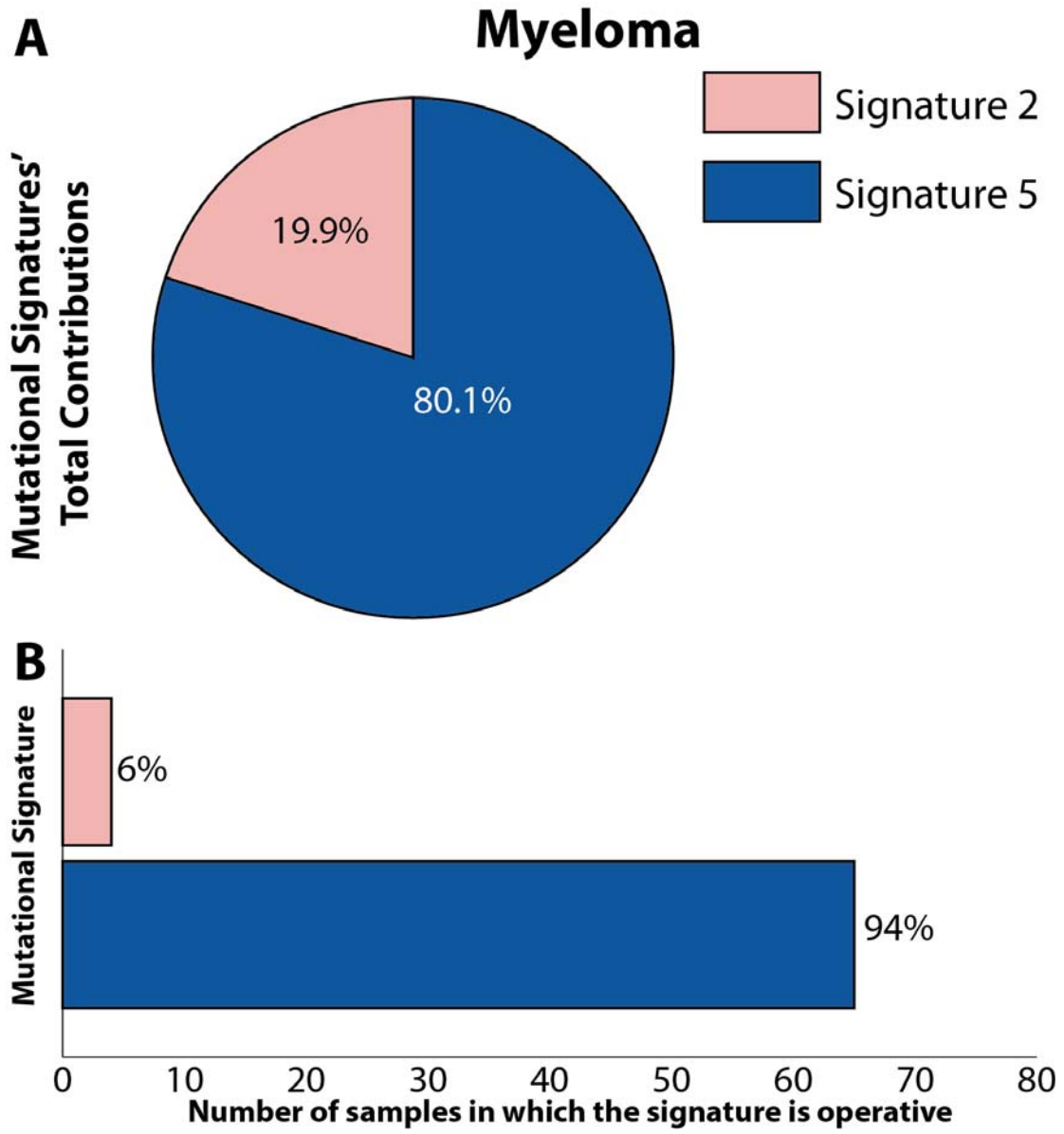


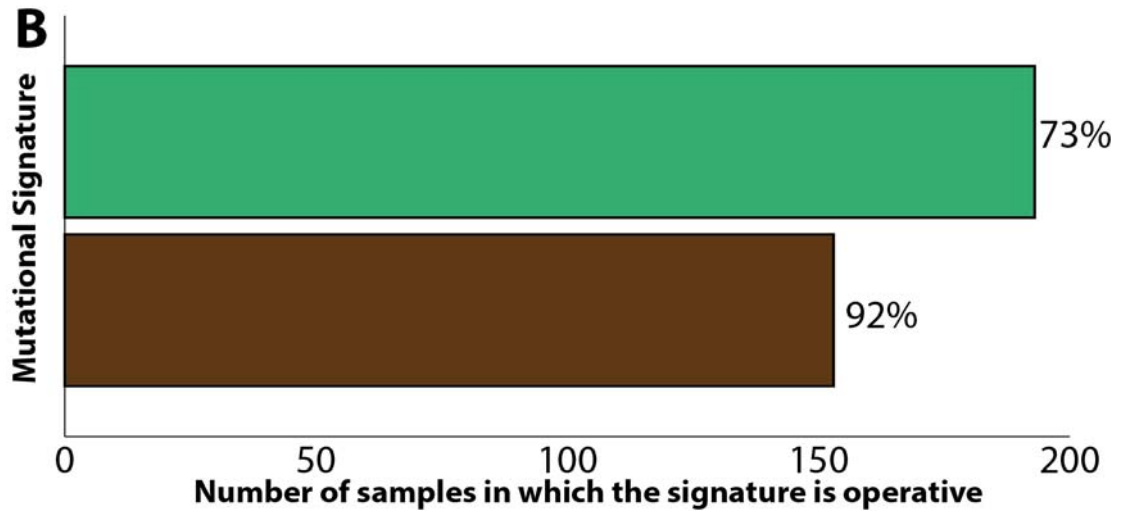
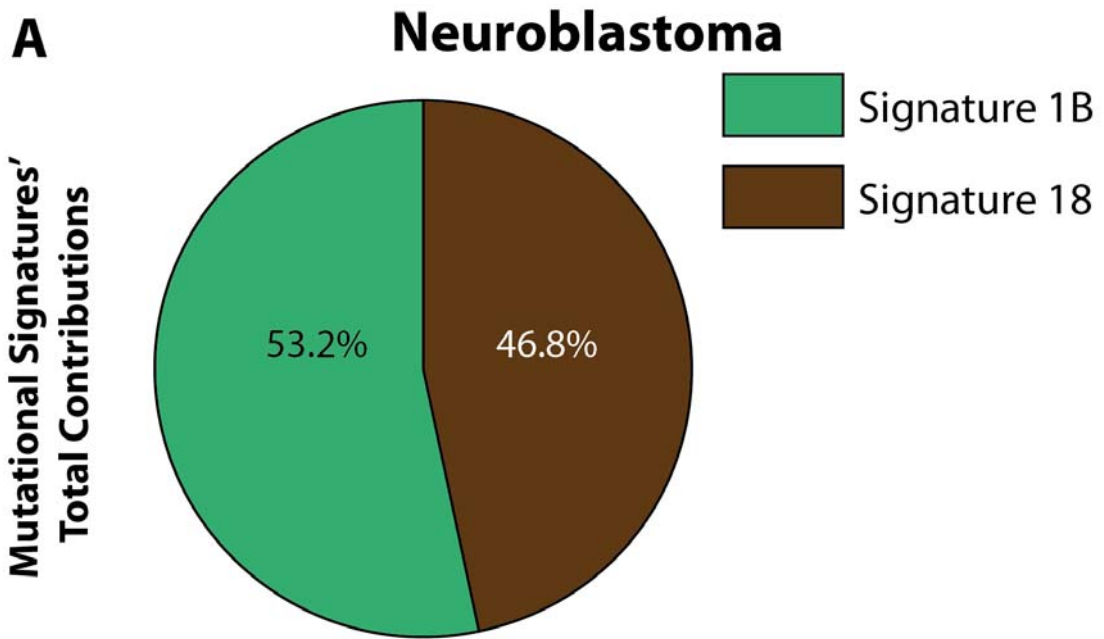


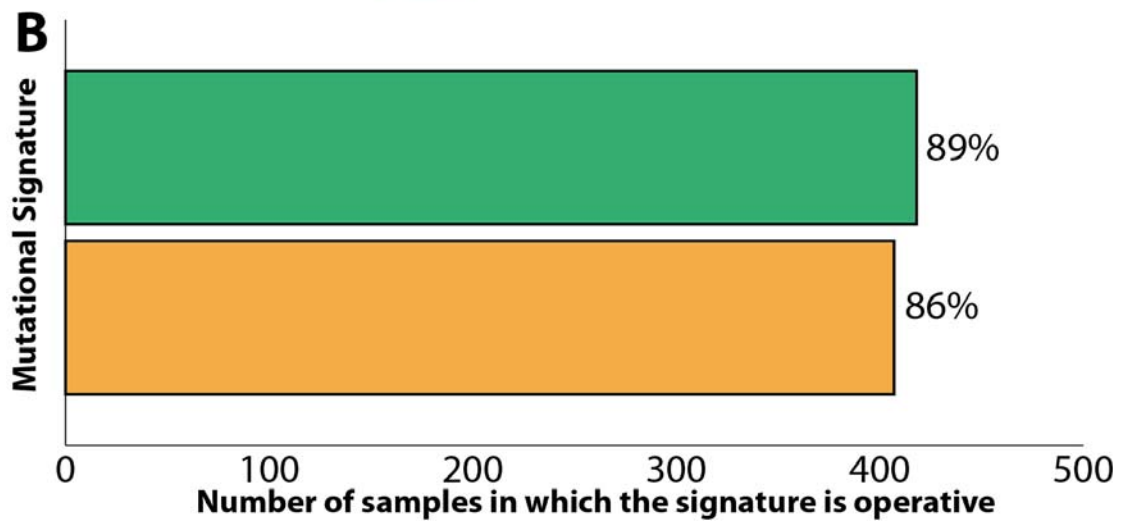
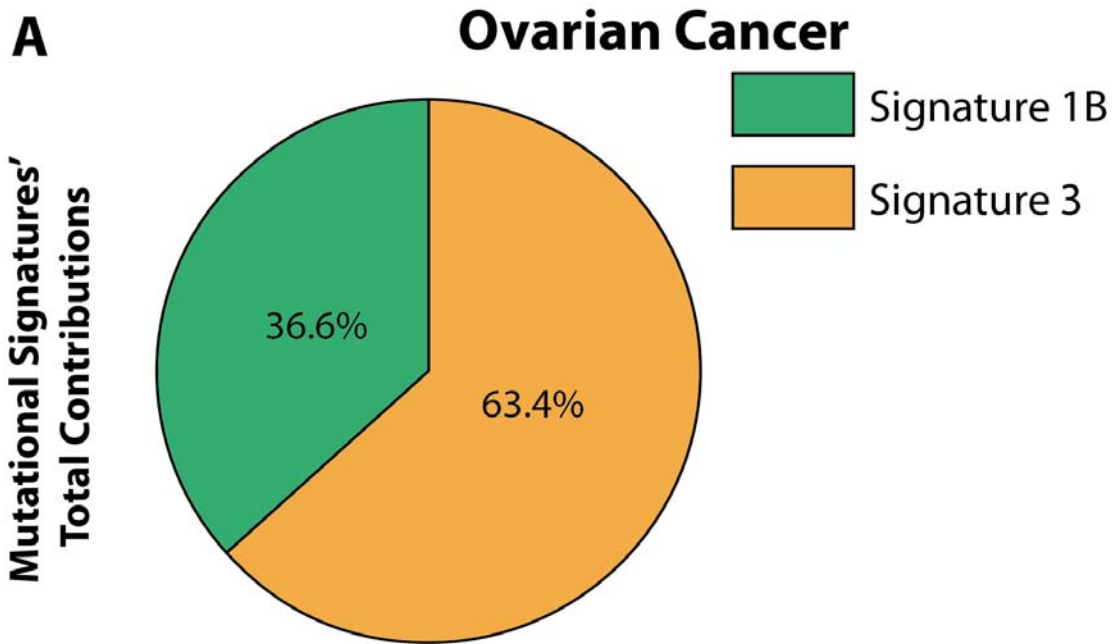


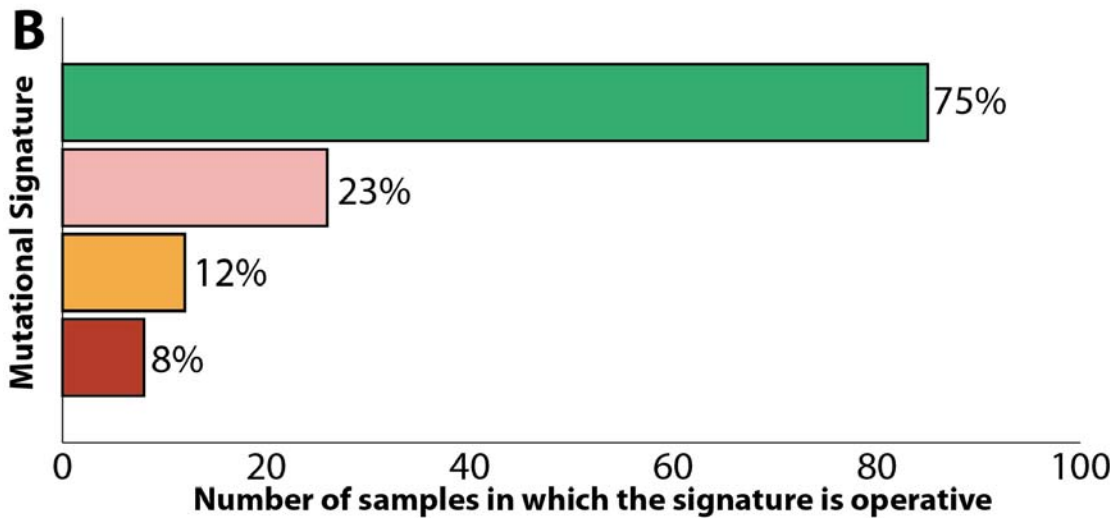
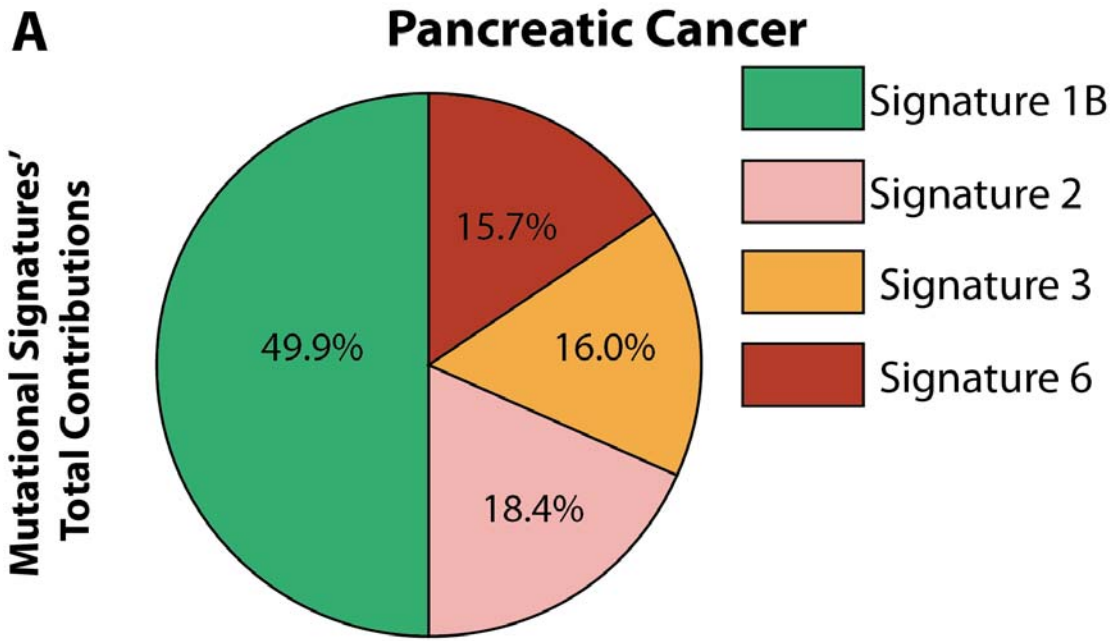


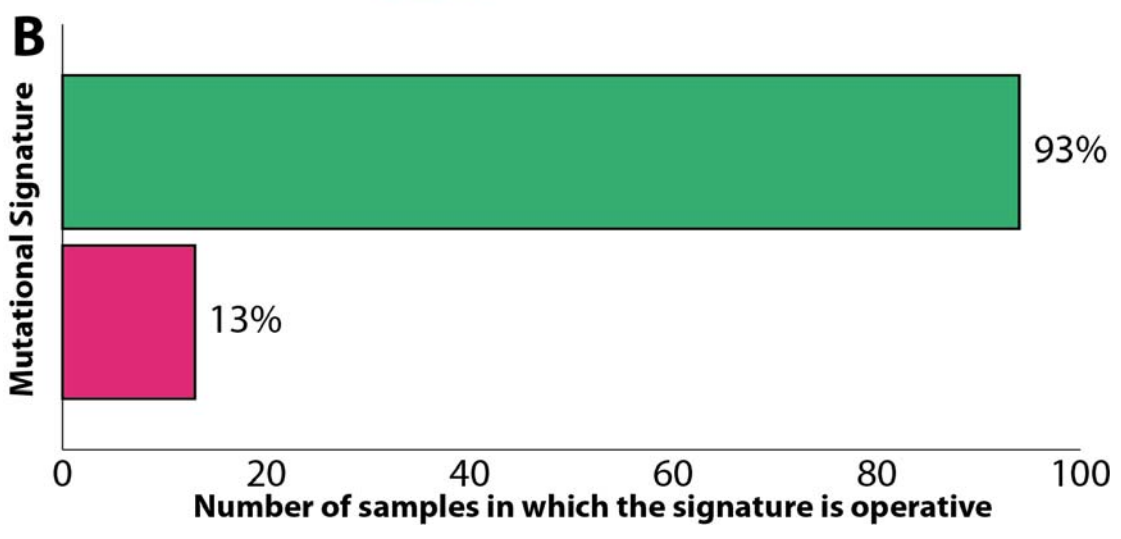
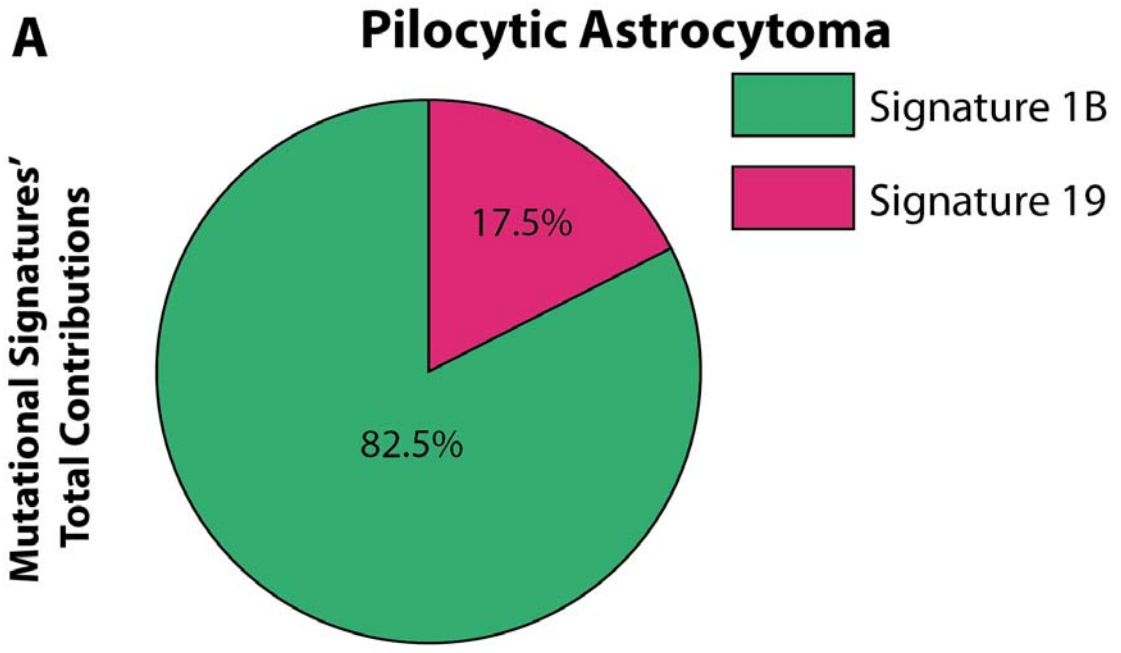


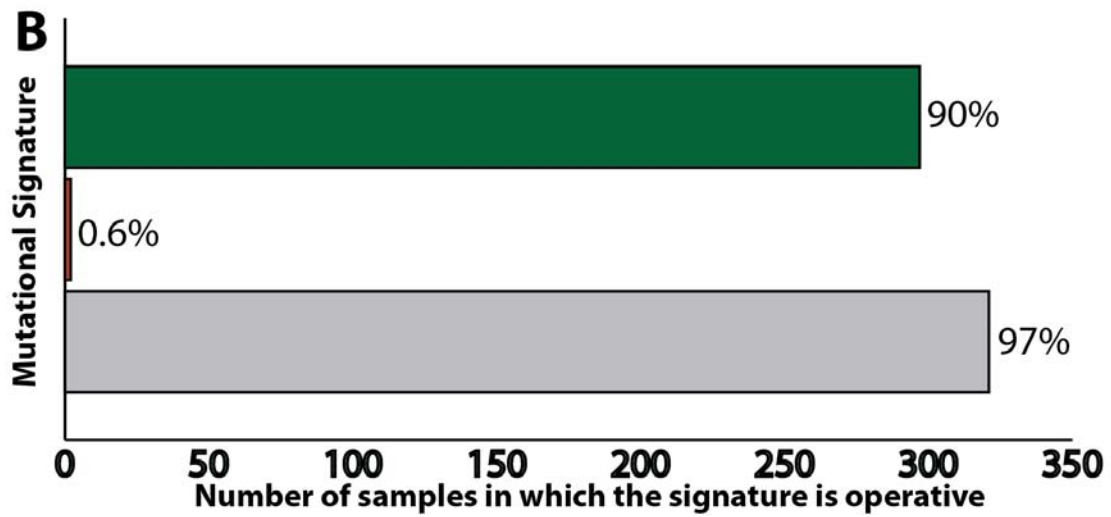
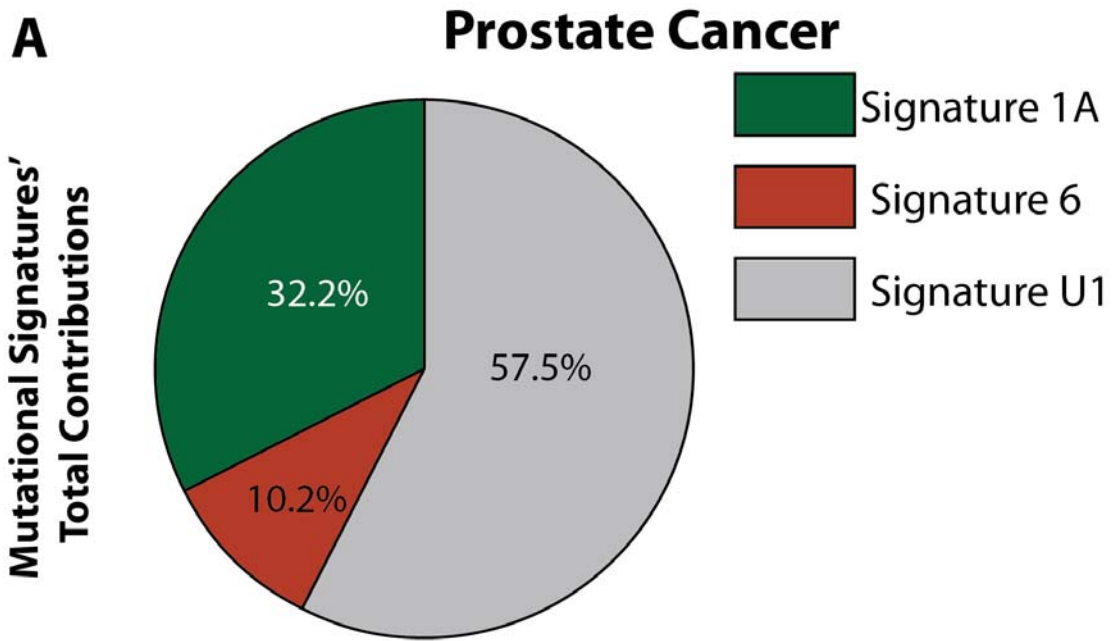


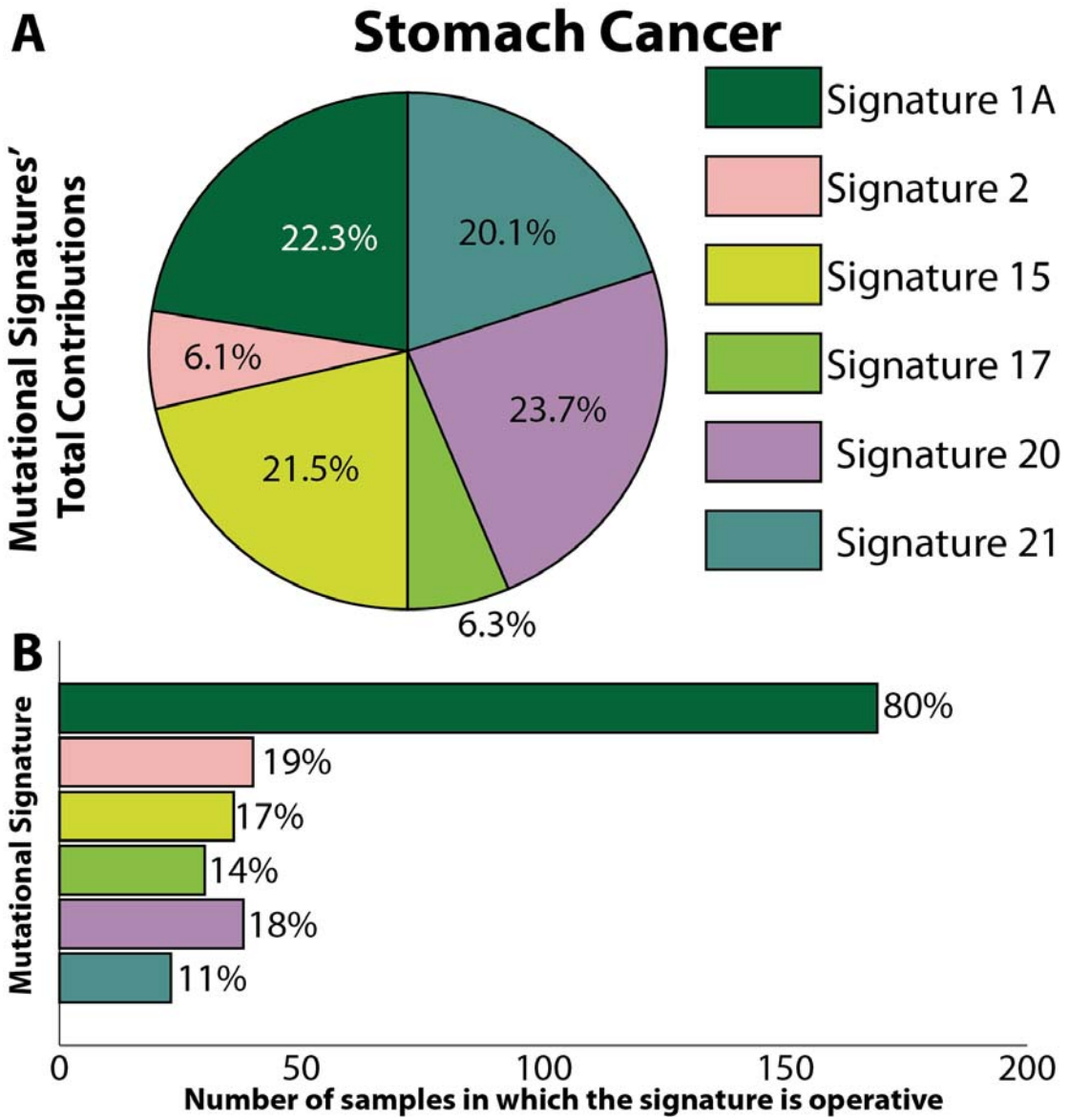


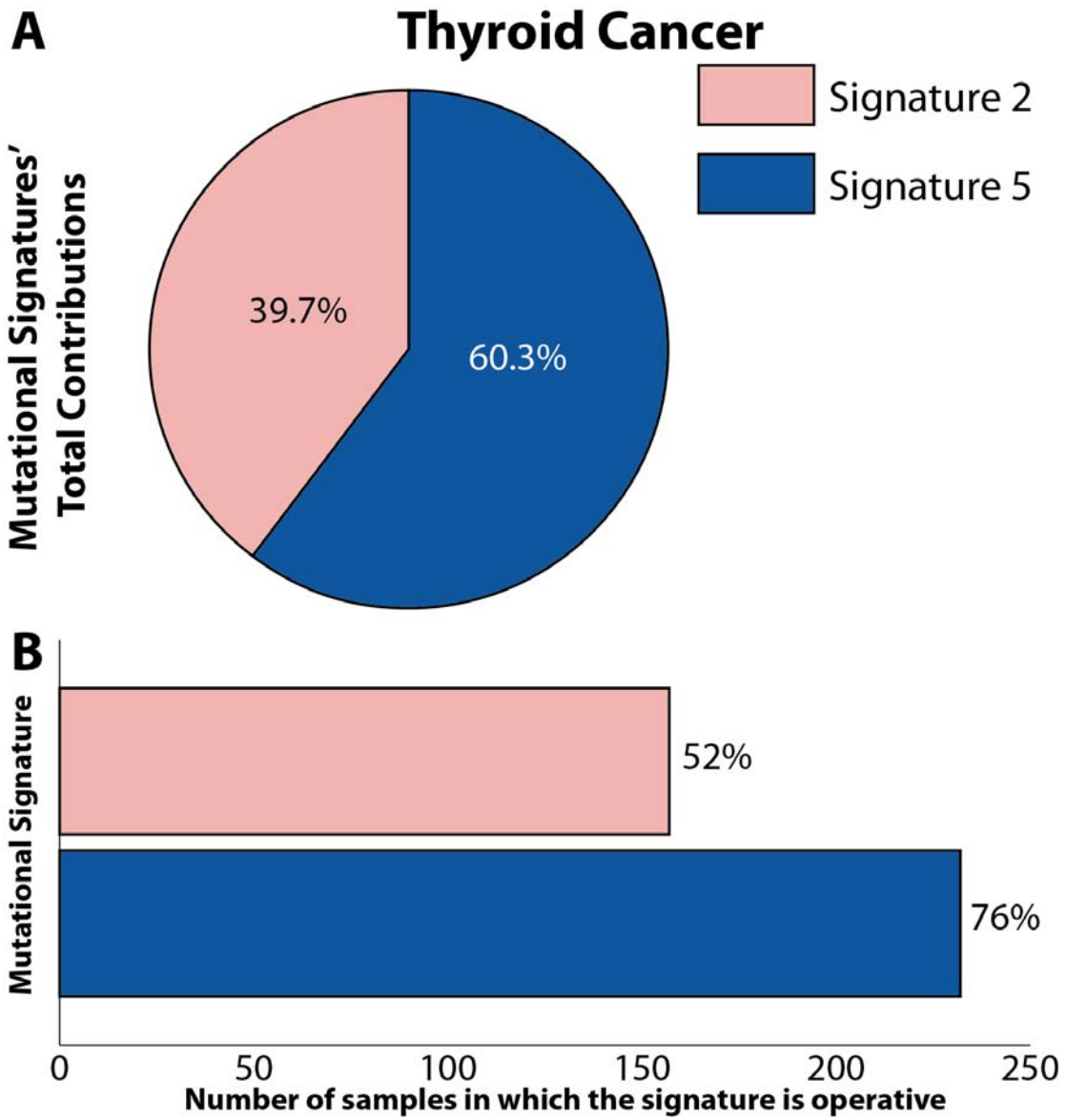


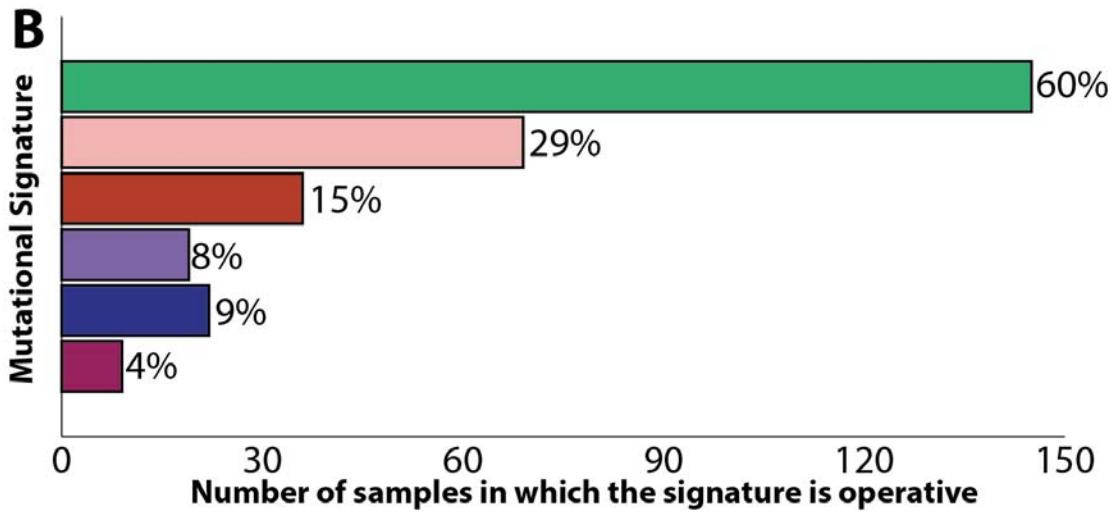
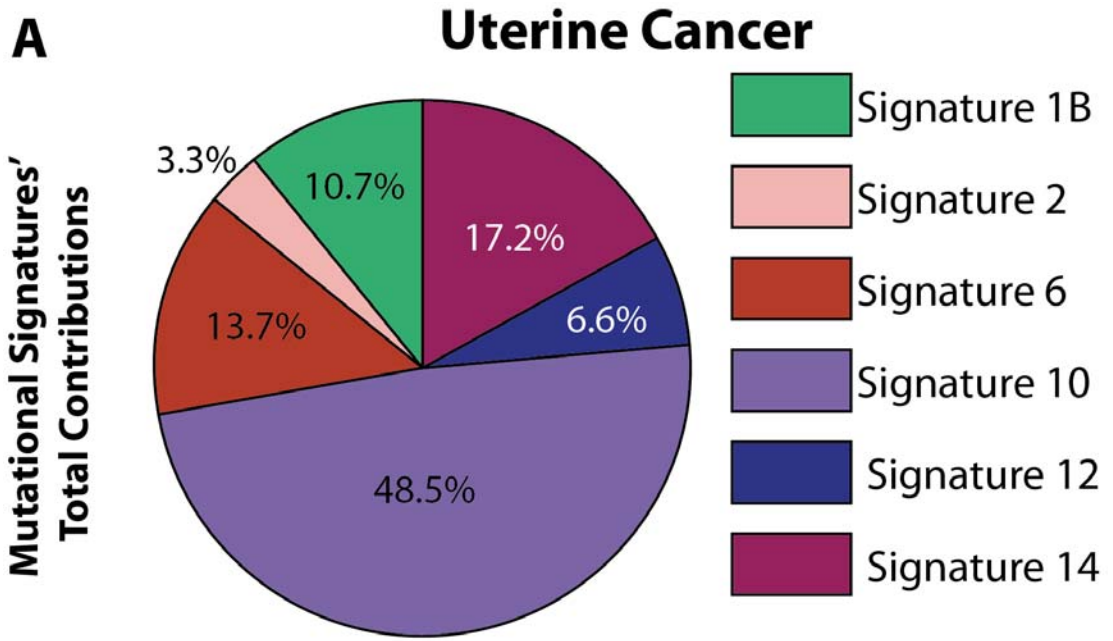












APPENDIX VII: Publications associated with this thesis

This appendix contains the references of the articles that have been written and published as part of this thesis. The articles are separated into two categories: (i) main articles – four manuscripts directly related to developing and presenting the approach for deciphering mutational signatures and applying this approach to a large scale of whole-genome and whole-exome sequencing data, and (ii) supporting articles – seven manuscripts in which mutational signatures (and/or patterns of somatic mutations) have been examined. It is worth noting that this list of manuscripts does not include another six published articles unrelated to mutational signatures and/or cancer nor does it include another seven articles currently under review with which I have been involved during the course of my doctoral studies. Lastly, it should be noted that this thesis is almost entirely written based on the four main mutational signatures articles.

Main articles

Alexandrov LB and Stratton MR (2014) Mutational Signatures: The Patterns of Somatic Mutations Hidden in Cancer Genomes. **Current Opinion in Genetics & Development** 24, 52-60 (invited review article/corresponding author).

Alexandrov LB, Nik-Zainal S, Wedge DC, Aparicio SA, Behjati S, Biankin AV, Bignell GR, Bolli N, Borg A, Borresen-Dale AL, Boyault S, Burkhardt B, Butler AP, Caldas C, Davies HR, Desmedt C, Eils R, Eyfjord JE, Foekens JA, Greaves M, Hosoda F, Hutter B, Ilicic T, Imbeaud S, Imielinski M, Jager N, Jones DT, Jones D, Knappskog S, Kool M, Lakhani SR, Lopez-Otin C, Martin S, Munshi NC, Nakamura H, Northcott PA, Pajic M, Papaemmanuil E, Paradiso A, Pearson JV, Puente XS, Raine K, Ramakrishna M, Richardson AL, Richter J, Rosenstiel P, Schlesner M, Schumacher TN, Span PN, Teague JW, Totoki Y, Tutt AN, Valdes-Mas R, van Buuren MM, van 't Veer L, Vincent-Salomon A, Waddell N, Yates LR, Zucman-Rossi J, Futreal PA, McDermott U, Lichter P, Meyerson M, Grimmond SM, Siebert R, Campo E, Shibata T, Pfister SM, Campbell PJ, and Stratton MR (2013) Signatures of mutational processes in human cancer. **Nature** 500:415-421.

Alexandrov LB, Nik-Zainal S, Wedge DC, Campbell PJ, and Stratton MR (2013) Deciphering signatures of mutational processes operative in human cancer. **Cell Reports** 3:246-259.

Nik-Zainal S, **Alexandrov LB**, Wedge DC, Van Loo P, Greenman CD, Raine K, Jones D, Hinton J, Marshall J, Stebbings LA, Menzies A, Martin S, Leung K, Chen L, Leroy C, Ramakrishna M, Rance R, Lau KW, Mudie LJ, Varela I, McBride DJ, Bignell GR, Cooke SL, Shlien A, Gamble J, Whitmore I, Maddison M, Tarpey PS, Davies HR, Papaemmanuil E, Stephens PJ, McLaren S, Butler AP, Teague JW, Jonsson G, Garber JE, Silver D, Miron P, Fatima A, Boyault S, Langerod A, Tutt A, Martens JW, Aparicio SA, Borg A, Salomon AV, Thomas G, Borresen-Dale AL, Richardson AL, Neuberger MS, Futreal PA, Campbell PJ, Stratton MR (2012) Mutational processes molding the genomes of 21 breast cancers. **Cell** 149:979-993.

Supporting articles

Behjati S, Huch M, van Boxtel R, Karthaus W, Wedge DC, Tamuri AU, Martincorena I, Petljak M, **Alexandrov LB**, Gundem G, Tarpey PS, Roerink S, Blokker J, Maddison M, Mudie L, Robinson B, Nik-Zainal S, Campbell P, Goldman N, van de Wetering M, Cuppen E, Clevers H, and Stratton MR (2014) Genome sequencing of normal cells reveals developmental lineages and mutational processes. **Nature (AOP)** doi:10.1038/nature13448

Murchison EP, Wedge DC, **Alexandrov LB**, Fu B, Martincorena I, Ning Z, Tubio J, Werner EI, Allen J, Barboza di Nardi A, Donelan EM, Marino G, Fassati A, Campbell PJ, Yang F, Burt A, Weiss RA, and Stratton MR (2014) Transmissible dog cancer genome reveals the origin and history of an ancient cell lineage. **Science** 343:437-440.

Bolli B, Avet-Loiseau H, Wedge D, Van Loo P, **Alexandrov LB**, Martincorena I, Dawson K, Iorio F, Nik-Zainal S, Bignell G, Hinton H, Li Y, Tubio J, McLaren S, O'Meara S, Butler AS, Teague J, Mudie L, Anderson E, Rashid N, Tai YT, Shammas M, Sperling A, Fulciniti M, Richardson P, Parmigiani G, Magrangeas F, Minvielle S, Moreau P, Attal M, Facon T, Futreal A, Anderson K, and Campbell PJ (2014) Heterogeneity of genomic architecture and evolution in multiple myeloma. **Nature Communications** 5 (2997).

Papaemmanuil E, Rapado I, Li Y, Potter NE, Wedge DC, Tubio J, **Alexandrov LB**, Loo PV, Cooke SL, Marshall J, Martincorena I, Hinton J, Gundem G, van Delft FW, Nik-Zainal S, Jones DR, Ramakrishna M, Tittley I, Stebbings L, Leroy C, Menzies A, Gamble K, Robinson B, Mudie L, Raine K, O'Meara S, Teague JW, Butler AP, Cazzaniga G, Biondi A, Zuna J, Kempinski H, Muschen M, Ford AM, Stratton MR, Greaves M, and Campbell PJ (2014) RAG-mediated recombination is the predominant driver of oncogenic rearrangement in ETV6-RUNX1 acute lymphoblastic leukemia. **Nature Genetics** 46 (2): 116-125.

Wong CC, Martincorena I, Rust AG, Rashid M, Alifrangis C, **Alexandrov LB**,

Tiffen JC, Kober C, Green AR, Massie CE, Nangalia J, Lempidaki S, Döhner H, Döhner K, Bray SJ, McDermott U, Papaemmanuil E, Campbell PJ, and Adams DJ (2013) Inactivating *CUX1* mutations promote tumorigenesis. **Nature Genetics** 46 (1): 33-38.

Nik-Zainal S, Van Loo P, Wedge DC, **Alexandrov LB**, Greenman CD, Lau KW, Raine K, Jones D, Marshall J, Ramakrishna M, Shlien A, Cooke SL, Hinton J, Menzies A, Stebbings LA, Leroy C, Jia M, Rance R, Mudie LJ, Gamble SJ, Stephens PJ, McLaren S, Tarpey PS, Papaemmanuil E, Davies HR, Varela I, McBride DJ, Bignell GR, Leung K, Butler AP, Teague JW, Martin S, Jonsson G, Mariani O, Boyault S, Miron P, Fatima A, Langerod A, Aparicio SA, Tutt A, Sieuwerts AM, Borg A, Thomas G, Salomon AV, Richardson AL, Borresen-Dale AL, Futreal PA, Stratton MR, Campbell PJ, and Breast Cancer Working Group of the International Cancer Genome C (2012) The life history of 21 breast cancers. **Cell** 149:994-1007

Murchison EP, Schulz-Trieglaff OB, Ning Z, **Alexandrov LB**, Bauer MJ, Fu B, Hims M, Ding Z, Ivakhno S, Stewart C, Ng BL, Wong W, Aken B, White S, Alsop A, Becq J, Bignell GR, Cheetham RK, Cheng W, Connor TR, Cox AJ, Feng ZP, Gu Y, Grocock RJ, Harris SR, Khrebtukova I, Kingsbury Z, Kowarsky M, Kreiss A, Luo S, Marshall J, McBride DJ, Murray L, Pearse AM, Raine K, Rasolonjatovo I, Shaw R, Tedder P, Tregidgo C, Vilella AJ, Wedge DC, Woods GM, Gormley N, Humphray S, Schroth G, Smith G, Hall K, Searle SM, Carter NP, Papenfuss AT, Futreal PA, Campbell PJ, Yang F, Bentley DR, Evers DJ, and Stratton MR (2012) Genome sequencing and analysis of the Tasmanian devil and its transmissible cancer. **Cell** 148:780-791